

NPS ARCHIVE

1961.06

HILL, R.

A DESIGN STUDY FOR A
POLAR ICEBREAKER

RALPH C. HILL
and
JOSEPH L. COBURN, JR.

LIBRARY
U.S. NAVAL POSTGRADUATE SCHOOL
MONTEREY, CALIFORNIA

A DESIGN STUDY FOR A
POLAR ICEBREAKER

by

RALPH C. HILL, LIEUTENANT, U.S. COAST GUARD

B.S., U.S. Coast Guard Academy
(1953)

and

JOSEPH L. COBURN, JR., LIEUTENANT, U.S. COAST GUARD

B.S., U.S. Coast Guard Academy
(1955)

SUBMITTED IN PARTIAL FULFILLMENT
OF THE REQUIREMENTS FOR THE
DEGREE OF NAVAL ENGINEER
AND THE DEGREE OF
MASTER OF SCIENCE IN NAVAL ARCHITECTURE
AND MARINE ENGINEERING
at the
MASSACHUSETTS INSTITUTE OF TECHNOLOGY

June 1961

Signatures of Authors _____

Department of Naval Architecture and
Marine Engineering, 20 May 1961

Certified by _____ Thesis Supervisor

Accepted by _____ Chairman, Departmental Committee
on Graduate Students

A DESIGN STUDY FOR A POLAR ICEBREAKER, by RALPH C. HILL and JOSEPH L. COBURN, JR. Submitted to the Department of Naval Architecture and Marine Engineering on 20 May 1961 in partial fulfillment of the requirements for the Master of Science degree in Naval Architecture and Marine Engineering and the Professional Degree, Naval Engineer.

ABSTRACT

Theoretical and conceptual investigations are made of several aspects of icebreaker design. In particular, the following items are investigated thoroughly:

- (1) An expression for icebreaking force was derived by Vinogradov. His approach is followed, and the effects on icebreaking force of several variables are investigated. It is found that an approximately linear relationship exists between this force and both displacement and thrust-to-displacement ratio.
- (2) A stern shape for a triple screw icebreaker is developed. This development is illustrated by photographs of models used in the development. The final lines are offered as a parent form for further work. Protection of the propellers was the sole governing factor in this development.
- (3) The feasibility of nuclear propulsion for an icebreaker is investigated. Four possible preliminary designs are evaluated by cost estimates. It is concluded that nuclear propulsion is not economically feasible for the current requirements of icebreakers, and at the current costs of nuclear power.
- (4) The feasibility of applying present day roll stabilization techniques to icebreakers is studied. Complete stabilization is neither required nor feasible. It is concluded that a passive tank stabilizing system is the best system for ice-breaker application.

Part of this work was done on the IBM 709 computer of the M.I.T. Computation Center.

Thesis Supervisor: Captain E. S. Arentzen, U.S.N.

Title: Professor of Naval Construction

TABLE OF CONTENTS

	<u>Page</u>
Title	1
Abstract	ii
Table of Contents	iii
List of Figures	v
List of Tables	vii
List of Plates	vii
I INTRODUCTION	1
II PROCEDURE	6
II.1 General	6
II.1.1 Displacement	6
II.1.2 Length-beam ratio	8
II.1.3 Beam	9
II.1.4 Length	10
II.1.5 Draft	10
II.1.6 Summary	11
II.2 The Effect of Ship Characteristics on Icebreaking Capabilities	17
II.3 Stern Configuration and Propeller Arrangement	20
II.4 Nuclear Propulsion	26
II.4.1 Variables of Concept	27
II.4.2 Physical Variables	28
II.4.3 Relationships Between Variables	33
II.4.4 Specific Assumptions and Limitations Imposed on Pressurized Water Reactors	33
II.4.5 Specific Assumptions and Limitations Imposed on the Gas Cooled Reactor	37
II.4.6 Steam Cycle Design	39
II.4.7 Brayton Cycle Design	40
II.5 Roll Stabilization	42

TABLE OF CONTENTS
(continued)

	<u>Page</u>
III RESULTS AND DISCUSSION	52
III.1 The Effect of Ship Characteristics on Icebreaking Capabilities	52
III.2 Stern Configuration and Propeller Arrangement	61
III.2.1 Propeller Selection	61
III.2.2 Stern Configuration	74
III.3 Nuclear Propulsion	84
III.3.1 Reactors	84
III.3.2 Steam Plants	93
III.3.3 Brayton Cycle	94
III.3.4 Costs of Nuclear Power Plants	98
III.4 Roll Stabilization	107
IV CONCLUSIONS AND RECOMMENDATIONS	121
BIBLIOGRAPHY	125
APPENDICES	
A. Brayton Cycle Analysis	131
B. Details of EHP Calculation	137
C. Ice Breaking Analysis	140
D. Reactor Thermal Design Techniques Used	149
E. Cost Estimating Procedure	162
F. Details of Roll Stabilization Studies	175
F.1 Activated Tank System Based on the Characteristics of the USS GLACIER (AGB-4)	179
F.2 Analysis of Passive Anti-Roll Tanks Installed on the USS ATKA	195

LIST OF FIGURES

<u>Figure</u>	<u>Title</u>	<u>Page</u>
II-1	Comparison of Midship Sections	14
II-2	Curves of Performance, Cost and Effectiveness Versus System Capacity	44
II-3	Effective Waveslope Versus Displacement	46
III-1	Icebreaking Force Versus Displacement	56
III-2	Cost of Icebreaker Versus Thickness of Ice	56
III-3	Icebreaking Force Versus Angle of Bow with Horizontal	57
III-4	Bow Angle for Maximum Icebreaking Force Versus Thrust/Displacement Ratio	58
III-5	Ice Breaking Force Versus Thrust/Displacement Ratio	59
III-6	Ice Breaking Force Versus Waterplane Coefficient	60
III-7	Ice Breaking Force Versus Position of LCB	60
III-8	Speed and Power Estimates for Proposed Design	64
III-9	Thrust Versus RPM for 4 and 5 Bladed Propellers.Centerline Propeller	65
III-10	Thrust Versus RPM for 4 Bladed Propellers. Wing Propellers.	66
III-11	Cavitation Data	68
III-12	Cross Section of PWR No. 1 Core	89
III-13	Cross Section of PWR No. 2 Core	90
III-14	Cross Section of PWR No. 2' Core	91
III-15	Cross Section of GCR Core	92

LIST OF FIGURES
(continued)

<u>Figure</u>	<u>Title</u>	<u>Page</u>
III-16	Maximum Wall Temperature Versus Number of Fuel Elements for GCR	93
III-17	Maximum Heat Flux and Safety Factor on Burnout Heat Flux Versus Number of Fuel Rods for PWR	93
III-18	Reactor Thermal Power Versus Turbine Cross-over Pressure, PWR No. 1 and PWR No. 2	96
III-19	Reactor Thermal Power Versus Turbine Cross-over Pressure. PWR No. 2'	96
III-20	Steam Cycle Heat Balance, PWR No. 1	97
III-21	Steam Cycle Heat Balance, PWR No. 2'	98
III-22	Gas Turbine Cycle Efficiency Versus Pressure Loss	100
III-23	Gas Turbine Cycle Efficiency Versus Compressor. Isentropic Temperature Ratio	100
III-24	Gas Turbine Cycle Heat Balance	101
III-25	Location of Heeling Tanks on the GLACIER	110
III-26	Dimensions of One Set of Heeling Tanks on the GLACIER	110
III-27	Magnification of Roll and Tank Water Angles for a Stabilized Missile-Range Ship	114
III-28	Location of Heeling Tanks on the ATKA	116
III-29	Details of Anti-Roll Tank Installation on ATKA	117
III-30	Sequence of Events	119
A-1	Temperature-Entropy Diagram for CICBTX Brayton Cycle	136
F-1	Cross-Section of Ships and Tanks, Showing Nomenclature	178

LIST OF TABLES

<u>Table</u>	<u>Title</u>	<u>Page</u>
I	Characteristics of Modern Polar Ice-breakers (following page one)	
II-1	Beam and Draft of Navy Supply Ships	9
II-2	Proposed Design Characteristics	11
II-3	Shaft Horsepower to Displacement Ratios	12
III-1	Table of Offsets for the Proposed Stern	75
III-2	Technical Data on Reactors	87
III-3	Nuclear Propulsion Plant Equipment Costs	106
III-4	Fuel Cycle Cost Estimates	107
III-5	Particulars for the USS GLACIER (AGB-4)	109
III-6	Results of Roll Stabilization Study on the GLACIER Using Activated U-tube Tank	111
III-7	Particulars of the ATKA	115
B-1	Residual Resistance R_r/Δ from Ref. (10)	139
E-1	Cost Estimates for 7500 HP Cross-Compounded Steam Turbine and Auxiliary Equipment	169
E-2	Cost Estimates for Gas Turbine Cycle Power Producing Equipment	169
E-3	Base Charge for Uranium Established by U.S. Atomic Energy Commission	171
F-1	Comparison of Critical Ship Parameters	180
<u>Plate</u>		
III-1	Pictures of Models (following page 74)	

I. INTRODUCTION

The design of ships specifically intended for breaking ice is a relatively new branch in the field of naval architecture. Interest in the polar regions, as recorded by the expeditions to these areas in the early 19th century, predicated by many years the development of materials and power plants required by ships to operate in these regions. The first seagoing icebreaker, ERMAK, was built for the Russian government in 1899. The ship was built of steel, with $1\frac{1}{4}$ inch plating along the waterline. ERMAK displaced 10,000 tons and had engines of over 10,000 HP. Her design proved successful and she is generally regarded as the prototype of seagoing icebreakers.

Table 1 lists the characteristics of modern icebreakers designed for, or capable of, operation in polar ice. The characteristics of polar icebreakers built in the last decade indicate the interesting contributions by designers of several nations in regard to hull form and proportions, propulsion and endurance.

The Russians were the early leaders in the development of icebreaking vessels. This was due to a strong desire by their government to keep the Northern Sea Route between Murmansk and Vladivostok, along the northern coast of the

TABLE I CHARACTERISTICS OF MODERN POLAR ICEBREAKERS

Name	STALIN CLASS USSR	WIND CLASS USA	D'IBER -VILLE CANADA	KAPITAN CLASS USSR	GLACIER USA	LENIN USSR	MAC- DONALD CANADA	MOSCOW CLASS USSR	PROPOSED 1959 Reference	PROPOSED 1959 Reference
Nation									1	4
Where Built	Lenni- grad	San Pedro	Lauzon	Helsin- ki	Pasca- goula		Lauzon	Helsi- nki	-	-
Year built	1937	1944	1952	1954	1955	1958	1960	1960-62 Bldg.	-	-
LOA	349'9"	269'0"	310'0"	273'0"	309'6"	440'0"	315'0"	390'0"	-	360'0"
LWL	335'0"	250'0"	300'0"	265'0"	290'0"	420'0" (a)	307'3"	363'4"	320'0"	340'0" (a)
Beam, max.	76'0"	63'6"	66'6"	63'8"	74'0"	90'6"	70'0"	80'5"	64'0" (a)	75'6"
Beam, DWL	74'6" (a)	62'0"	65'0" (a)	63'0"	72'6"	90'0" (a)	69'0"	79'0" (a)	62'0"	74'
Draft, max.	29'6"	29'1;"	30'3"	23'0"	28'0"	30'3"	29'0"	34'6"	24'0"	29'0"
Depth	41'3"	37'9"	40'3"	31'2"	38'0"	-	41'0"	46'0"	39'2"	38'0"
Disp., full load, tons	11,000	6,500	9,930	5,360	8,640	16,000	8,974	15,000	7,875	10,500
Complement	157	182	61	117	360 20 pass.	900	77	-	-	450
Speed, max. knots	15.5	16.0	14.5	-	18.0	15.5	19.5	-	-	50 pass. 18.0
Cruising radius, miles	-	25,000	12,000	-	-	unlimited	20,000	20,000	-	unlimited
Block coefficient	.52	.47	.59	-	.513	.49	.53	.52	.50	.50
Prismatic coefficient	.610	.62	.70	-	-	-	-	.61	.59	-
Midship section coefficient	.85	.754	.84	-	-	-	-	.85	.85	-
Waterplane coefficient	.72	.75	-	-	.80(a)	-	-	.65	-	.80
LWL/BDWL	4.5	4.0	4.6	4.2	4.0	4.7	4.5	4.6	5.16	4.6
Rise of forefoot with horizontal Flare, side at DWL, amidships	25°	30°	30°	22°	30°	30°(a)	30°	26°	33°	-
Tumblehome	-	70°	84°	70°	70°	-	84°	72°	77°	-
Angle of entrance										
1/2 a	21°	21.5°	-	-	21.5°	-	-	24°	-	21.5°
Machinery	Steam recip.	Diesel	Steam Elect.	Diesel recip.	Diesel Elect.	Turbo- elect.(b)	Diesel Elect.	Diesel Elect.	-	Turbo- elect.(b)
Shafts	fwd	1	-	2	-	-	-	-	-	-
aft	3	2	2	2	2	3	3	3	2	2
SHP aft -- Centerline	5,000	-	-	-	-	19,600	5,000	11,000	-	15,000
Wing	2,500	5,000	5,400	-	10,500	9,800	-	5,500	-	-
SHP total	10,000	10,000	10,800	10,500	21,000	39,200	15,000	22,000	-	30,000
RPM, C _L -- bollard	-	-	-	-	-	185	136/170	-	-	-
-- free running										
RPM, wing - bollard	-	105/ 145	145	120	175	205	136/170	-	-	135/190
- free running										
SHP/Displacement	.91	1.53	1.01	1.96	2.43	2.45	1.67	1.72	-	2.86
SHP/B _{DWL}	132	161	167	166	290	435	221	286	-	406
Propeller ----- ^L	-	-	-	-	-	-	-	-	-	-
Diameter ----- ^{Wing}		17'0"			17'6"					18'0"
P/D ----- ^{Wing}	-		-	-		-	-	-	-	.7
----- ^{Wing}		.70			.692					

Footnote:
a - Estimated
b - Nuclear

U.S.S.R. open for as many months each year as possible. In 1933 the Russian government started a grand program for the construction of a large fleet of heavy duty ice-breakers, resulting in the STALIN class. Although coal burning power plants for marine use were rapidly disappearing, a coal fired, triple expansion steam plant was adopted due to the ready accessibility of coal fields along the Northern Route for fuel replenishment.

The United States jumped into the icebreaker business in a big way with the development of the WIND class ice-breakers during World War II. This class ship was deemed necessary to afford protection to Greenland, which was in danger of falling under Nazi control. Seven vessels of this class were built, three of which were loaned to the Russians for use during the war.

Since World War II there has been an increasing interest in the polar regions of a military, commercial and scientific nature. The United States sponsored "Operation Highjump" to the ^tAnarctic in 1946 and the "Deepfreeze" operations starting in 1955. The latter have been continued every year since 1955. Twelve of 50 countries participating in the International Geophysical Year Program set up special studies in the ^tAnarctic. The United States and Canada jointly have set up a number of weather stations in the Arctic. In 1955, a string of Distant Early Warning (DEWLINE) radar stations were set up along the northern coasts of Canada.

All of these activities required the extensive use of heavy duty icebreakers.

One of the most recent and certainly one of the most publicized icebreakers is the nuclear-powered LENIN completed by the Russians in 1958. As is readily seen from Table 1 the LENIN is much larger and more powerful than any of its predecessors and is the subject of considerable propaganda put out by the Russian government. However, very little has been published about her success since sea trials in 1958.

In 1959 the Society of Naval Architects and Marine Engineers recognized the importance of icebreakers as a class by devoting their entire spring meeting to icebreaker design and construction. The articles presented at this meeting, held on the St. Lawrence Seaway, are listed in references 1 through 6 of the bibliography. They provide an excellent coverage of the subject, including a much more extensive historical development than is given above.

In June and July of 1958, the U. S. House of Representatives Committee on Merchant Marine and Fisheries and the U. S. Senate Committee on Interstate and Foreign Commerce (14)* reported favorably on a bill to authorize the construction of a nuclear-powered icebreaker for the

* Numbers in parenthesis refer to references given in the Bibliography.

U. S. Coast Guard. Although the bill was not enacted into law, it had the effect of stimulating considerable interest in the subject. Since the Coast Guard has the primary responsibility for icebreaker design for the United States government, this interest is quite naturally reflected in the decision by the authors, both Coast Guard officers, to do their graduate thesis work in the field of icebreaker design.

A thorough study of existing and proposed designs brought to light the many problems peculiar to icebreaker operation and design. Among other things icebreakers seem to be one type of surface vessel where nuclear propulsion might be feasible. A complete investigation into all aspects of icebreaker design would be impossible in the time allotted for thesis work; therefore, the following topics were selected for detailed study:

1. The development of a stern configuration in combination with three stern propellers with 50% of the power on the centerline screw, which would offer greater propeller protection than that afforded on present twin screw icebreakers used by the United States.

2. An analysis of the effects of various form parameters on icebreaking capabilities, based on Vinogradov's equation given in the appendix of reference (1).

3. An analytical investigation into the feasibility of nuclear propulsion.

4. A study of the various possibilities for roll stabilization.

During the course of their graduate work Lieutenant Coburn specialized in nuclear engineering, while Lieutenant Hill specialized in hull design and construction. Lieutenant Hill served for two years on the icebreaker NORTHWIND, 1954 to 1956, making three trips to the Arctic regions.

II. PROCEDURE

II.1. General

Before proceeding with the detailed studies of the problems selected, it was necessary to determine the major characteristics desired of a polar icebreaker with nuclear propulsion. The capabilities required vary somewhat for different governments. This design will be specifically for an icebreaker to be operated by the United States government. The following factors were given primary consideration.

II.1.1. Displacement

In trying to determine a required displacement the need arose for more operational data. In general a heavier ship can break through thicker ice and can force an opening through denser ice packs. Likewise a heavier ship costs more both to build and to operate. It must be determined, from an operational viewpoint, just how large a ship is required to perform the tasks expected of it. An icebreaker has two basic functions: (1) to escort conventional ships through ice fields;

(2) to operate individually in polar regions to gather hydrographic and scientific data. In carrying out both of these missions the time spent in the ice is a much stronger function of the season of the year than it is of the ice breaking capabilities of the ship. It is felt that the additional amount of time an ice-breaker of twice the icebreaking capabilities of the "WIND" class could remain in any of the polar regions, after the winter season sets in, is very limited.

Russia has limited access to ice free ports. Thus, they have a compelling reason for keeping their Northern Sea Route open as long as possible each year. This may give them a sufficient reason (other than for propaganda purposes) for building icebreakers the size of the LENIN (16,000 tons). The United States does not have a similar need. A survey of operational data found in the literature on the WIND class (6,500 tons) did not reveal a need for a larger ship as far as icebreaking capabilities are concerned. It may be that other considerations, such as a large beam to leave a broad track, or larger dead-weight capacity, will require a larger vessel. After giving the subject due consideration our preliminary calculations were based on a range of displacements from 6500 tons to 10,000 tons, as shown in Table II-2.

II.1.2. Length-beam ratio-Lwl/Bwl

The range of L/B ratios for existing icebreakers is 4.0 to 4.7. One advantage of a low L/B ratio is good maneuverability. A second consideration is the resulting broader beam for a given displacement. Also it is desirable that parallel middle body be avoided to facilitate working the ship loose when caught between two ice floes. This restricts the length if excessive beam is to be avoided. On the other side of the ledger as L/B increases maneuverability decreases and controllability increases, making it easier to maintain a straight course, a valuable feature for convoy work. Also for equal displacement a longer ship exerts a greater downward breaking force on the ice.

Except for U.S. design practice the trend has been towards higher ratios. Mr. Ferris (1) suggests an L/B of 5.0 to 5.5. Mr. German (2) states that Canadian experience indicates that maneuverability and power requirements limit the length of an Arctic icebreaker to about 320 feet. He suggests an L/B of 4.5 for a displacement of 10,000 tons. Mr. Lank and Mr. Oakley (4) propose a design with L/B equal to 4.6. Thus designers are tending away from the low L/B of the WIND class and the GLACIER (4.0). Operational reports on these

latter types have been good, but theoretical icebreaking formulas lead designers to higher ratios. An L/B of 4.0 would seem to be a lower limit. Going below this figure would give increasingly large GM, making the vessel even more stiff and uncomfortable to ride than the present WIND class.

II.1.3. Beam

The beam of the icebreaker determines the maximum breadth of the vessels it is capable of escorting through the ice. The track that the icebreaker leaves is about half a yard wider than the icebreaker itself (10). Table II-1 gives a list of most of the broadest of existing U.S. Navy supply ships.

TABLE II-1

Type	Beam, max, feet	Draft, max, feet
AE (Ammunition)	74	29
AKA (Attack transport)	63	28
AS (Sub tender)	70	27
AV (Seaplane tender)	72	27
AD (Destroyer tender)	70	27
AP (Troop transport)	72	26
APA (Attack troop transport)	62	24
AO (Oiler)	75	32

It appears that a beam of 75 feet is the maximum required and a beam of about 70 feet may be adequate.

However, the 63.5 foot beam of the WIND class is enough for escorting AKA and APA types, which were used in the DEWLINE project. If supply ships for use in polar regions could be limited to a 63 foot beam there would seem to be no need for going to an icebreaker much broader than this. At present there are not any conventional ships designed specifically for polar operation. This being the case, use of the supply ships noted in Table II-1 would indicate a desire for a maximum beam approaching 75 feet.

II.1.4. Length

Having determined the required beam the length will follow from the L/B ratio desired.

II.1.5. Draft

A deep draft permits installation of large diameter propellers with sufficient blade clearance below the surface to avoid striking solid ice. This clearance should be at least 8 to 10 feet. A trim by the stern helps.

In some areas, notably Northern Alaskan waters, shoal water tends to limit the maximum draft. However, an argument can be made against having a draft less than that of the supply ships. Table 2 shows this to be 28 to 29 feet.

II.1.6. Summary

Table II-2 gives the characteristics of the designs considered.

TABLE II-2
Proposed Design Characteristics

	No. 1	No. 2	No. 3	No. 4	No. 5
Displacement, tons	6,500	8,500	8,500	8,500*	10,000
LBP, feet	247	280.5	301	311	327
B(DWL), feet	61.7	70.6	62	74	74
H(DWL), feet	28	29	29	28**	30
L/B	4.0	4.0	4.85	4.2	4.4
SHP	19,500	25,500	25,500	25,500	30,000
SHP/disp.	3.0	3.0	3.0	3.0	3.0
SHP/B	316	361	411	345	405
C_b	0.52	0.49	0.55	0.46	0.48
C_x	0.85	0.85	0.85	0.85	0.85
C_p	0.62	0.59	0.64	0.54	0.58
Estimated Cost (mega-inches)	21.1	30.2	30.2	30.2	37.3

* Grew to 9,000 tons as the thesis progressed.

** Later changed to 29 feet in order to use larger propellers.

The SHP to displacement ratio was rather arbitrarily fixed at 3.0. The primary reason for this was that some starting point is necessary. If nuclear propulsion is feasible it would seem that a high SHP to displacement ratio is merited. Table II-3 compares this ratio on some of the latest icebreakers. For a more complete listing see Table I.

TABLE II-3
Shaft Horsepower to Displacement Ratios

<u>Ship</u>	<u>Disp.</u>	<u>SHP</u>	<u>SHP</u> <u>DISP</u>
WIND class	6,500	10,000	1.53
GLACIER	8,640	21,000	2.43
LENIN (nuclear power)	16,000	39,600	2.45
MACDONALD	8,974	15,000	1.67
MOSCOW class	15,000	22,000	1.72
Proposed design	---	---	3.00

For a given displacement fixing this ratio fixed the shaft horsepower.

The next step was to determine a draft which would provide some protection for propellers large enough to deliver this horsepower. Based on the propeller diameters of previous designs the minimum draft was set at 28 feet. However, a deeper draft is desired due to

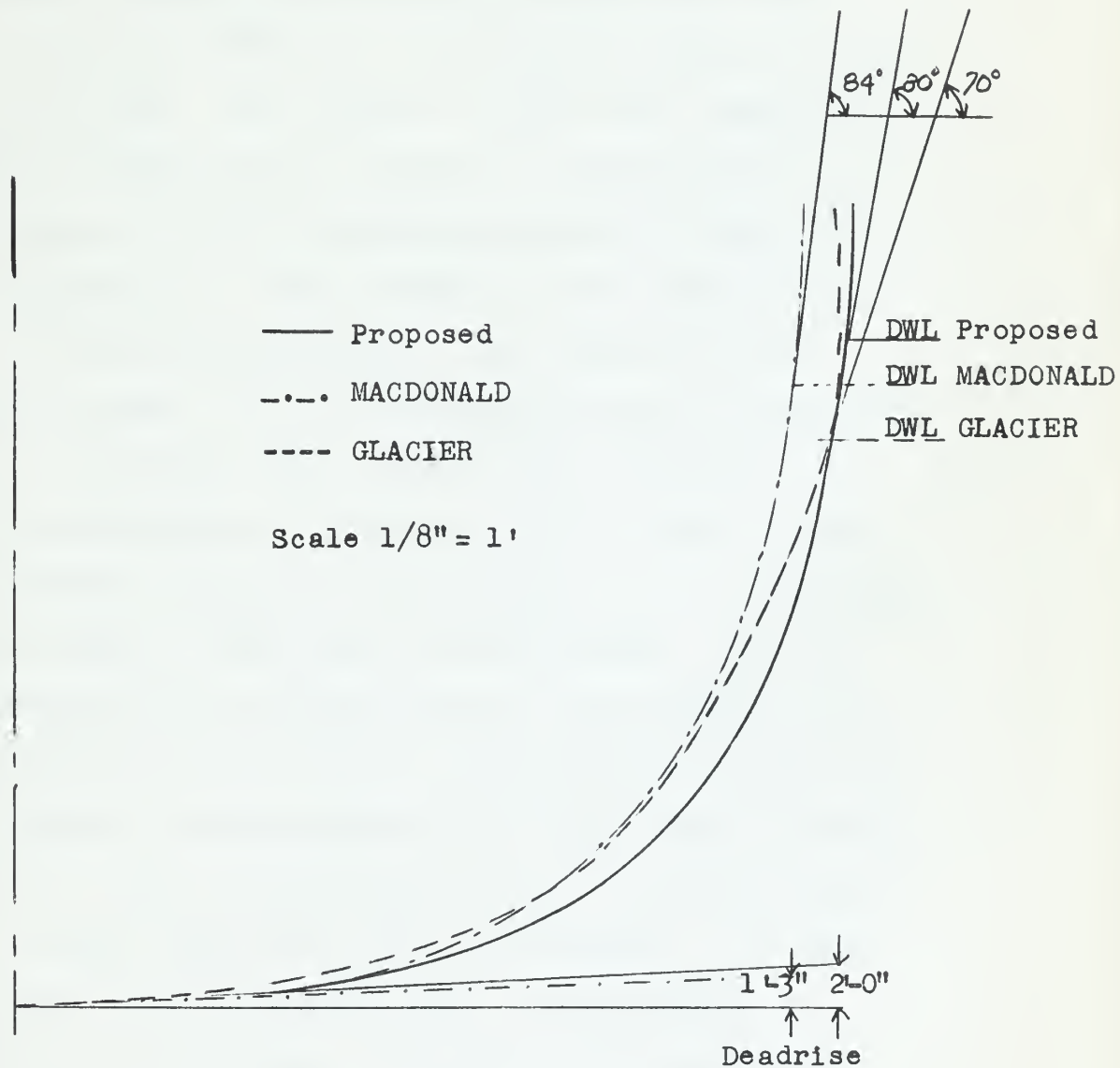
the large horsepower requirement. Therefore the draft of the different proposals was varied, as shown, between 28 and 30 feet.

Another characteristic which was set at the beginning and held fixed was the midship section coefficient C_x . The conventional shape of the midship section on U.S. icebreakers is almost a circular arc with very little dead rise, strong flare at the waterline, and moderate tumblehome above the waterline. A round bottom facilitates the use of the heeling tanks in working the ship loose when beset. As Admiral Thiele (6) points out, it also is an aid in steady breaking if the heeling tanks are continuously operated. However, it was felt that a somewhat flatter bottom could be used with less flare at the design waterline. This is more in accordance with Canadian design practices. A round section would still be maintained over that portion of the ship in contact with the ice. The result is a fuller section which decreases the possibility of ice going under the ship and coming up into the propellers. A comparison of different shapes is made in Figure II-1. For the fuller section the midship section coefficient was estimated at .85.

At this point the following features of the different proposals were specified: (1) displacement;

Figure II-1

Comparison of Midship Sections



(2) shaft horsepower, (3) draft, and (4) midship section coefficient. Two more independent characteristics had to be chosen. The beam required is subject to a tangible analysis depending on what convoy ships are used, therefore the beam for each proposal was specified next.

Finally a somewhat less tangible length-beam ratio was specified. Table II-2 could now be completed from specified data. The original figures were juggled, in order to better fit the purposes of each proposal, in arriving at the final figures presented in Table II-2.

Proposal No. 4 was selected as best representing all of the desired features. The reasons for this selection were: (1) A 75 foot maximum beam is necessary. Due to the slight flare at the design waterline this gave a design beam of 74 feet. (2) In spite of many conflicting opinions of both foreign and U. S. designers, a low length to beam ratio is recommended. The controllability of the WIND class and the GLACIER is not considered to be a problem by the operators, while the high degree of maneuverability of these ships is widely praised. Also, as previously noted, a low L/B results in a broader beam for a given displacement. (3) With a 75 foot beam and a deep draft a displacement of 8,500 tons is necessary. Even with this displacement the ship becomes very fine, the block coefficient, C_b ,

being 0.46. This is less than for any existing designs. For this reason the draft was held at 28 feet. As noted in a footnote to Table II-2 this was later changed to 29 feet which reduced C_b to 0.45. A first reaction to such a low block coefficient may be unfavorable. However, the authors see no real justification for such a reaction. The ship is designed solely for breaking ice. Proposal No. 4, with a 29 foot draft, meets the requirements of wide beam and deep draft, and has more than enough weight for ice breaking capabilities.

II.2. The Effect of Ship Characteristics on Ice-breaking Capabilities, Procedure.

To state that a ship is an icebreaker and must, therefore, break ice, is not enough to determine the desirable features of the ship. The word "polar" in the title of this thesis implies some of the particular kinds of ice to be broken and also implies something of the conditions under which the ship will operate. However, even if the ship's mission is carefully spelled out and a particular location and kind of ice are specified, the problem of selecting parameters for the best ice breaking ability is not simple.

The prediction of a ship's icebreaking ability is mainly dependent on experience, and very little has been recorded of the experience accumulated in this field to date. There have been no systematic studies of the effect of ship parameters on icebreaking as there have been in the field of resistance and powering. Little effort has been expended to overcome the difficulties of experimental approaches.

In spite of these handicaps, some successful ice-breakers have been built. This success, in a way, may handicap further development of this type of ship by encouraging the reproduction of the features of the successful icebreakers without inquiring into and experimenting

with other features. Full scale testing is too expensive of course, so there exists a need for either an analytical or a scale model experimental approach.

Of the two main analytical approaches, the most recent, by Vinogradov (1) is considered to more nearly represent the physical process of ice breaking in polar regions. Simonson (11), in his analysis in 1936, expressed the opinion that it was undesirable to crash into the ice with any appreciable velocity. His concept of ice breaking was limited mainly to harbor and river ice.

The Vinogradov approach accounts for the presence, now deemed a necessity, of the kinetic energy of the ship when it hits the ice. No attempt is made to include the dynamic forces in this analysis. However, it is reasoned that these forces act when the static force is smallest and are non-existent when the static force is largest. Thus the neglect of dynamic forces is within the accuracy of other assumptions. The major source of inaccuracy in this treatment is in the selection of numerical values for two important parameters of the ice, the coefficient of restitution and the coefficient of friction.

However difficult it may be to determine these ice characteristics, the Vinogradov analysis is considered valid for comparing the ice breaking performance of different ships, or for studying the effect of varying certain

parameters on any one ship. The influence of displacement, power (or thrust), angle of bow, location of LCB and the waterplane coefficient on the ice breaking force developed by ice breakers has been calculated by programming Vinogradov's formula on the M.I.T., IBM, 709 computer. This has enabled a systematic study of the five characteristics named. The details of this study are given in Appendix C.

II.3. Stern Configuration and Propeller Arrangement, Procedure

The shape of the stern is influenced by a number of considerations, some of which are conflicting and need to be compromised. Factors which should be recognized are width of path left behind the ship, controllability of the ship while going ahead and astern, reserve buoyancy and stability, and protection of propellers and rudder. Since one of the most troublesome problems in ice breaking operations is propeller damage, it is felt that any compromise should favor protection of the stern gear. This does not seem to be the case on existing ships. A fine afterbody, similar to the forebody, has been an essential requirement. It is strongly felt that a blunter stern would improve the design. It would give better protection, increased reserve buoyancy, increased transverse stability, and would provide a clearer path. Mr. Ferris (1) persists in the idea that an icebreaker must have a pointed stern for backing into the ice, while admitting that damage to stern gear can hardly be avoided under these circumstances. In freeing a ship beset in the ice, backing is sometimes necessary, but only at slow speed through broken ice where a fine stern is only an aid, not an absolute necessity. It is the wash of the propeller that is

valuable under these circumstances. The same argument holds under conditions where the ship is backing down prior to making a run at heavy ice.

It is believed that a triple screw arrangement has definite advantages for ships approaching 10,000 tons with high SHP displacement ratios. With twin screws damage to one propeller seriously reduces the ability of the ship to turn in the ice, aside from the loss of up to 50% power. A triple screw arrangement with 50% of the power on the centerline seems to offer some advantages. The centerline screw can be well protected. The wing screws may be slightly more vulnerable, but damage to one, or even both, will not be nearly as serious as the loss of one propeller on a twin screw ship. The ship will still be able to turn in either direction using the 50% power available on the centerline. There is nothing new in this idea as the Russians have done this for many years. A different, in general broader, stern configuration will be required, but as previously noted this is not considered to be a drawback.

The U. S. designers have not used a triple screw arrangement to date. The Canadians had not done so until very recently. Their latest icebreaker, the JOHN A. MACDONALD, does have triple screws aft with

5,000 SHP on each shaft. A discussion of this ship by Mr. J. Gordon German (2) did not reveal the reasons why a triple screw arrangement was chosen. However, in reply to a request made to him by the authors the following reasons were cited:

- "(1) reduced vulnerability of the wing screws, viz. smaller proportion of total power on each wing shaft resulted in smaller screws, deeper below the surface and better protected by hull.
- (2) in event of damage of one screw, more power remained to aid vessel in her operations for escape from closing ice fields. In addition, a twin screw vessel is almost helpless in ice with one screw disabled.
- (3) with three screws it was possible to arrange machinery spaces such that total flooding or fire in any one complete engine room would not render vessel helpless.
- (4) with one screw directly ahead of rudder ahead steering is greatly improved over twin screw vessels having a centerline rudder."

In designing a stern configuration, with the basic requirement being to provide maximum propeller protection, the physical arrangement of the hull and the propeller is very important. The best way to observe this arrangement is with three dimensional models with the propellers in place. Construction of wooden models would be very desirable. Self-propulsion tests could then be run

in simulated ice fields using paraffin blocks or other suitable model "ice", and the action of the ice in the region of the propellers observed. The first step in the above procedure is to design a parent stern form. Systematic variations of important features of the stern could then be made to obtain a series of models for testing. The design of such a parent form, using the three propeller arrangement proposed with 50% power on the centerline propeller, is one of the major purposes of this thesis. To this end, three dimensional models were made out of heavy cardboard. They did not float very well, but they did show the physical arrangement much better than lines drawings.

It seemed impractical to start off trying to draw up a set of lines without first looking at some existing ships; therefore the first model built was based on the twin screwed GLACIER. The scale used was $1/4" = 1'$, and only that portion of the ship from station 13 aft (20 stations in all) was constructed. This scale and practice was continued with all of the models built for consideration in arriving at the final design of the parent.

Next the lines of the JOHN A. MACDONALD were laid out from the small scale drawing in reference (2), and

a model constructed from these lines. The actual propeller diameter was not available but it was estimated at fifteen feet for all three propellers. This was based primarily on the diameter of the LABRADOR's propellers which are fifteen feet. Both are Canadian ships and both have 5000 SHP on each shaft. Also the stern of the MACDONALD did not allow room for a much larger diameter.

In the initial plan it was expected that from a comparison of the twin screw arrangement of the GLACIER and the triple screw arrangement of the MACDONALD, an original set of lines could be drawn using our own concepts. However, an icebreaker with a triple screw arrangement designed in 1956, at M.I.T. by a course XIII-A design team, had one of the concepts deemed to be desirable. Namely, a sharply cut-away stern which allowed greater propeller tip clearance, while still allowing the propellers to remain well under the overhang. Therefore, these lines were used for a third model. Like the MACDONALD this design had equal power on all three shafts; however, it had seventeen foot diameter propellers, this size being more nearly in the range required of our design. All of these first three models had the same length between perpendiculars of 290 feet, the same draft of 28 feet

and nearly the same displacement. Thus a very good comparison could be made.

A fourth and final model was made using the three previous models as a guide, as well as the previously selected overall characteristics for our design. Pictures of the models of the GLACIER, the MACDONALD and the proposed parent design are shown in Section III.2.2.

The propellers for this design were selected using Troost's design charts (28). Fifty percent of the total SHP was to be developed on the centerline propeller, with twenty-five percent on each wing propeller. The criterion used was maximum thrust at zero speed with due consideration being given to cavitation. After selecting the best propellers on this basis a check was made on free running conditions. Finally estimated curves of EHP and SHP versus ship speed were drawn.

II.4. Nuclear Propulsion, Procedure

The promise of long core life indicates the possible use of a nuclear reactor for propulsion in an icebreaking ship, where a long endurance is required. The construction of the LENIN by the USSR has added a great deal of interest, both technical (4) and political (14) in this possibility. The costs of this endurance must be established to enable an evaluation of the suitability of nuclear power for an icebreaker.

It is shown in Appendix D that thrust is more significant than power in the ice breaking process. However, thrust is related through the propellers and machinery components to the SHP of the ship. The results of an investigation into the effect of thrust or SHP on a ship's ice breaking ability is included in Section III.1. Based on these results and a certain degree of arbitrariness a SHP of 25,500 HP was chosen for this design. It is interesting to note the required open sea speed did not determine the SHP, as is the usual case for conventional ships. The application of various component efficiencies to the specified SHP results in the required power at the turbine flange and the required thermal power of the reactor. Tentative assumptions of 30,000 horse power at the turbine and 100 megawatts will be subjected to reevaluation later.

An investigation of the many variables involved will offer a method to approach the design of the reactor.

II.4.1. Variables of Concept

There are currently many kinds of reactors in operation and even more in a conceptual state (32). This paper will be limited to the consideration of only the following:

PWR No. 1. A pressurized light water moderated and cooled thermal reactor. This is a "conventional design" using the Nuclear Merchant Ship Reactor (NMSR) of the N.S. SAVANNAH as a prototype (46). Saturated steam cycle is used to drive D.C. turbine-generator sets for the main propulsion motors.

PWR No. 2. A pressurized light water moderated and cooled thermal reactor of an "advanced design". The design study of reference (43) is used as the prototype. The secondary cycle is the same as for PWR No. 1, but the steam condition will not necessarily be the same.

GCR. A graphite moderated, helium cooled thermal reactor using the Marine Gas Cooled

Reactor (MGCR) design as a prototype (47,48).

The power generation will be by direct circulation of the helium through a Brayton cycle. The gas turbines will drive D.C. generators.

II.4.2. Physical Variables

The significant physical variables encountered in the design of a reactor may be categorized as: 1) temperatures, 2) pressures, 3) geometry, 4) nuclear properties, 5) flow variables, and 6) others.

II.4.2.1. Temperatures

The bulk temperature entering the reactor, t_{c1} , sets the basic temperature level of the primary system. This level is often limited by consideration of material properties.

The bulk temperature of the coolant leaving the reactor, t_{c2} , establishes the top temperature of the cycle, and through heat exchangers, sets the top temperature of the secondary loop of multiple loop systems. t_{c2} is often limited by material limitations as well as by design uncertainties embodied in safety considerations.

The temperature rise of the coolant in the reactor, $\Delta t_c = t_{c2} - t_{c1}$, is a significant temperature variable.

This temperature rise determines the coolant flow rate through the reactor to remove a given amount of heat. In certain cases Δt_c may be limited by the thermal stresses imposed upon reactor internals and the pressure vessel itself. In other cases this temperature may be limited to keep heat exchanger temperature differences as large as possible.

The maximum temperature of the coolant as it leaves the hottest fuel element, t_{cmax} , is limited in the same manner as t_{c2} .

The maximum wall temperature, t_{wo} , again may be limited by the materials of the wall or cladding as well as the heat removal fluid. t_{wo} is often limited to avoid surface film boiling.

The maximum cladding material temperature, $t_{cladmax}$, is primarily determined by considering the high temperature strength of the cladding material, and its compatibility with the fuel material at elevated temperatures.

The maximum fuel temperature may be limited by changes that the fuel may undergo at various temperatures, or by the melting temperature of the fuel. Both of these considerations depend on the fuel material.

II.4.2.2. Pressures

The pressure, p_1 , at the entrance of the reactor

is the pressure the circulating machinery sees and essentially the operating pressure of the reactor itself. This pressure is almost an independent parameter. It influences the whole system indirectly and can be optimized more or less independently of the rest of the system. This is the case in a system having two separate loops in which the heat exchanger equipment is the connecting link. The pressure p_1 may also be directly involved in the power cycle as in the case of direct cycle boiling water reactors or direct cycle gas cooled reactors. In this case there is no way to separately consider the effect of varying p_1 on the whole system.

The pressure drop Δp in the system or in a given component as the reactor, Δp_r , is significant in that Δp , along with the flow rate, determines the power involved in circulating the coolant. Reduction of Δp generally involves increased size of components.

II.4.2.3. Geometry

The flow area, A_f , presented to the coolant by the fuel elements, and the heat transfer area A_{ht} , available in a fuel element depend upon the configuration and size of the fuel element chosen. There is essentially an infinite number of combinations of fuel rod size and arrangements, and the final choice must represent a com-

promise between pressure loss and heat transfer requirements.

The path of the coolant may be varied as in one-pass versus two- or three-pass concepts.

II.4.2.4. Nuclear Properties

Surprisingly enough, nuclear considerations are in general separable from other problems in this treatment. Nuclear characteristics of materials used primarily affect the economics of the reactor design through fuel costs. For example, low neutron absorption materials are usually more expensive than stainless steels. However, the use of low absorption materials such as ziralloy for cladding generally allows the use of fuel of lower enrichment and hence the fuel cycle costs are reduced. The species and enrichment of the fuel enter similarly but the form of the fuel; i.e., metallic uranium versus uranium dioxide pellets, is mainly a material problem related to temperatures and heat removal.

II.4.2.5. Flow Variables

The flow rates, both the total mass flow rate through the reactor, w_T , and the mass flow rate per fuel channel or element, w , are related to the rate of heat removal through the temperature rise Δt_c in the reactor.

Individual velocities of coolant through components of the system may be limited by vibration and erosion considerations or by some maximum acceptable pressure loss. In general, however, heat transfer is enhanced by high fluid velocities.

II.4.2.6. Other Variables

One of the most significant variables in the thermal design of a pressurized water reactor is the maximum heat flux per unit area, $(q/A)_{max}$, and its value relative to the heat flux at which boiling burnout, $(q/A)_{bo}$, occurs (29). Boiling burnout occurs as a result of the formation of a complete film of vapor between the heating surface and the heat transfer liquid. This results in a sudden and extremely large temperature increase at the surface. A material failure due to this temperature is inevitably associated with burn out.

$(q/A)_{bo}$ may be calculated by any one of several empirical relationships or may be observed directly in an experiment. There is a great deal of uncertainty in the results of any generalized correlation for $(q/A)_{bo}$ and the experimental approach is superior. The correlation used in Appendix D is the so-called Jens-Lottes equation, the limitations of which are included in Appendix D.

II.4.3. Relationships Between Variables

The basic physical laws to be applied will be those of heat generation and heat transfer. Reactor theory and criticality calculations will not directly enter the discussion, except that nuclear characteristics must be considered when discussing fuel cycle costs.

The equations of heat generation and heat transfer may be combined in many forms (30,31,49). Working equations are derived in the appendix based on the especially useful approach of Rhosenow and Lewins (49).

II.4.4. Specific Assumptions and Limitations Imposed on Pressurized Water Reactors

II.4.4.1. The rapid emergence of nuclear engineering and the possible grave results of a mistake have influenced reactor designers. Thus, current designs are justifiably conservative and factors of safety have been modified very little.

The reactor powering the Nuclear Ship SAVANNAH is an example of current PWR design practice (44,45,46).

A nuclear powered icebreaker conceived and contracted for early completion now would almost certainly have a reactor embodying the safety factors and limitations of the

NMSR in the SAVANNAH. For this reason, the first reactor to be considered will use the NMSR as a prototype.

General Characteristics of PWR No. 1.

Single region, uniformly loaded, pressurized light water moderated and cooled thermal reactor. Single coolant pass through the core.

$$p_1 = 2000 \text{ psia}$$

$$\Delta t = 30^\circ\text{F}.$$

$$(q/A)_{\max} / (q/A)_{bo} = \sim 9/1$$

$$t_{c2} \leq t_{sat} - 100^\circ$$

$$two \leq t_{sat} - 5.0$$

These temperatures specify, in effect, that in normal operation there will be no boiling anywhere in the reactor. The underlying reason for this philosophy has been a fear that the unknown response of a reactor to the formation of vapor would be unstable. This fear has been vindicated for certain designs, and under certain conditions when an instability called "chugging" has been observed (34). As previously mentioned, the general correlations relating pressures and temperatures to the burn-out heat flux are not satisfactory, hence the large factor of safety used on the maximum allowable heat flux is really a factor of ignorance.

The physical make-up of fuel elements used is essentially that of the NMSR (46). The number of elements in the core and the length of these elements depend upon the relations developed in Appendix D and are given in Section III.

II.4.4.2. Nuclear engineering is in the transition out of its initial stage and as experience accumulates designers are weighing more carefully the costs of extreme conservatism against the decreasing likelihood of an accident. These new thoughts are reflected in the many "preliminary designs", "design studies", or "paper reactors" which are available now from the U. S. Atomic Energy Commission or the General Printing Office of the Department of Commerce.

It is interesting to compare and possibly weigh some of the advantages of a PWR of this era with a reactor of the first stage, specifically PWR No. 1 of this report.

General Characteristics of PWR No. 2

$$p_1 = 2000 \text{ psia}$$

$$\Delta t = 40^\circ$$

$$(q/A)_{\max} / (q/A)_{bo} = \sim 2.3/1$$

$$t_{c2} \leq t_{\text{sat}} - 25^\circ$$

two not specified

$$t_{c2\max} \leq t_{\text{sat}}$$

These temperatures imply that under normal operating conditions some local sub-cooled boiling is allowed (30). Designers of so-called "advanced PWR's" justify this by noting the stable operation of boiling water reactors and the knowledge gained from the EBWR and VBWR where chugging has been intentionally induced and the factors contributing to this instability were established (34). The higher temperatures allowed by this approach influence the entire system and is reflected in the results in Section III.2.

In the design stage of new reactors many experiments are carried out and it is expected that accurate burn out heat flux data can be obtained for the specific conditions contemplated. If the burnout heat flux can be predicted accurately, a reasonable safety factor to apply to this quantity is one in the range of 2 to 3.

If the design heat flux of PWR No. 2 is markedly increased over that of PWR No. 1, as is proposed, the reactor itself will be smaller. For the same pressure, the pressure vessel wall will be thinner and the reactor internals will have generally smaller dimensions. This reduction in size will allow a larger temperature rise in the coolant while the thermal stresses are maintained at the same level.

The fuel element geometry of this reactor will be specified as the same as that of PWR No. 1, but the over-

all size will be of course reduced to take advantage of the reduced safety factors.

II.4.5. Specific Assumption and Limitations Imposed on the Gas Cooled Reactor Design

The hope of improved thermal efficiency and reduced complexity has led reactor designers to consideration of direct cycle nuclear reactor power plants. These are systems in which the thermodynamic working fluid is the reactor coolant as well. The system chosen for this comparison uses the MGCR as a prototype.

General Characteristics of GCR

Single region, uniformly loaded, graphite moderated, helium cooled thermal reactor. Single coolant pass through the core. Brayton cycle of the CICBTX type with single pass regenerator and intercooler.

$$t_{c1} = 1300^{\circ}\text{F}$$

$$t_{wo} = 1500^{\circ}\text{F}$$

Other pressures and temperatures are determined by the thermodynamic analysis of the cycle. The basic limitation on the maximum wall temperature is based on the maximum temperature that can be expected to be endured

by the cladding material. The top temperature is the result of a compromise between the desire for high thermodynamic efficiency and an effort to keep metal temperatures low enough for proper strength requirements.

In the analysis in Appendix A the cycle is analyzed and the basic parameters are chosen to result in the best available thermodynamic efficiency.

II.4.6. Steam Cycle Design

For the purpose of the PWR designs, the secondary systems were fixed as follows:

(1) Four main turbo-generator sets will be employed, each consisting of cross compounded 7500 HP turbines. The high pressure and low pressure turbines are each to drive separate 2600 KW D.C. generators.

(2) Moisture separation and a single extraction for feed water heating are both to be accomplished at the cross over between high and low pressure turbines. The optimum pressure for the extraction was determined by performing a series of heat balances for different extraction pressures.

(3) The key condition imposed by the heat balance is that, at rated load, the power delivered by the low pressure and the high pressure turbines is to be the same.

Turbine efficiency, η_T , defined here as the ratio of actual enthalpy drop to isentropic enthalpy drop in a turbine, was assumed to be a function of the moisture content of the steam in the last stages of the turbine. The

function

$$\gamma_T = 0.80 (1 - m)$$

was used to describe this dependence on moisture. m is the weight fraction of moisture in the steam at exit from the turbine.

Other efficiencies used throughout the calculations are:

$$\gamma_{\text{motor}} = 0.930$$

$$\gamma_{\text{turbo-generator}} = 0.915$$

Note that a penalty of about ten percentage points of efficiency is paid for the use of electric drive.

II.4.7. Brayton Cycle Design

The gas turbine cycle analysis was based on the assumption of perfect gas behaviour of the helium. Again the assumptions of propulsion motor and turbo generator efficiencies were made to require a total of 30,000 horse power at the turbine flanges. To provide flexibility and to limit the size of the D.C. generators, four loops are used, each complete and capable of independent operation. Four double-armature D.C. generators of 2600 KW capacity on each armature are to be employed.

The crucial component efficiencies have been estimated, based on those of the prototype, as follows:

compressor efficiency, $\gamma_c = 0.85$

turbine efficiency , $\gamma_T = 0.90$

pressure loss parameter, $\gamma = 0.96$

Calculations of the various state points are made following the standard techniques of gas turbine design (38,51). The pressure of 1150 psia was chosen as a compromise between the added weights and sealing difficulties of high pressures and the reduced size of ducting and turbomachinery made available by high pressures.

II.5. Roll Stabilization, Procedure

Icebreakers are notoriously heavy rollers, a feature which is inherent in their design. A large GM with an almost round underwater shape, both deemed necessary for carrying out icebreaking operations, combine to produce bad roll characteristics. The most common method of reducing roll is through the use of bilge keels. Expendable bilge keels have been used on United States and Canadian icebreakers. These were of light construction and were easily installed. The idea being to provide some degree of stabilization on the voyage to the ice field, with the realization that they would be torn off once in the ice, without doing structural damage to the hull. They were then reinstalled during the next dry docking. This is an expensive process for something that only does a half-way job. It also leaves one with the feeling that there must be a better method.

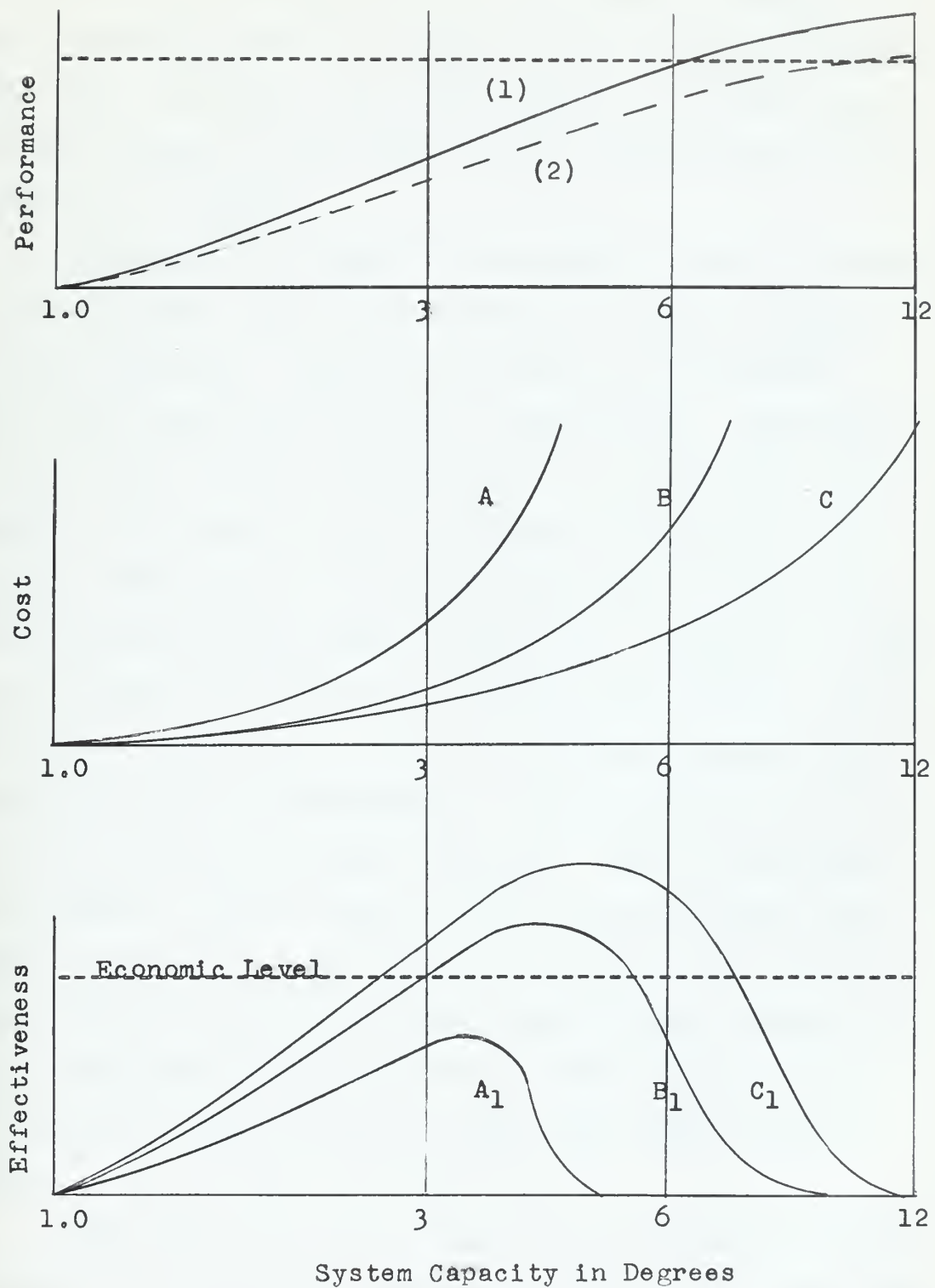
Many methods of roll stabilization have been tried on different type ships over the past 80 years. These methods were classified by Chadwick (52). After discussing what would seem to be all possible methods he concludes that U-tube tanks (active or passive), sea-ducted tanks, and fin stabilizers have the greatest future for the stabilization of ships.

Before any further discussion of specific systems it seems advantageous to first consider methods for comparing different systems. Performance and cost are the two items uppermost in the mind of a prospective buyer. Both are directly related to the capacity of the system. Another useful term is effectiveness, defined as the ratio of performance to cost. More will be said about how performance, cost and capacity are defined in relation to roll stabilization, but for the moment, using these terms in their general sense, consider the three sets of curves presented by Chadwick (52). These show the general features of performance, cost and effectiveness versus system capacity.

The performance versus capacity curves indicate that after a capacity of about 10 degrees is reached, there is very little improvement in performance. Curve 1 represents a typical Naval vessel, while curve 2 represents a typical commercial vessel. The curves of cost are monotonic-increasing and have an ever-increasing slope. The curves of effectiveness which combine cost and performance have distinct peaks. Picking an arbitrary economic level, it is shown that for ship A, a difficult ship to stabilize, it is not economically feasible to attempt any degree of stabilization. Ships B and C have a range over which it is economically feasible to provide stabilization. Ship C, less difficult than the average ship to stabilize, has the widest range. Chadwick is of the opinion that "no

Figure II-2

Curves of performance, cost and effectiveness
versus system capacity



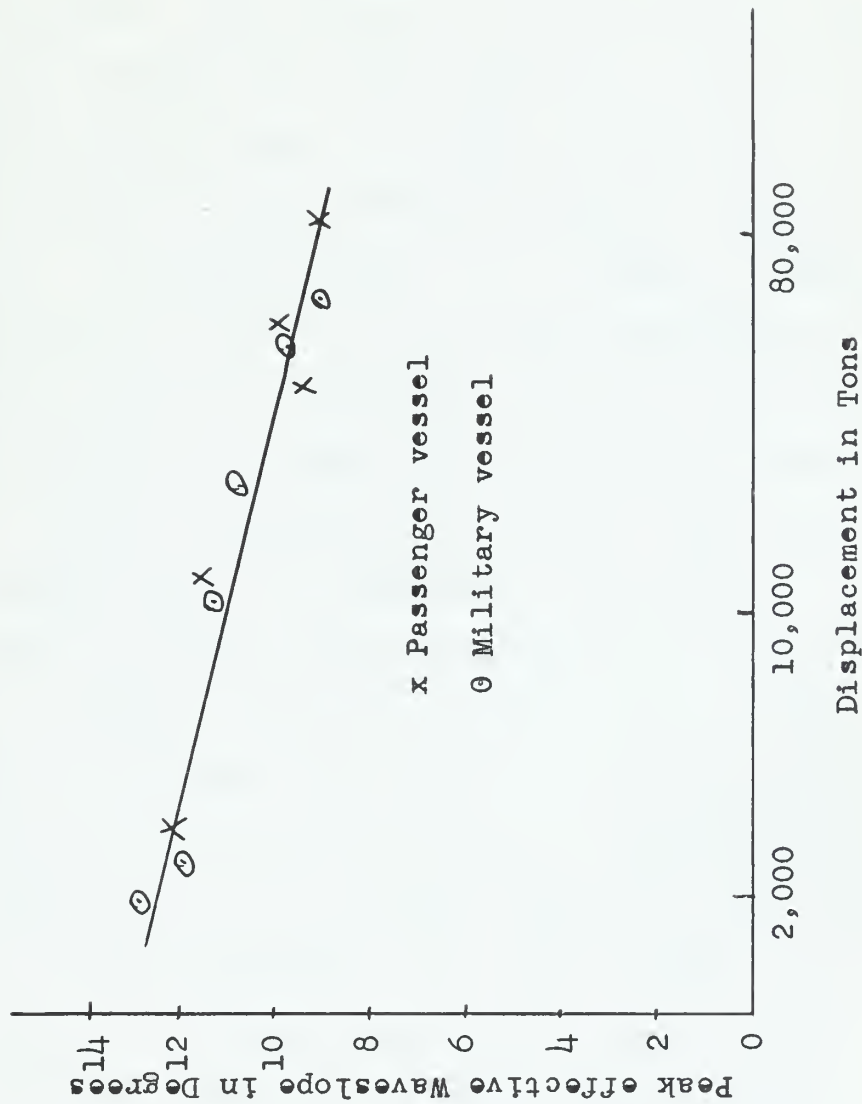
system with a capacity of less than 2.5 degrees will be successful in the long run, and that even 3.0 degrees will generally result in barely tolerable effectiveness." The upper limits are less well defined but he feels that it will rarely be profitable to go to capacities greater than 6 or 7 degrees.

Performance is judged by the degree to which the ship is stabilized. Cost will be defined in terms of space, weight and power. Capacity is defined as the maximum effective waveslope that can be neutralized. Waveslope is the most suitable variable to use in describing ocean waves. True waveslope is the actual waveslope measured at the ocean surface. Effective waveslope is simply the total destabilizing torque on the ship, expressed in terms of the static list which this torque would produce. Thus effective waveslope is equal to the destabilizing torque divided by (GM x displacement). Determination of the effective waveslope is quite difficult. This is discussed by Chadwick, and will not be gone into other than to present an empirical curve taken from Chadwick (52) showing peak effective waveslope versus displacement. Because of the integrating action of the hull, peak effective waveslopes are slightly less for large ships than for small ones, as can be seen from Figure II-3.

Going back now to the discussion of different systems, Chadwick (53) gives an excellent discussion of U-tube tank,

Figure II-3

Peak Effective Waveslope vs. Displacement



activated fin, and gyro stabilizing systems, stressing the activated U-tube system. His conclusions favored the activated fin stabilizer for a ship of normal characteristics in terms of space, weight, and power costs for equal performance. There seems to be some general agreement in the literature with this conclusion. The Canadian Navy adopted a Denny-Brown, activated, retractable, fin stabilizer for use on the icebreaker LABRADOR, completed in 1955 (3). The percent weight, i.e., weight of complete stabilizing system divided by full load displacement, of the LABRADOR installation was given as 1.2%. This is considerably less than the figure of 1.85 given by Chadwick (53) for a "normal" retractable fin system. The capacity of the LABRADOR system is undoubtedly less than the 5.2 degrees used by Chadwick since icebreakers are much more difficult to stabilize than the "normal" ship no matter how "normal" is defined. But from the sea experience of the LABRADOR the stabilizer has served a useful purpose. Quoting from Captain F. W. Matthews' paper on "Stability and Control of HMCS LABRADOR" (3) - "As a general rule, in complicated wave systems experienced, a roll of 25 degrees is normally reduced to between 8 to 10 degrees, and 15° roll is reduced to between 4 to 5 degrees. The speed of the ship for all observations made subsequent to trials is between 13 to 14 knots." The opening in the ship's side, for retraction of the fins, apparently has not caused any trouble.

Thus there seems to be a good case built up for the retractable, activated fin system for use on icebreakers; however, there are some other considerations, namely:

(1) The fin system effectiveness decreases with speed. The optimum open water cruising speed for fuel economy for the existing U.S. polar icebreakers is about 11.5 knots. The LABRADOR also falls in this grouping. This is getting into the speed range where the performance of fin stabilizers is falling off rapidly. One of the author's worst experiences during three Arctic patrols on a WIND class icebreaker was while the ship was riding at anchor. Rolls averaging 15 to 20° with peak rolls up to 30° were suffered for a three-day period. Also, icebreakers frequently are used for gathering oceanographic data at low speed. In both of the latter situations fins are of little or no value.

(2) Large capacity heeling tanks are built into icebreakers for use in working the ice. These are considered to be very desirable for this purpose, (6). Thus it may be possible to considerably reduce the cost, in terms of

weight and space, for a tank system by designing the stabilizing system into the heeling system, or vice-versa. The only additional space and weight required would be for larger transverse ducts, and if an activated tank system is used, for more elaborate control equipment.

3) On a nuclear powered icebreaker the volume normally used for fuel tanks will be available for other purposes. Part of this is taken up by the larger machinery spaces required, but it is expected that the volume required by a tank stabilizing system will still be available. This space could also be used for cargo oil, however, cargo carrying capacity of an icebreaker is not a governing design feature.

4) Roll stabilization on icebreakers may be definitely desirable, but is it economically practical? The activated fin system used on the LABRADOR is apparently successful. However, the cost of roll stabilization on icebreakers must be charged primarily to habitability. Just the weight addition alone, using an average cost figure of \$3,000 per ton of total displacement

and 1.2% of 6,500 tons or 78 tons for the stabilizing system weight of the LABRADOR, adds a cost of \$234,000. This amount, plus the space taken up by the system, would go a long way towards improving other habitability features; features that could be used a much larger percentage of the time, such as improved berthing quarters. Therefore, aside from its other limitations, a retractable fin system is considered to be too costly.

The purpose of the rest of this study was to determine what could be done in the way of stabilization, utilizing the tank space presently used for heeling. Tests with activated anti-rolling tanks installed on the USS PEREGRINE (E-AM373) (49) were not wholly successful. However, the tests were a big step forward. It was felt that many of the troubles encountered during these tests were due to using equipment not specifically designed for the job. Also refinements were needed in the control systems. Even with these difficulties 20 to 50% stabilization was obtained under varied operating conditions.

In DTMB report 950 (59) Grant R. Hagen reports the results of feasibility studies for the roll stabilization of the USS BOSTON (GAG-1). The method he used was based on Chadwick's work. In conducting this study, that part of Hagen's pro-

cedure pertaining to activated U-tube tanks was applied to the known characteristics of the GLACIER, these characteristics being similar to those selected for our design study.

At a later stage it was discovered, quite by accident, as nothing has been printed on the subject, that the U.S. Navy had installed a passive anti-roll tank on the ATKA, a WIND class icebreaker. The installation was completed in early 1961 by the Boston Naval Shipyard. An initial trial run was completed late in April, 1961. Since the ATKA is stationed in Boston, the dimensions and other details of the anti-roll tanks were obtained from personnel attached to the ship. An analysis of the system as installed was then made.

The results of both of the above studies are presented in Chapter III, Section III.4. Detailed calculations are given in Appendix F.

III. RESULTS AND DISCUSSION

III.1 The Effect of Ship Characteristics on Icebreaking Capabilities, Results and Discussion

The initial effort of this analysis was channeled into a study of the effect of displacement on a ship's ice-breaking ability. The results of these calculations are shown in Figure III-1. As near as can be determined, this plot is a straight line for the restrictions imposed. These restrictions are: (a) similarity of ships, and (b) constant thrust to displacement ratio of 0.022. It is proposed by Simonson (11) that the thickness of ice that can be broken is proportional to the square root of the applied force. A reasonable approximation of costs of similar ships is that the cost is directly proportional to the displacement. These two observations have been combined with Figure III-1 qualitatively in Figure III-2. No attempt was made to numerically evaluate the axes because of all the unknown factors. The important observations here is, that, if a proposed icebreaker's ability is specified in terms of some thickness of ice to be broken, this specification should be well considered. The cost of the ship is about proportional to the square of the thickness of ice specified.

The effect of the angle of the stem with the water-line ϕ on the icebreaking force was investigated through the programmed version of Vinogradov's analysis. The dependence of force on ϕ depends in turn upon the thrust to displacement ratio. Figure III-3 is a plot of these results. It should be noted that ordinate is discontinuous to accommodate the wide range of forces plotted. From these calculations, it does appear that there is an optimum bow angle for any given set of ship and ice parameters, and that this optimum angle is a strong function of thrust to displacement ratio. Examination of the scale against which the icebreaking force is plotted shows that the curves are quite flat in the region of the maximum force. Therefore, there is a range of bow angles, depending on the thrust to displacement ratio, for which the icebreaking force is near optimum. This is illustrated in Figure III-4. The solid line shows a linear relation-

ship for the optimum bow angle, and the dashed lines show the range of bow angles that maintain the ice breaking force within 1% of the maximum. It would appear from this analysis, that the angle of the bow with the horizontal is not an important variable in icebreaker design. This may explain the relatively equal success of icebreaker designs with bow angles ranging between 22° and 33°.

The wide separation of the curves of Figure III-3 indicates that the thrust to displacement ratio is a significant variable in the design of an icebreaker. Figure III-5 illustrates the results of calculating the icebreaking force for various thrust to displacement ratios.

The two curves plotted are the extremes of a family of curves for various values of the parameters, C_{wp} and the position of LCB. It is significant to note, that while the curves are practically linear for thrust to displacement ratios greater than 0.0158, there is a region of more rapidly increasing force at thrust to displacement ratios less than 0.0158. Here again, above the specific value mentioned, cost will increase linearly with the specified icebreaking force and will increase roughly as the square of the thickness of ice to be broken. Ratios of thrust to displacement greater

than 0.0158 should be justified in the light of performance required.

The results of varying the other parameters studied, C_{wp} and position of LCB, are plotted in Figures III-6 and III-7. These variations are virtually linear and the change in icebreaking force over a reasonable range of C_{wp} is hardly significant. The position of the longitudinal center of buoyancy has a more significant effect on the force developed, but the variation is only around 5% for a move of 10 feet.

FIGURE III-1
ICE BREAKING FORCE
VS
DISPLACEMENT

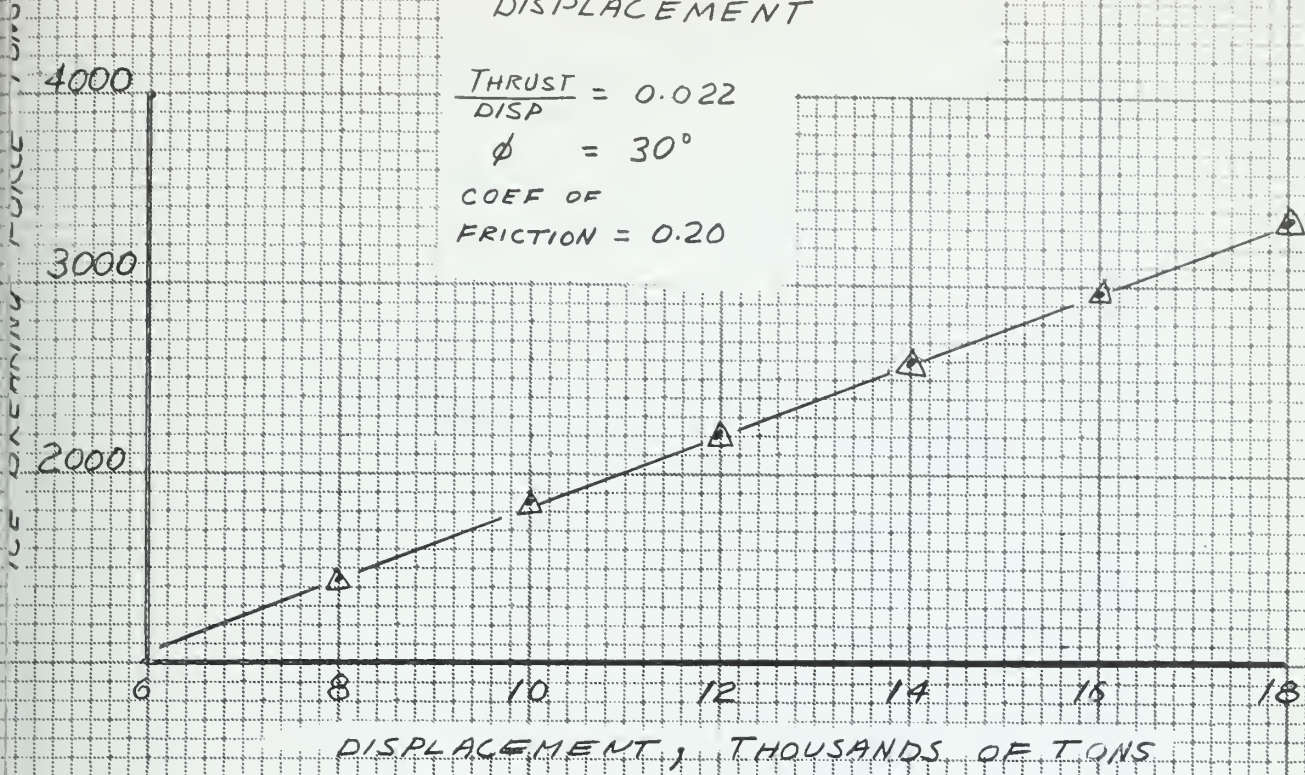


FIGURE III-2
COST OF ICEBREAKER
VS
THICKNESS OF ICE

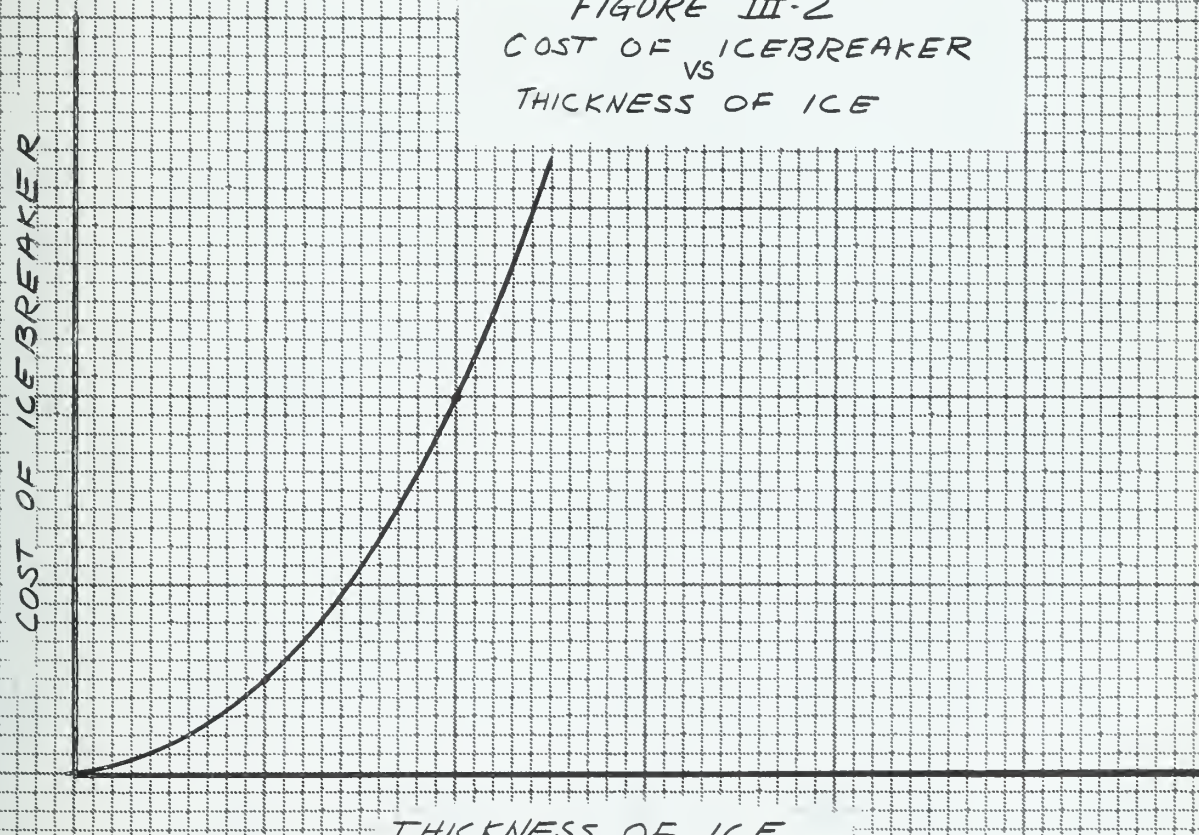


FIGURE III-3
 ICEBREAKING FORCE
 VS
 ANGLE OF BOW WITH HORIZONTAL
 $DISP = 8500 \text{ T}$ $LCF = 5' \text{ FWD} \otimes$
 $C_{WP} = 0.80$ $f = 0.20$

NOTE DISCONTINUOUS SCALE
 FOR FORCE

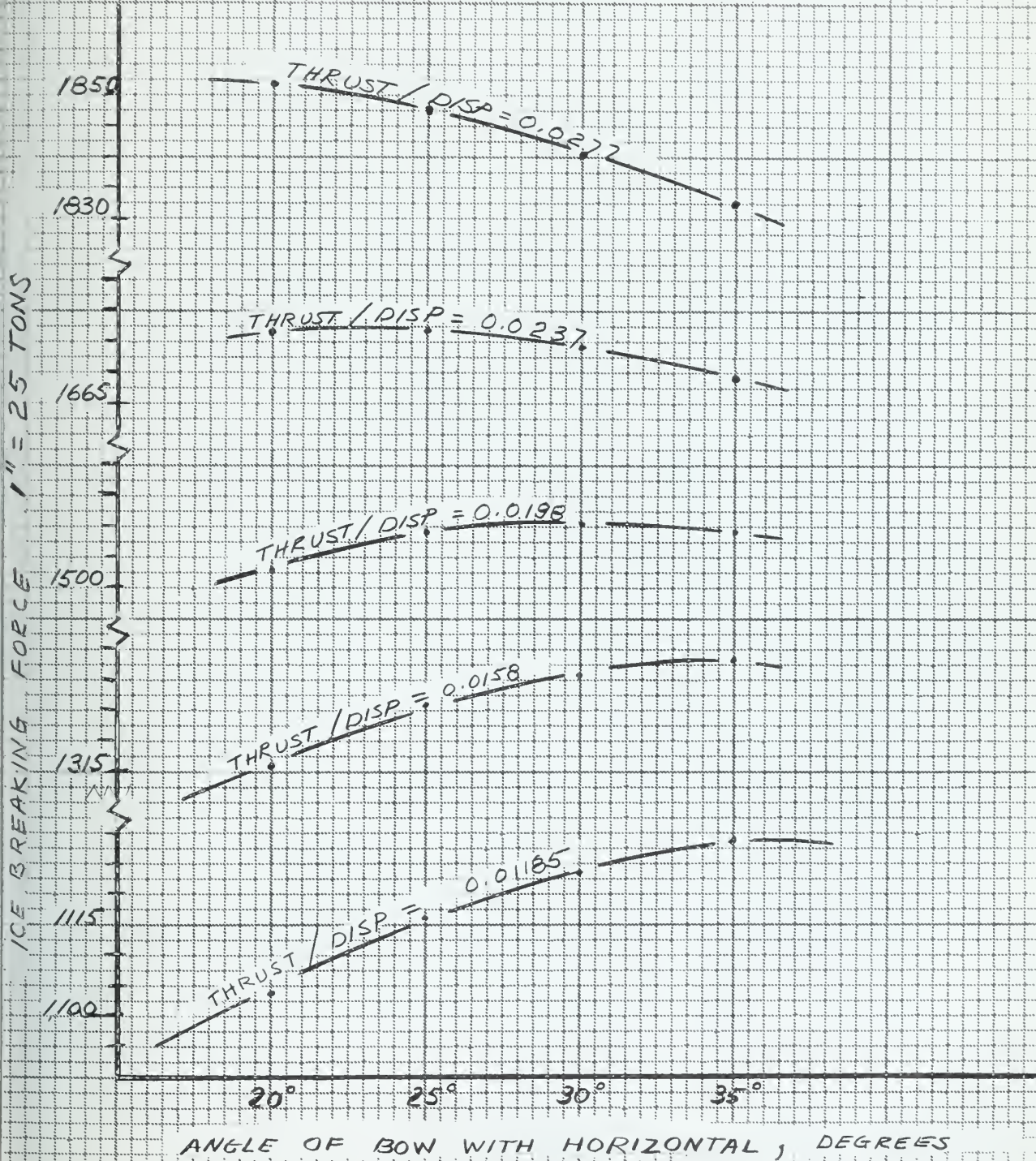
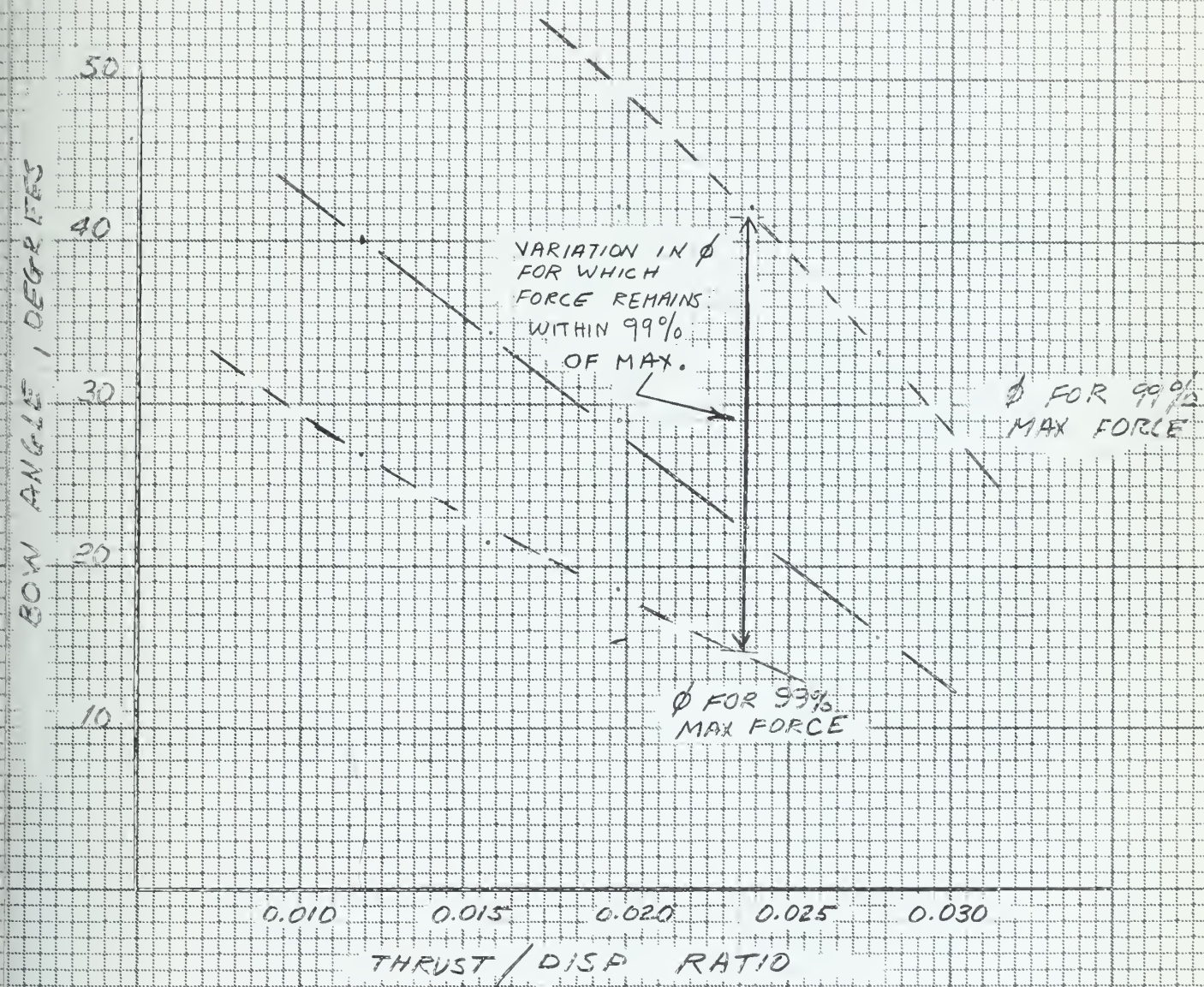


FIGURE III-4
 BOW ANGLE FOR MAXIMUM
 ICE BREAKING FORCE
 VS
 THRUST / DISP RATIO



ICE BREAKING FORCE

VS

THRUST / DISP RATIO
DISP = 8500 T $\phi = 30^\circ$

2000

1800

1600

1400

1200

1000

ICEBREAKING FORCE, TONS

FIGURE III-5

THRUST / DISPLACEMENT

0.010 0.015 0.020 0.025

$C_{WP} = 0.80$
 $LCF = +5.0$

$C_{WP} = 0.70$
 $LCF = -5.0$

FIGURE III-6
 ICEBREAKING FORCE
 VS
 WATER PLANE COEFFICIENT
 $DISP = 8500 \text{ t}$ $\phi = 30^\circ$
 THRUST / DISP RATIO = 0.0158

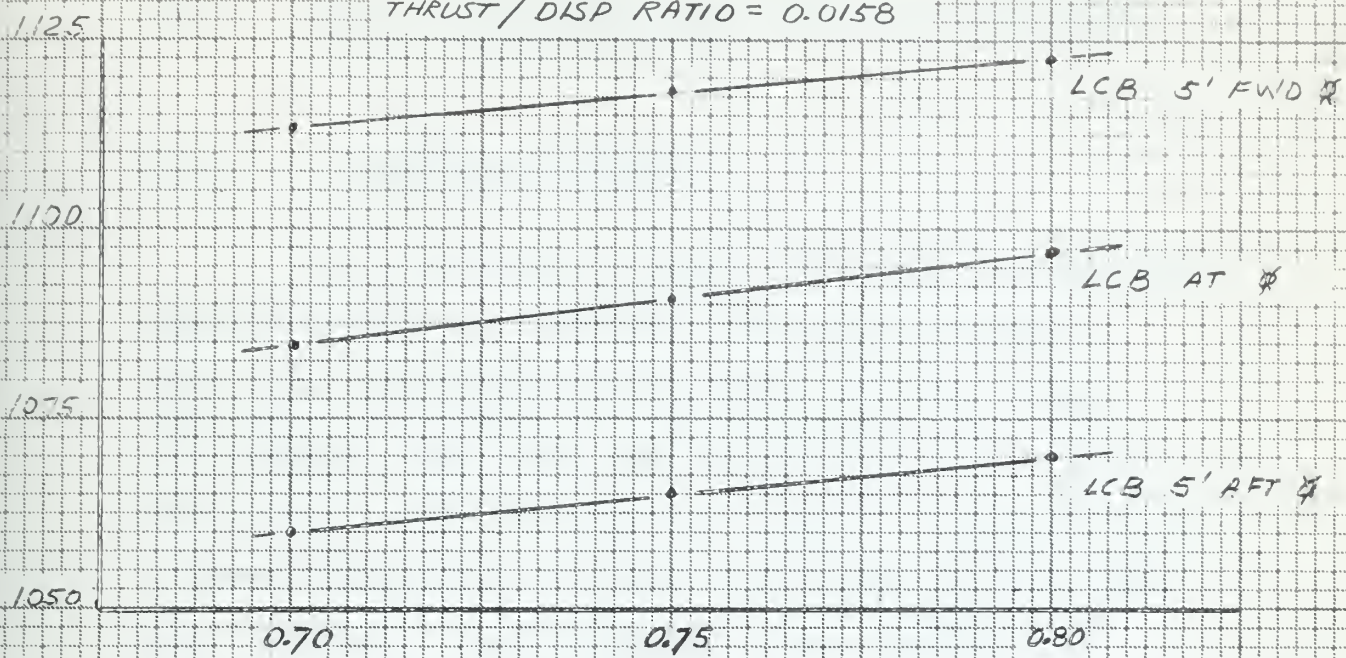
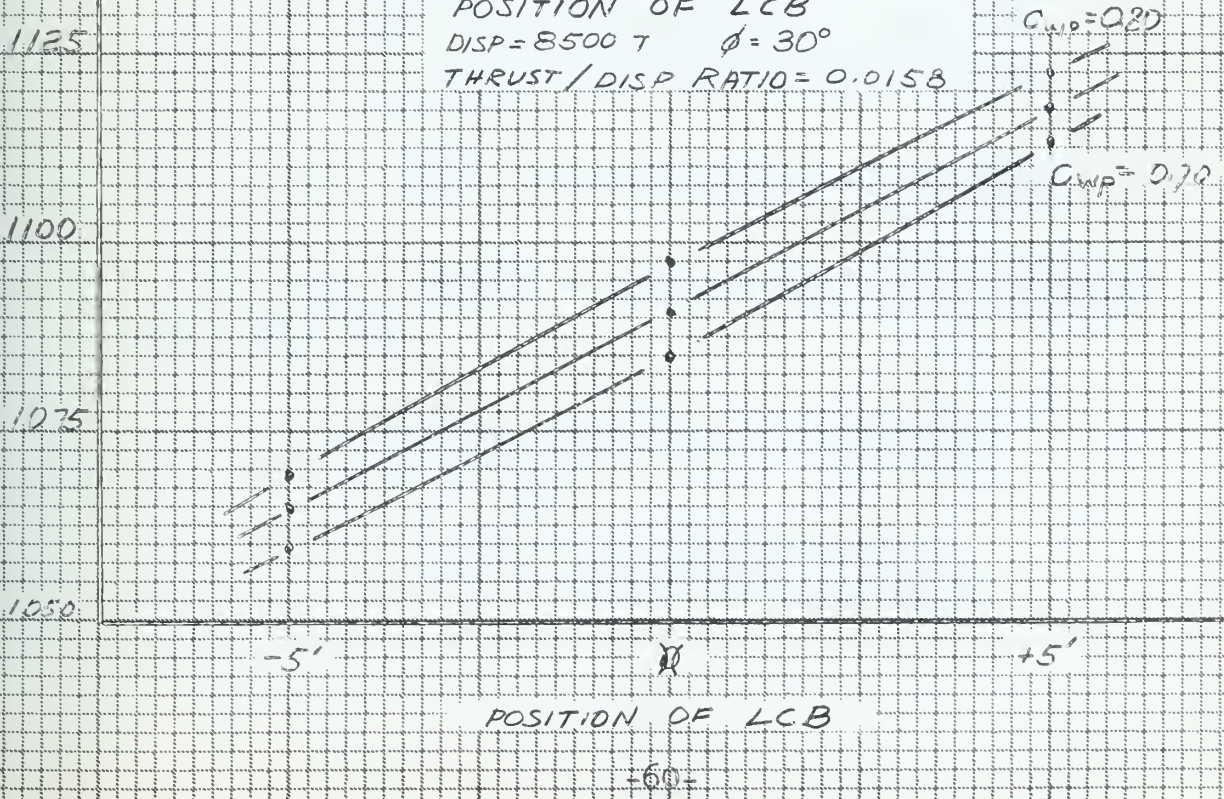


FIGURE III-7
 ICEBREAKING FORCE
 VS
 POSITION OF LCB
 $DISP = 8500 \text{ t}$ $\phi = 30^\circ$
 THRUST / DISP RATIO = 0.0158



III.2. Stern Configuration and Propeller Arrangement, Results and Discussion

III.2.1. Propeller Selection

One of the first things that comes to mind when improved propeller protection and maximum thrust at zero speed are desired is the feasibility of using Kort nozzles. The work done by van Manen (17), (18) and (19) with Kort nozzles was studied. Also an article by Deros Argyriadis on modern tug design (20) was read with interest. The advantages of Kort nozzles for icebreaker application are:

- (1) Increased efficiency at high slip (zero speed condition).
- (2) Smaller diameter propeller required. The optimum diameter in a nozzle is much less than the optimum without a nozzle.
- (3) Propeller is protected by the nozzle.

The disadvantages of a Kort nozzle for icebreaker application are:

- (1) Backing efficiency is less with the nozzles.
- (2) Very small tip clearance is required to attain the increase in

efficiency. The clearance recommended by van Manen is less than one-half inch for a 17' diameter propeller. This is difficult to attain in practice and would be especially difficult on an icebreaker due to the possibility of ice damage. With such smaller clearances it would only take relatively small distortions of the nozzle to completely bind the propeller.

(3) Best results are obtained when the nozzle is kept intact (not made a part of the hull) with a minimum of structural members. This condition would be very difficult to meet with the added strength requirements for icebreaker application. Also with a full ring, as well as with a partial ring, the ice would tend to hang on the nozzle.

Thus it seems that a great deal of advanced design work towards a special application for icebreakers will have to be done before Kort nozzles will see any use on these rugged, heavy duty ships. Therefore standard propellers are used in the design of the parent form.

The EHP was computed by the Froude method. An attempt was first made to use Gertler's reanalysis of

Taylor's data (29). However, icebreaker coefficients do not fall within the range of Taylor's curves and the estimate of EHP obtained was very crude. A much more accurate method was used for the final results. Dr. Jansson, in reference 10, gives curves of Rr/Δ for icebreaker hulls very similar to the proposed design. His data was based on model tests. Using this data C_r was readily computed. C_f was taken from Schoenherr frictional-resistance coefficients given in Gertler's report. A roughness coefficient ΔC_f of .0004 was used. The resulting curve of EHP versus speed is shown in Figure III-8. Details of the EHP calculation are given in Appendix B.

Figures III-9 and III-10 give the results of the calculations used in selecting the propellers. These are based on the design charts of L. Troost (28). The primary objective was to develop maximum thrust at zero speed utilizing full power capabilities. For the centerline propeller data are given for both four and five bladed propellers. Only the four bladed propeller was considered for the wing propellers due to the adverse cavitation effects of the five bladed propeller which has a lower expanded area ratio.

Cavitation is a problem with the heavily loaded propellers of icebreakers; therefore, a rough check

Figure III-8

Speed and power estimates for proposed design

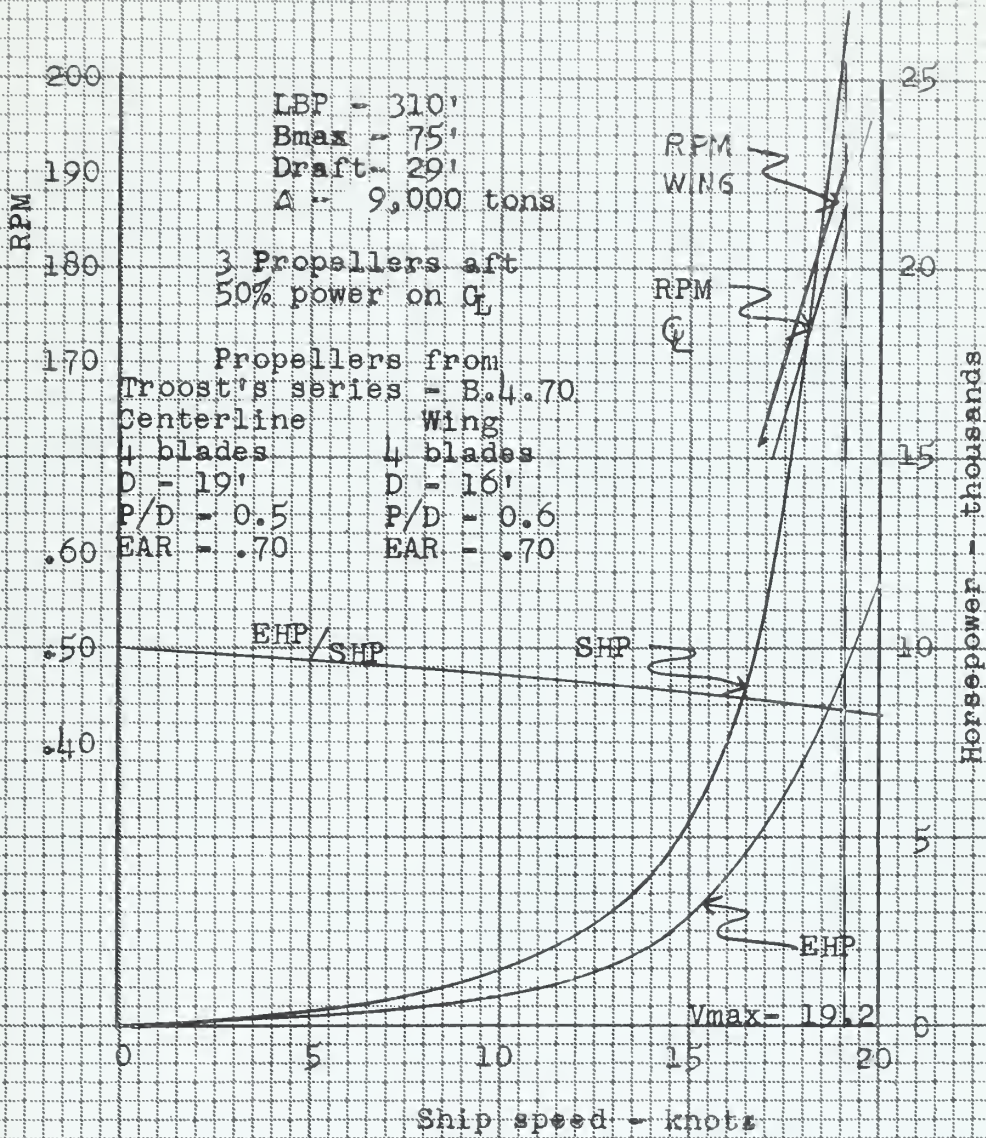
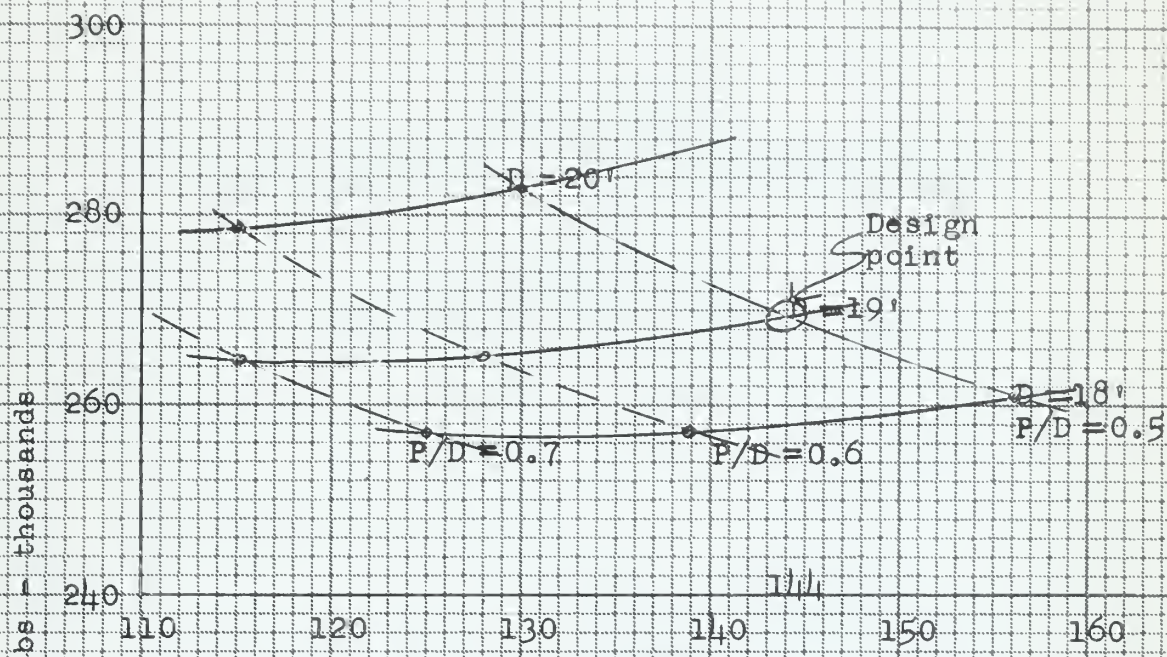


Figure III-9

Thrust versus RPM for 4 and 5 bladed propellers at zero ship speed. Centerline propeller = 12,750 SHP

Troost
M-G series B.4.70
Type B. 4 blades. EAR = 0.70
BTR = .045



Troost
M-G series B.5.60
Type B. 5 blades. EAR = 0.60
BTR = .040

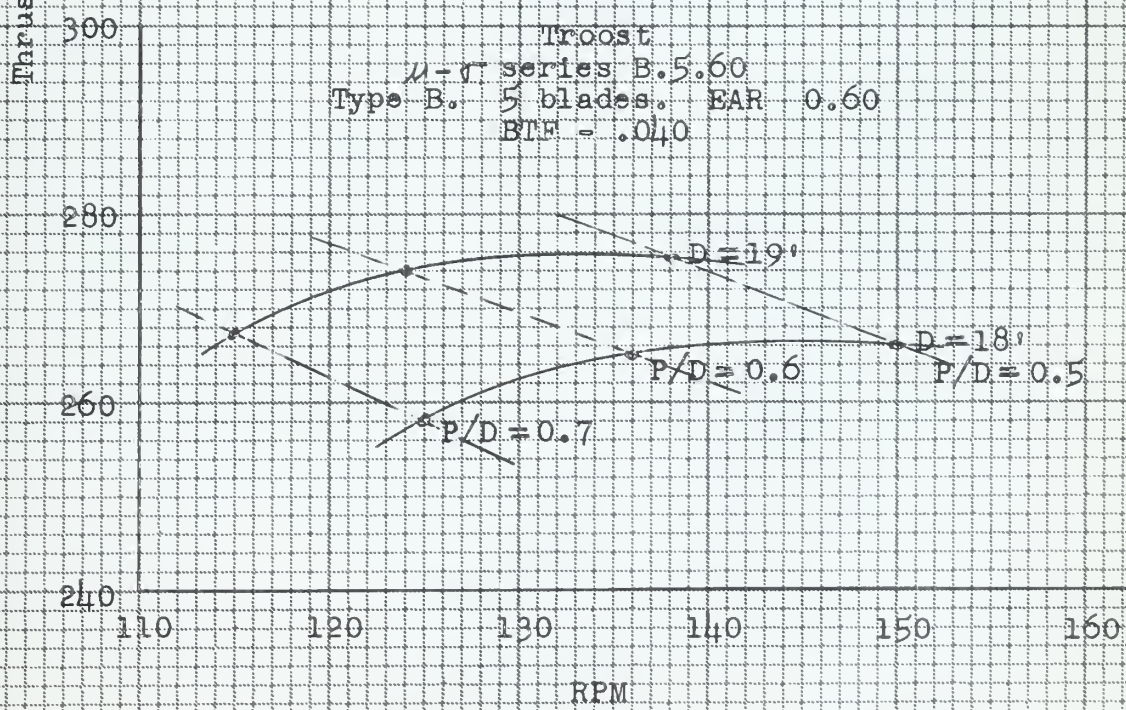
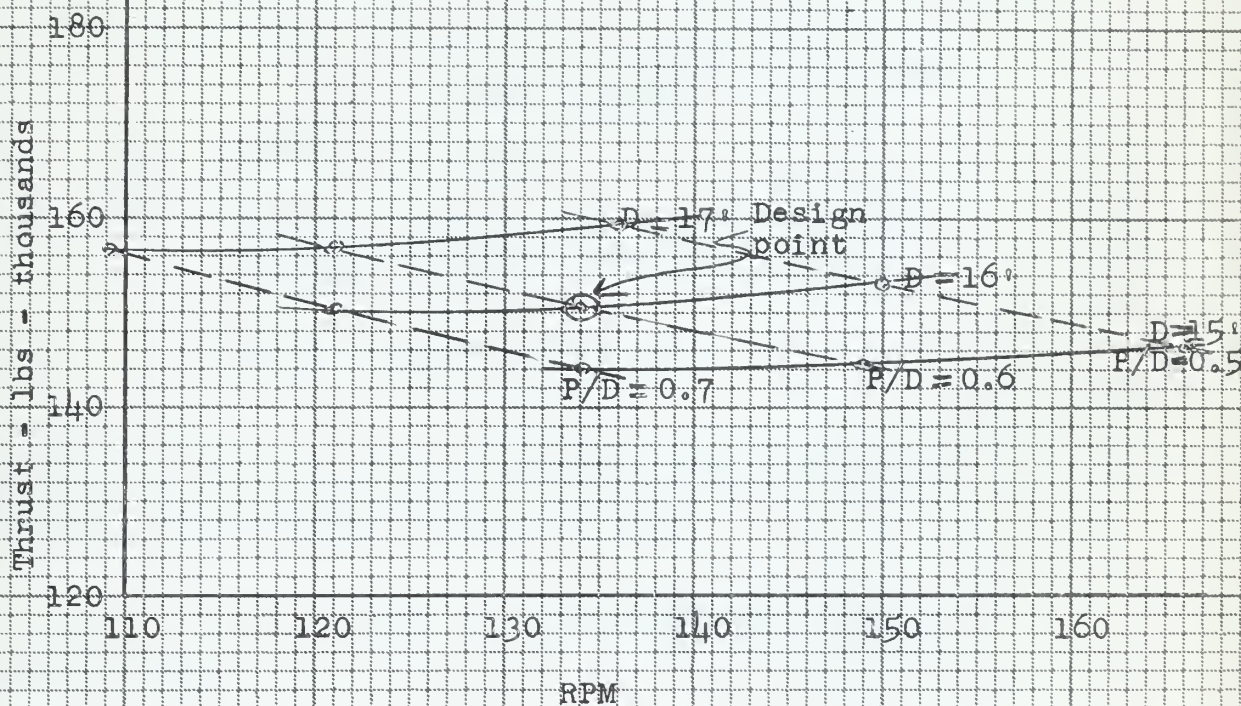


Figure III-10

Thrust versus RPM for 4 bladed propeller at zero ship speed. Wing propellers - 6,375 SHP.

Troost
M-C series B.4.70
Type B. 4 blades. EAR = 0.70
BTF = .045



for cavitation was made. The results of this investigation are shown in Figure III-11. The required projected area to avoid cavitation is based on a formulation given by Troost

$$F_{pr} = \frac{T}{.276 V (P_o - e)^{\frac{1}{2}}} \quad \text{equals the required projected area.}$$

where

T = thrust

$$V = \sqrt{u^2 + V_o^2}$$

$u = .7D \pi n$ = tangential velocity at seven-tenths radius.

V_o = speed of advance.

P_o = static pressure head at $.7R$ with the blade in vertical position at its highest point.

e = vapor pressure of water.

The actual projected area was also taken from an approximate relationship given by Troost

$$F_{Pa} = (1.067 - 0.229 P/D) F_a \quad \text{equals the actual projected area}$$

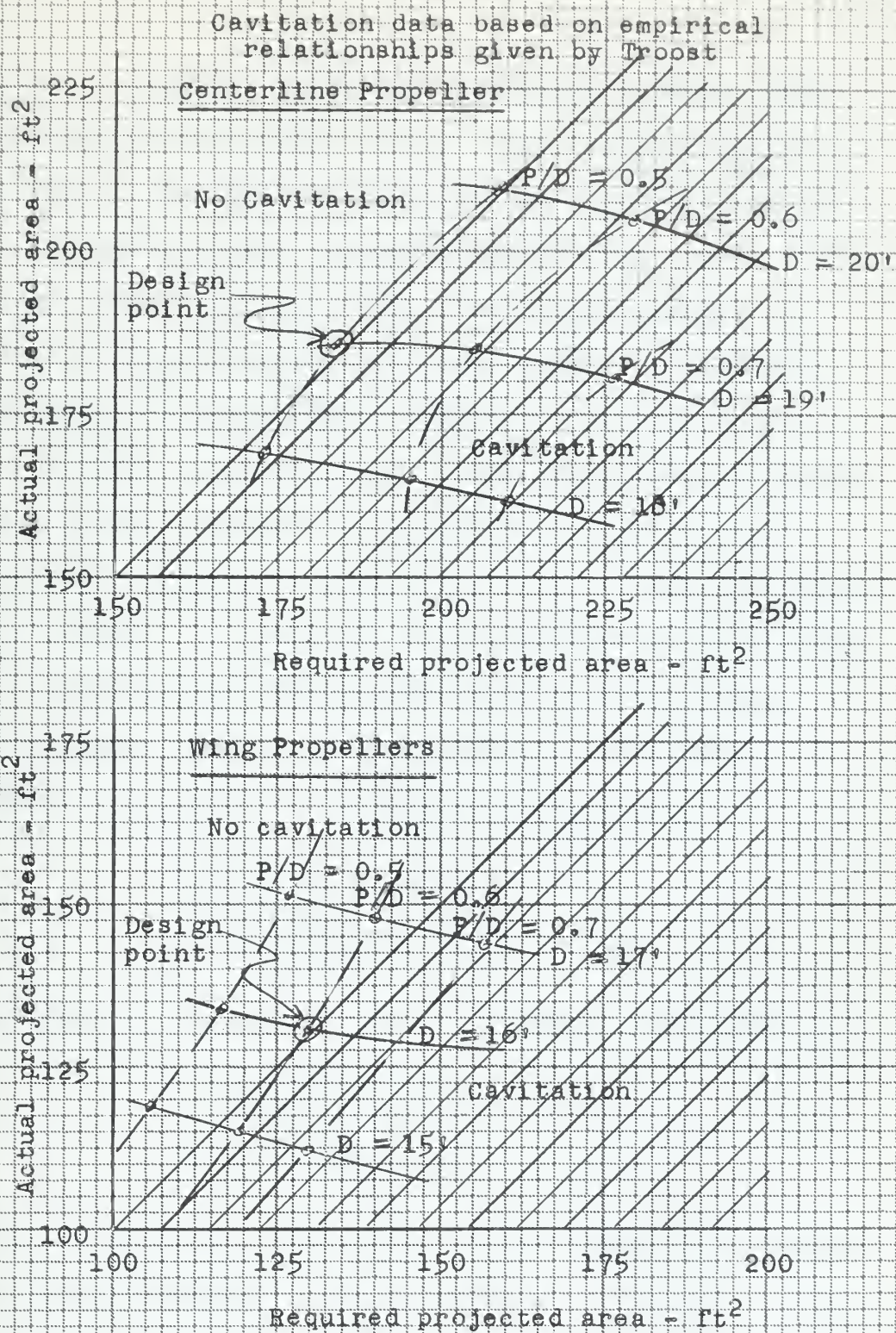
where

P/D = pitch-diameter ratio

$$F_a = \text{expanded area} = \text{EAR} \times \pi D^2 / 4$$

From the curves it is apparent that for a given propeller diameter lowering P/D increases thrust and reduces cavi-

Figure III-17



tation. Likewise increasing propeller diameter with constant P/D increases thrust while reducing cavitation. Therefore, for maximum thrust at zero speed a low P/D is desired with the biggest diameter than can be fitted on the ship consistent with other requirements. In order to take advantage of large diameter propellers the draft of the proposed design was increased to 29'. The maximum diameter of the centerline propeller which would leave adequate tip clearance was set at 19'. From the cavitation criteria a P/D of 0.5 was the maximum allowed. A lower P/D is not desired as decreasing P/D decreases propeller efficiency at free running conditions. Thus the design point as indicated in Figure III-9 for the centerline propeller is

Propeller diameter -- 19'

Pitch-diameter ratio -- 0.5

For the wing propeller based on similar considerations

Propeller diameter -- 16'

Pitch-diameter ratio -- 0.6

Using these propellers free running speeds were computed by standard methods using Troost's μ - σ charts. Figure III-8 also gives the curve of speed versus SHP and an estimate of the propulsive coefficient EHP/SHP. Values

used for the wake fraction w and thrust deduction coefficient t were as follows:

For the centerline propeller

$$t = .20$$

$$w = .20$$

For the wing propellers

$$t = .25$$

$$w = .14$$

The values for the wing propellers were based on model test data on twin screwed hulls presented by Dr. Jansson (10) and should be fairly accurate. No such data was available to use in estimating values for the centerline propeller. Data from single screw ships is not directly applicable as the centerline screw, in this case, is working partially in the wake of the wing screws. The values selected are nothing more than reasonable guesses. Relative rotative efficiency e_r and mechanical shafting efficiency e_m were taken as 1.025 and .97 respectively. The same values were used for all propellers.

Full power was developed at 19.2 knots. The propeller efficiencies at this speed were .42 for the centerline propeller and .47 for the wing propellers. These are low due to the low pitch diameter ratios selected. The

propulsive efficiency EHP/SHP at a maximum speed of 19.2 knots is estimated at .43. However, it is not felt that this speed has any real significance. Only under very unusual circumstances "should" the ship be run at this speed. A much more economical speed of 14 knots requires only 4000 SHP. The power capabilities of the ship were based on thrust at zero speed, not on a high free running speed. At lower speeds the propulsive efficiency will improve slightly as shown.

Before concluding this section a few more words about cavitation are in order. One might gather from looking at Figure III-11 that the authors feel they will not have any cavitation if the selected propellers are used. This is not true. In the first place ice-breaker propellers are made considerably thicker for added strength than the propellers used in making propeller design charts. In modern circulation theory of propeller design the effect of thickness on the pressure coefficient $\Delta P/q$ is clearly shown.

$$\Delta P/q = (v/V)^2 - 1 = \frac{P_o - P_{local}}{1/2 \rho V^2}$$

where

V = free stream velocity

v = local velocity on the blade

P_o = free stream pressure

In using this theory v/V is made up of three distinct parts; that due to camber, that due to angle of attack, and that due to thickness. The part due to thickness is an order of magnitude larger than the other two parts. Therefore a small increase in thickness can cause a significant increase in $\Delta P/q$. Of course the higher $\Delta P/q$ the harder it becomes to avoid cavitation.

It must also be pointed out that the cavitation criterion of Troost is based on data from typical merchant ships. Therefore its applicability to ice-breaker propellers may be questioned. In general it is very difficult, and probably not too wise, to make any definite statements about the possibilities of having cavitation in a given problem without testing the propellers in question in a propeller tunnel. The results shown in Figure III-11 are, nevertheless, quite interesting in that they do show general trends.

Nothing has been said about propeller materials, although this is certainly an important aspect of the problem. The metallurgy of propeller materials and current usage is covered quite well by Admiral Thiele in reference 6. The original purpose of the authors was only to arrive at reasonable diameters to use in conjunction with the stern design. But the results were of enough interest that it was decided to include

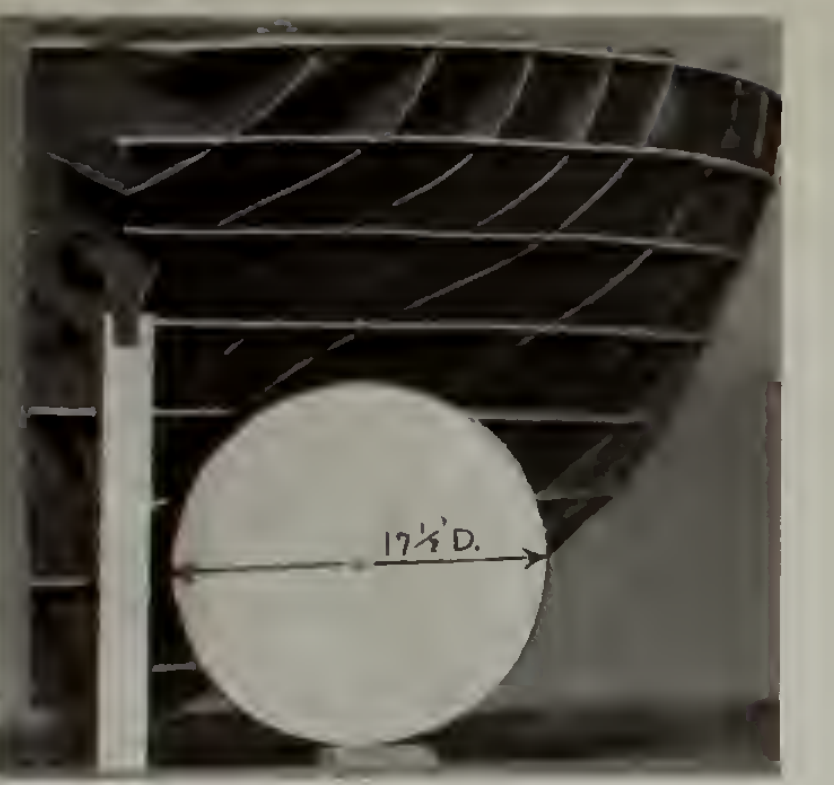
them. The one conclusion that can be drawn from this study is that controllable pitch propellers are certainly desirable. As already mentioned, at 100% slip lowering the pitch diameter ratio reduces cavitation while increasing thrust. Therefore, a low P/D is definitely called for. On the other hand at free running speeds the propeller efficiency falls off rapidly as P/D is lowered. A compromise is required unless controllable pitch propellers could be used, but the severe conditions under which the propellers operate are enough to make a designer shudder. However, only two settings are needed, one for free running, and one for working the ice. This would considerably reduce the control mechanisms involved. Looked at in this light there may be some hope yet for the application of controllable pitch propellers to icebreakers.

III.2.2. Stern Configurations

Three different views of three of the four models constructed are shown on Plate III-1. The other model served its purpose as a conceptual aid in arriving at the final parent form, but there did not seem to be any advantage in its presentation here. Table III-1 gives the offsets of the proposed parent form.

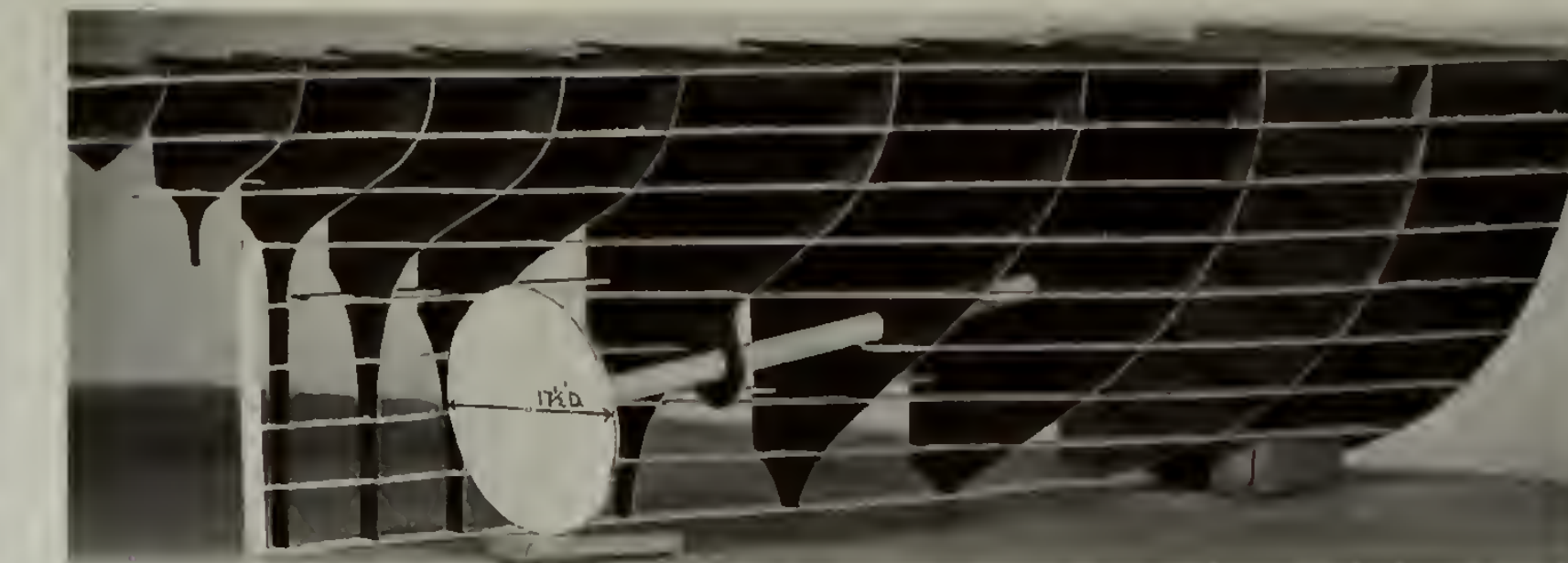
The lines of all models were based on 20 stations numbered from forward aft. In accordance with U.S. Navy practice the after perpendicular for the GLACIER and the proposed parent is at the design waterline. The after perpendicular for the MACDONALD is at the centerline of the rudder post. The scale used was $\frac{1}{4}'' = 1'$. The forward station of the models of the GLACIER and the proposed parent is station 13. The forward station of the model of the MACDONALD is station 14. This is due to the difference in the location of the after perpendicular. In all cases the design waterline is the second waterline from the top. Other data for the models is given in Figure III-12.

Offsets for the lines of the MACDONALD were taken from a very small scale drawing presented in reference (2). Thus a good deal of fairing was required and the final lines as used to construct the model undoubtedly are not

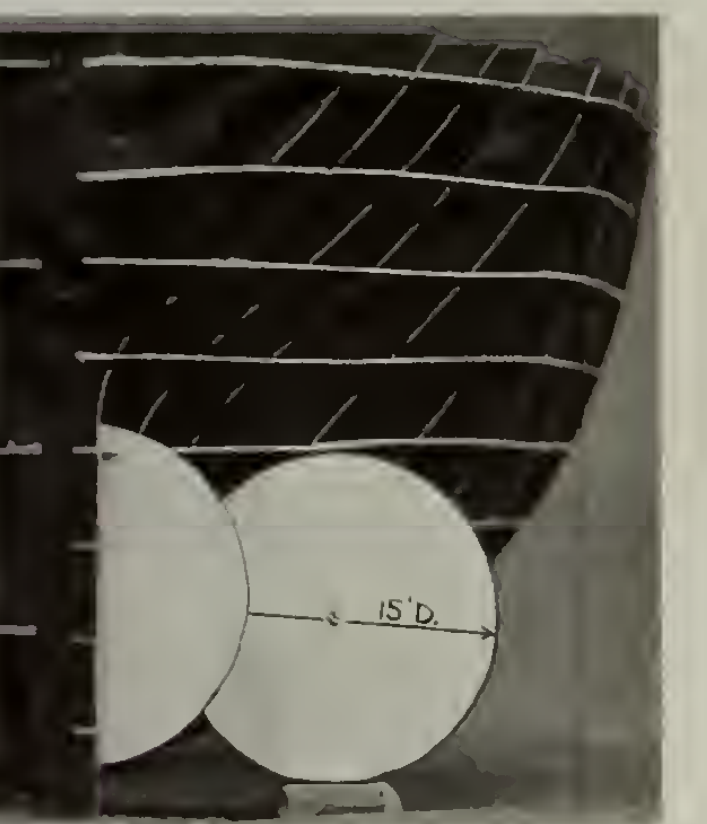


GLACIER

LBP ----- 290'
BEAM, MAX. ----- 74'
DRAFT, MAX. ----- 28'
DISP., TONS, MAX. ----- 8,640
SHP ----- 21,000
L/B ----- 4.0
SHP/DISP. ----- 2.43
TWIN SCREW
THRUST, ZERO SPEED, ----- 195 TONS
SPEED, OPEN WATER ----- 19 KNOTS

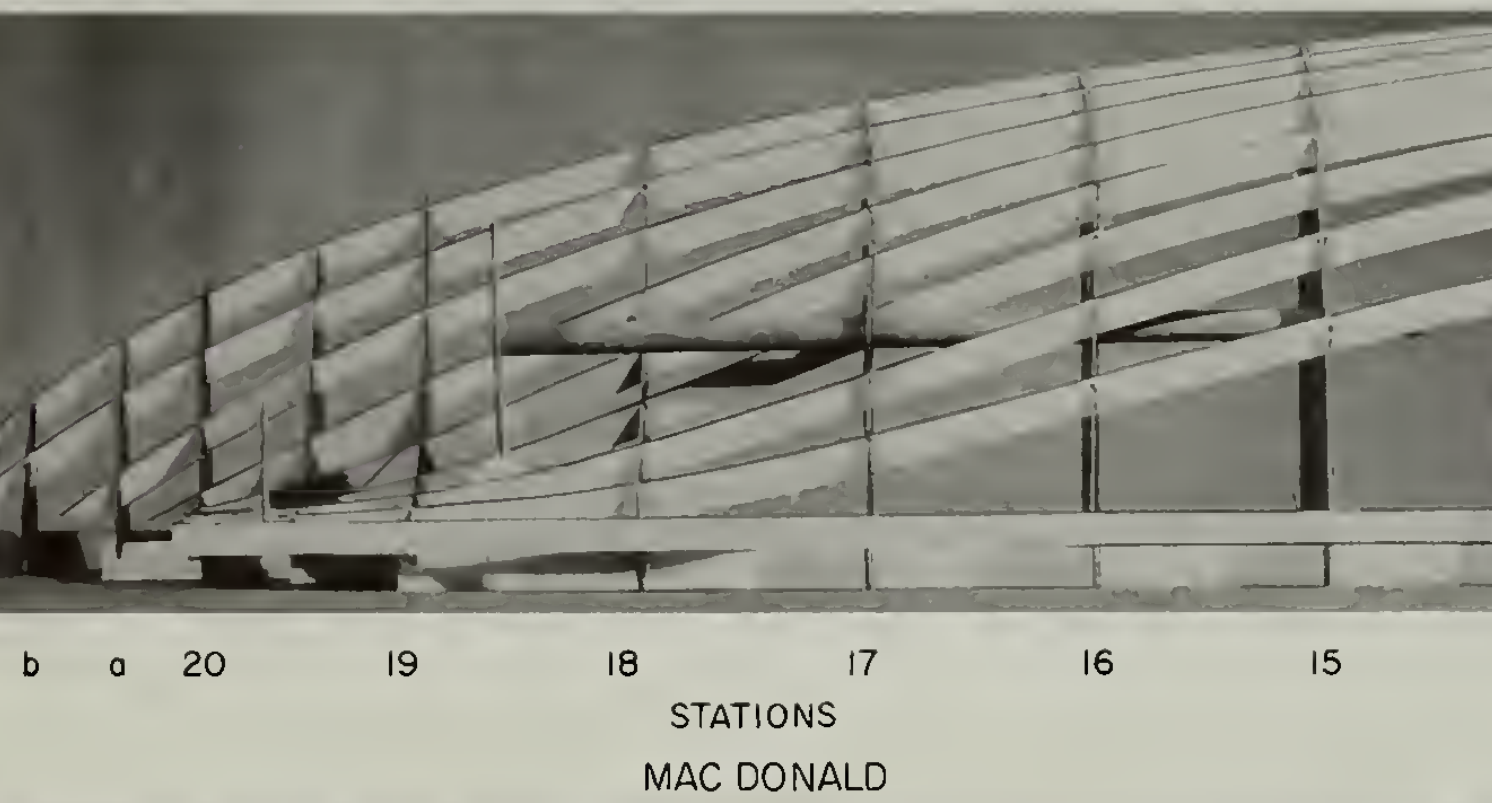


GLACIER

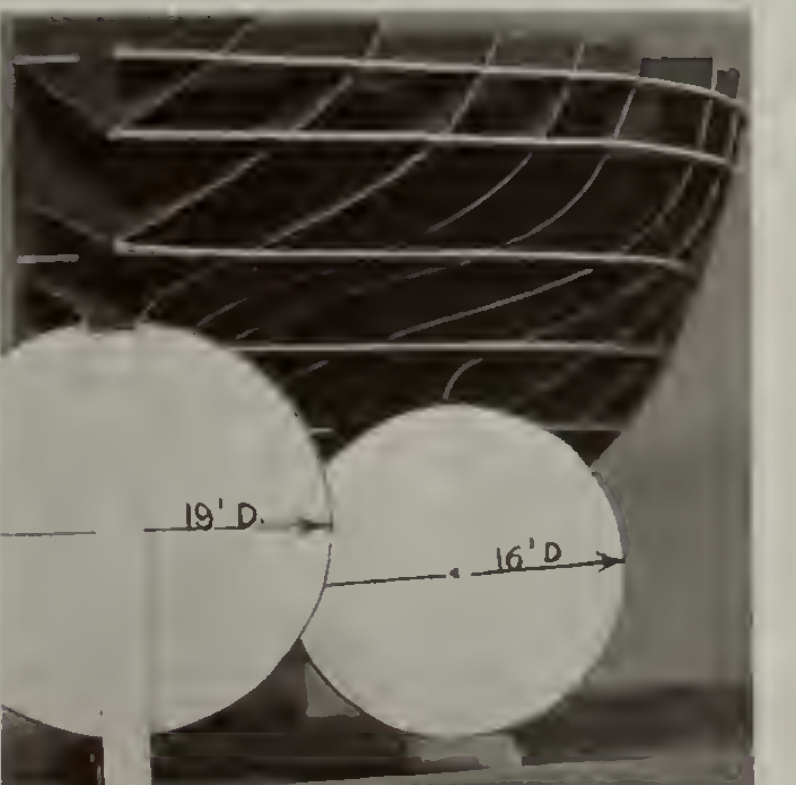


JOHN A. MAC DONALD

LBP ----- 290'
BEAM, MAX. ----- 75'
DRAFT, MAX. ----- 28'
DISP., TONS, MAX. ----- 8,974
SHP ----- 15,000
L/B ----- 4.6
SHP/DISP. ----- 1.67
TRIPLE SCREW (1-1-1)
THRUST, ZERO SPEED, -----
SPEED, OPEN WATER ----- 16.5 KNOTS

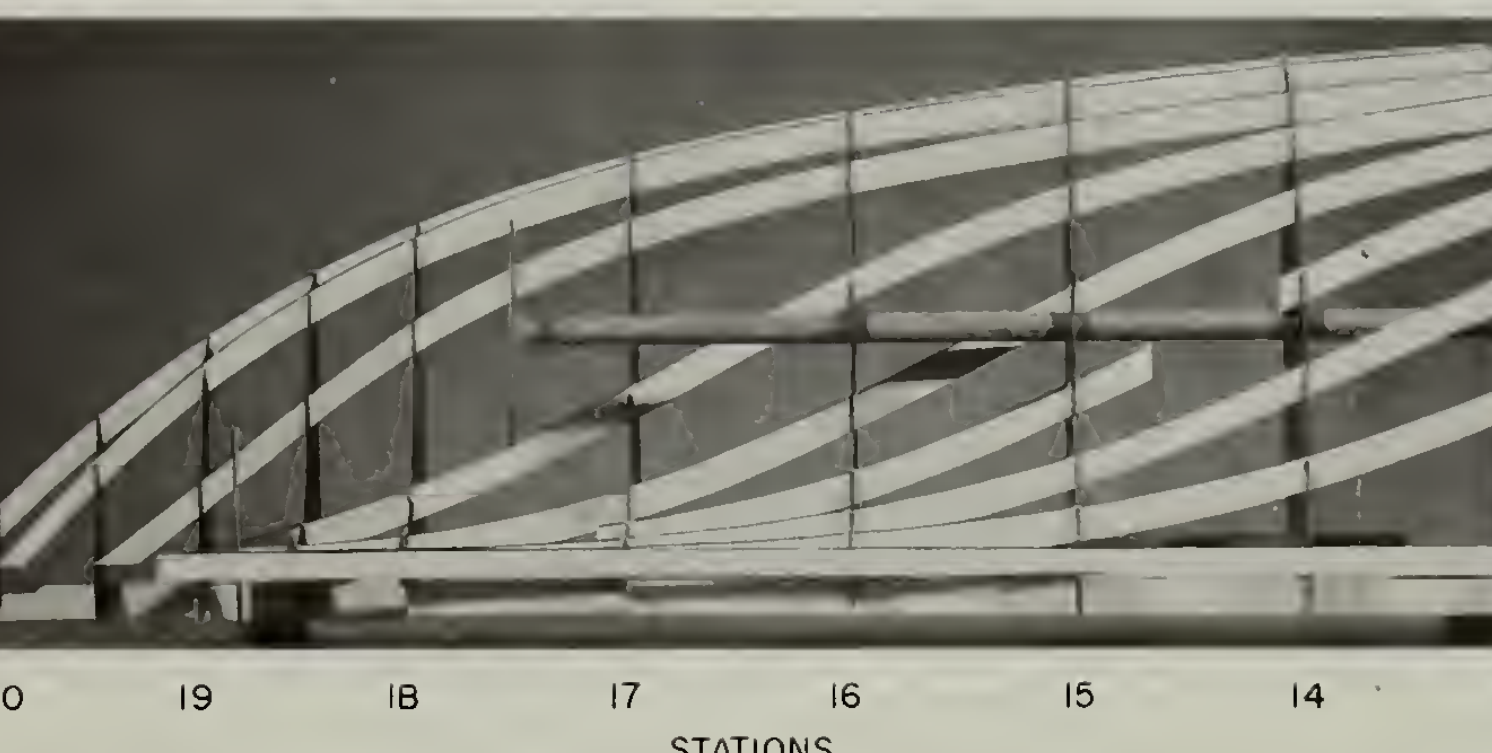


MAC DONALD



PROPOSED PARENT FORM

LBP ----- 310'
BEAM, MAX. ----- 75'
DRAFT, MAX. ----- 29'
DISP., TONS, MAX. ----- 9,000
SHP ----- 25,500
L/B ----- 4.2
SHP/DISP. ----- 2.84
TRIPLE SCREW (1-2-1)
THRUST, ZERO SPEED ----- 254 TONS
SPEED, OPEN WATER ----- 19.2 KNOTS



PROPOSED PARENT

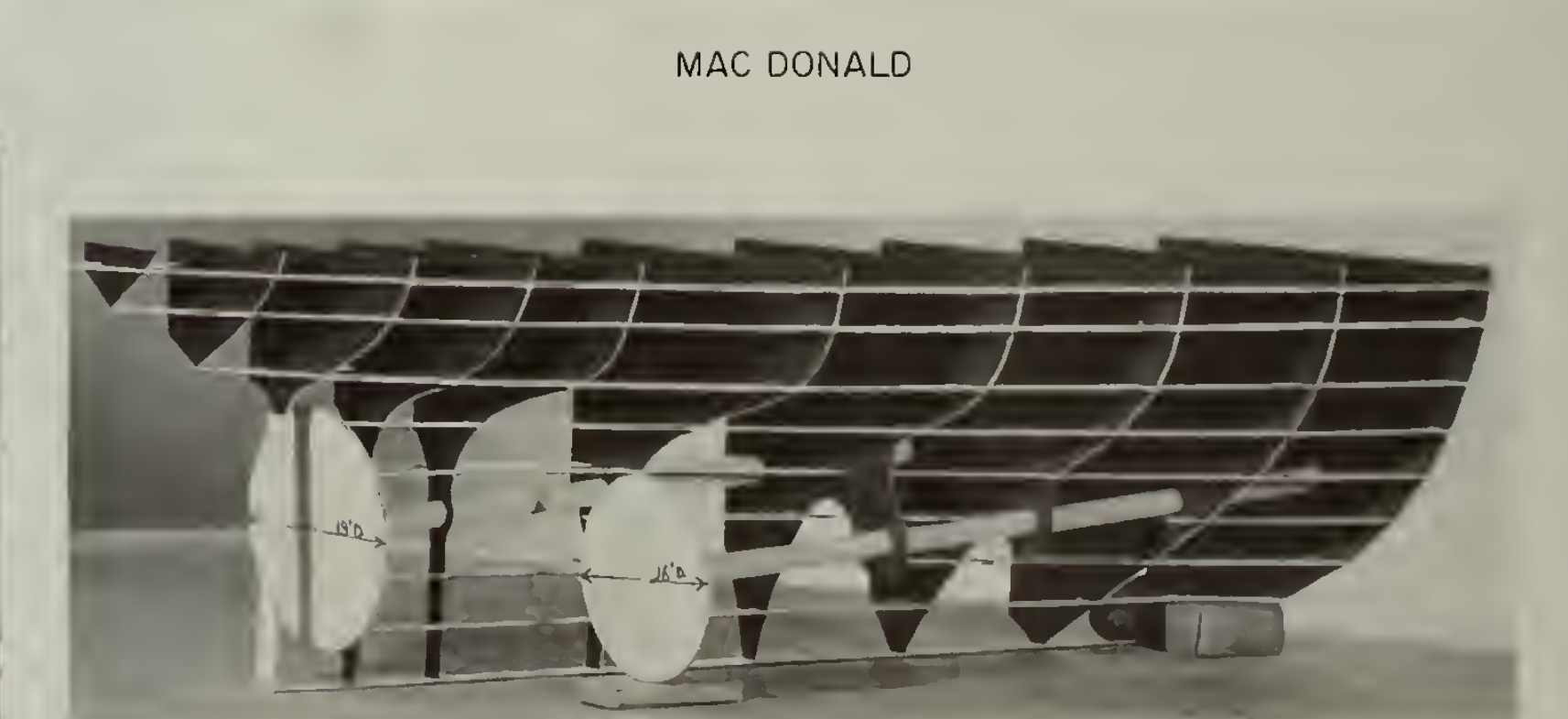


TABLE III-1

Table of Offsets for the Proposed Stern

Waterline Half Breadths

Station	2	4	8	12	16	20	24	28	32
10	19'-11"	23'-11"	28'-4"	31'-2"	33'-1"	34'-7 $\frac{1}{2}$ "	35'-10"	36'-9"	37'-4"
11	19'-11"	23'-11"	28'-4"	31'-2"	33'-1"	34'-5 $\frac{1}{2}$ "	35'-11"	36'-7"	36'-7"
12	12'-7"	18'-6"	25'-1"	29'-1"	31'-8"	33'-5"	34'-11"	35'-11"	34'-10"
13	7'-2 $\frac{1}{2}$ "	13'-7"	20'-0"	25'-7"	29'-8 $\frac{1}{2}$ "	32'-5"	34'-11"	31'-11"	31'-11"
14	4'-0"	7'-2 $\frac{1}{2}$ "	13'-7"	20'-0"	25'-7"	20'-1 $\frac{1}{2}$ "	28'-1 $\frac{1}{2}$ "	30'-10"	31'-10"
15	1'-5"	2'-2 $\frac{1}{2}$ "	3'-7"	6'-4"	11'-1 $\frac{1}{2}$ "	12'-1"	24'-1 $\frac{1}{2}$ "	27'-11"	29'-2"
16	1'-0"	1'-1 $\frac{1}{2}$ "	2'-7 $\frac{1}{2}$ "	2'-8"	5'-1"	12'-1"	24'-1 $\frac{1}{2}$ "	27'-11"	29'-2"
17	1'-0"	1'-0"	1'-0"	1'-0"	1'-2"	8'-2"	21'-1"	25'-9"	27'-1"
18	1'-0"	1'-0"	1'-0"	1'-0"	1'-0"	1'-9"	5'-2"	17'-2"	24'-5"
19	1'-0"	1'-0"	1'-0"	1'-0"	1'-0"	1'-2"	2'-9"	11'-10"	18'-8"
AP	0	0	0	0	0	1'-0"	1'-0"	5'-9"	13'-4"
	0	0	0	0	0	0	0	6'-4"	16'-6"
						0	0	0	10'-11"
							0	0	4'-3"

Buttock Heights

Station	4	8	16	24
10	0'-2"	0'-3"	0'-11"	4'-0"
11	0'-5"	1'-0"	3'-0"	7'-1"
12	1'-11"	4'-6"	9'-5"	14'-9"
13	8'-10"	11'-8"	18'-5"	21'-7"
14	14'-7"	18'-2"	21'-2"	23'-11"
15	17'-7 $\frac{1}{2}$ "	18'-11"	22'-5"	25'-9"
16	18'-1 $\frac{1}{2}$ "	21'-4"	23'-7"	30'-6"
17	19'-1 $\frac{1}{2}$ "	22'-10"	25'-10"	30'-10"
18	19'-1 $\frac{1}{2}$ "	22'-10"	25'-10"	30'-10"
19	23'-1 $\frac{1}{2}$ "	29'-2"	30'-10"	30'-10"
AP	26'-6"			

the exact lines of this ship. Also as noted previously the propeller diameters and locations of propellers of the MACDONALD are only estimates. This is of little consequence as the model was used only as an aid in arriving at the final design. The model of the GLACIER is a true replica.

The three models provide a good contrast of the different stern configurations which are possible. All three models are of ships of approximately the same displacement. The installed SHP does vary considerably which naturally must influence the design. The high SHP of the proposed design lends added weight to the advantages of using three propellers, although it is not a necessary condition.

Data on triple screw vessels of any kind is very scarce. The German navy has built triple screw warships from time to time, more so than any other navy, but due to their very nature nothing has been published about them. The major source of information on triple screw icebreakers is Russia. Nothing more need be said about obtaining information from this source. It is just not available. The United Nations paper on the LENIN (41) is a notable exception to this. The LENIN has the same type of triple screw and power arrangement as proposed by the authors. The paper gives a fairly good discussion

of the machinery and reactor, but says nothing of the hull design. The one other source of information on the triple screw was the Canadian icebreaker JOHN A. MACDONALD, which is why this design was chosen for one of the models.

The avowed purpose of this study was to seek better propeller protection. This concept must be kept in mind. Improved propulsive efficiency was not sought. It was for this reason that resistance and self-propulsion tests were not considered from the very beginning of the project. Before tests can be made, a model or models suitable for the tests must be built. Before a model is built it must be designed. Before it is designed a thorough study must be made of the why, how, and what for's of the design. An attempt was made to do the latter two.

There is some general agreement on the conditions under which propeller damage occurs. These are:

- (1) Propeller blade nicking into a large mass of ice. The worst condition for this is when the ship is swinging.
- (2) Blocks of ice passing under the ship and wedging between the propeller blades and the hull.
- (3) Backing in ice.

The first condition can be avoided by a large amount of overhang. The second condition requires large tip clearances. These are contradictory on both twin screw and triple screw designs. Tip clearance can be increased by moving the propellers outboard. This reduces the overhang. If twin screws were used on the proposed design, both tip clearance and overhang could be quite large. The overhang is measured from the operating waterline, which, as previously stated, is the next to last waterline on the models. With twin screws on the proposed design the tip clearance and overhang would both be better than three feet. On the GLACIER the tip clearance is eleven inches, while the overhang is about three feet. On the MACDONALD the conditions are worse. The tip clearance is about a foot and the overhang is nil or a little on the minus side. The lines of the MACDONALD are very nice to look at, but they do not seem to reflect the requirements of good propeller protection. Again it must be repeated that the model shown in Plate III-1 may not be a true replica of the MACDONALD. It is the lines of the model which are being referred to.

The above comparison supposes twin screws on the proposed design. With triple screws the comparison is not quite as good, although still favorable. The more the overhang is increased by moving the wing propeller

inboard the more overlap there is with the centerline propeller. This will tend to cause a strong wake variation on the latter due to propeller wash, which is conducive to vibration and low efficiency. To avoid overlap as much as possible the overhang was decreased to a minimum of about a foot and a half. This increased the tip clearance to four and a half feet. The overlap is still less than that of the MACDONALD. This condition is one that must be accepted with a triple screw arrangement. In personal correspondence with Mr. German, concerning the MACDONALD, he noted that "fuel economy is slightly better with triple screw design for cruising speed than twin. This may not always be the case but was apparently the case for the JOHN A. MACDONALD. This opinion is based upon estimates, as model tests were not run for twin screw version." Thus if his estimates are accepted the adverse effect of the overlap is not too great.

The favorable tip clearance of the proposed design was brought about by making the stern broader and much shallower. Also the draft is a foot more than for the other two models. A direct result of a broad, shallow stern with a deep draft is a large skeg. This adds frictional resistance, but has two beneficial effects; first, it will tend to give the ship improved directional stability. This is desirable due to the low length beam

ratio. Second, it will act as a roll damper, helping to stabilize the ship in roll.

Other advantages of the proposed stern configuration are:

- (1) Larger, more efficient propellers can be used.
- (2) The large centerline propeller directly ahead of the rudder improves steering qualities at low speeds.
- (3) The wing propellers are twelve and a half feet below the design waterline compared to ten feet for the GLACIER. This will considerably reduce the liability to damage when backing in ice. The centerline propeller is only eight feet below the design waterline, but is well protected by the rudder and stern post.
- (4) By its very nature a triple screw arrangement reduces the possibility of disabling propeller damage.

Some of the possible disadvantages of the proposed design, other than the two already mentioned of increased skeg resistance and strong wake variation on the centerline propeller are:

(1) The flatter, broader stern might tend to cause heavy ice chunks, rolled under in the ice breaking process, to flow aft into the propellers, rather than to rise to the surface. It is believed that this tendency will be partially counteracted by the fuller midship section used, which will force the ice out away from the propellers. In the final analysis this will have to be determined by model tests using model "ice"; or by those little fellows used in fluid analysis, known generally as Maxwell's demons, who ride along on a chunk of the streamline. It is very difficult to observe the action of the ice under the hull in actual ice breaking operations.

(2) The wing propellers require long shafting runs external to the hull. This is partially offset by the increased flexibility of the machinery arrangement for the triple screw design. Also for equal total horsepower smaller shafting and bearing sizes can be used than for twin screw design.

Since the purpose of this part of the study was to design a parent form, it is proper that mention be made of variations in the design which should be considered. Some of these are:

- (1) The effect of variations in fullness of the midship section in deflecting the ice away from the propellers.
- (2) The effect on propulsive efficiency of moving the wing propellers inboard, thereby increasing the overhang.
- (3) The effect on propulsive efficiency of moving the wing propellers longitudinally to change the wash into, or wake fraction of, the centerline propeller.
- (4) The effect on propulsive efficiency of using smaller diameter wing propellers. This reduces the efficiency of the wing propeller, but this may be more than offset by the increase in efficiency of the centerline propeller due to a higher wake fraction. The latter being due to less wash effect. Smaller wing propellers would increase both the overhang and the tip clearance.

The last three items listed all have to do with propulsive efficiency. It has been previously stated that increased efficiency was not sought. Thus, there would seem to be a contradiction. This is not really so. Even though improved propeller protection was the goal, propulsive efficiency cannot be ignored. It is possible that changes in the location of the wing propellers will not have a significant effect on efficiency. This will have to be checked by tests, but if it is so, then the location should be such that it will provide optimum protection. Even if it is not so any compromise should favor increased protection.

There will be other variations, the effect of which will have to be tested. Many of these will arise during the course of model tests. However, it is concluded that the stern configuration proposed offers many distinct advantages, which outweigh the disadvantages. A triple screw arrangement with 50 percent of the power on the centerline screw should be given strong consideration in any future polar icebreaker designs.

III.3 Nuclear Propulsion, Results and Discussion

III.3.1 Reactors

Four power plants emerged from these calculations. They are identified as follows:

PWR No. 1 is a pressurized water reactor of the type in current operation. The coolant operating pressure is 2000 psia. The bulk temperature of the coolant leaving the reactor is 100° below the saturation temperature and there is a safety factor of about 9 on burnout heat flux. The secondary steam cycle operates on 600 psia saturated steam.

PWR No. 2 is a pressurized water reactor of the "advanced" type. There are no PWR's of this kind now operating. The main departures are first, a safety factor of only 2.3 on burnout heat flux, and second, the allowing of local subcooled boiling. There is no net boiling in any channel. The secondary steam is identical to that of PWR No. 1. Advantage is taken of the higher coolant temperatures to increase the log mean temperature difference in the steam generators. This results in smaller and cheaper

steam generators. Because of the higher power density, the reactor of PWR No. 2 is smaller and cheaper than that of PWR No. 1.

PWR No. 2' is a pressurized water reactor with the same safety factors and limitations of PWR No. 2. In this case, however, the higher coolant temperature was used to increase the secondary steam temperature and pressure. The secondary loop remained saturated but at 900 psia. This resulted in improved thermal efficiency and less power was required from the reactor. The reactor was therefore reduced in size from that of PWR No. 2.

GCR is a helium cooled reactor operating in a closed cycle with gas turbines for power production. The basic limitation on the reactor is the specification of the maximum wall temperature allowable. Gas cooled power reactors are in operation in England but differ from this GCR in three ways. First, the Calder Hall reactors are very large natural uranium reactors. Second, the maximum coolant tem-

perature is around 650°F. Third, at Calder Hall, the hot gas is used to produce steam for a conventional steam turbine power cycle. Another deviation of this design is the power cycle itself. To date there has been no closed cycle gas turbine power plant operated on any appreciable scale.

Table III-2 summarizes the pertinent technical data derived for the four designs. Figures III-12 through III-15 illustrate possible core arrangements for each of the designs. In the development of the PWR reactor designs, the critical restriction turned out to be that on the burnout heat flux safety factor. Figure III-17 is a plot of the preliminary calculations made. The abscissa is the number of fuel rods, which is roughly proportional to the core cross sectional area. The number obtained from this curve for a particular desired safety factor was slightly modified so the fuel rods and elements could be properly accommodated in a core lattice.

The GCR design was of course limited by the maximum wall temperature restriction. Preliminary calculations developed the variation of maximum wall temperature with number of elements as shown in Figure III-16. The actual number was again modified to physically fit the elements into a cylindrical core.

TABLE III-2

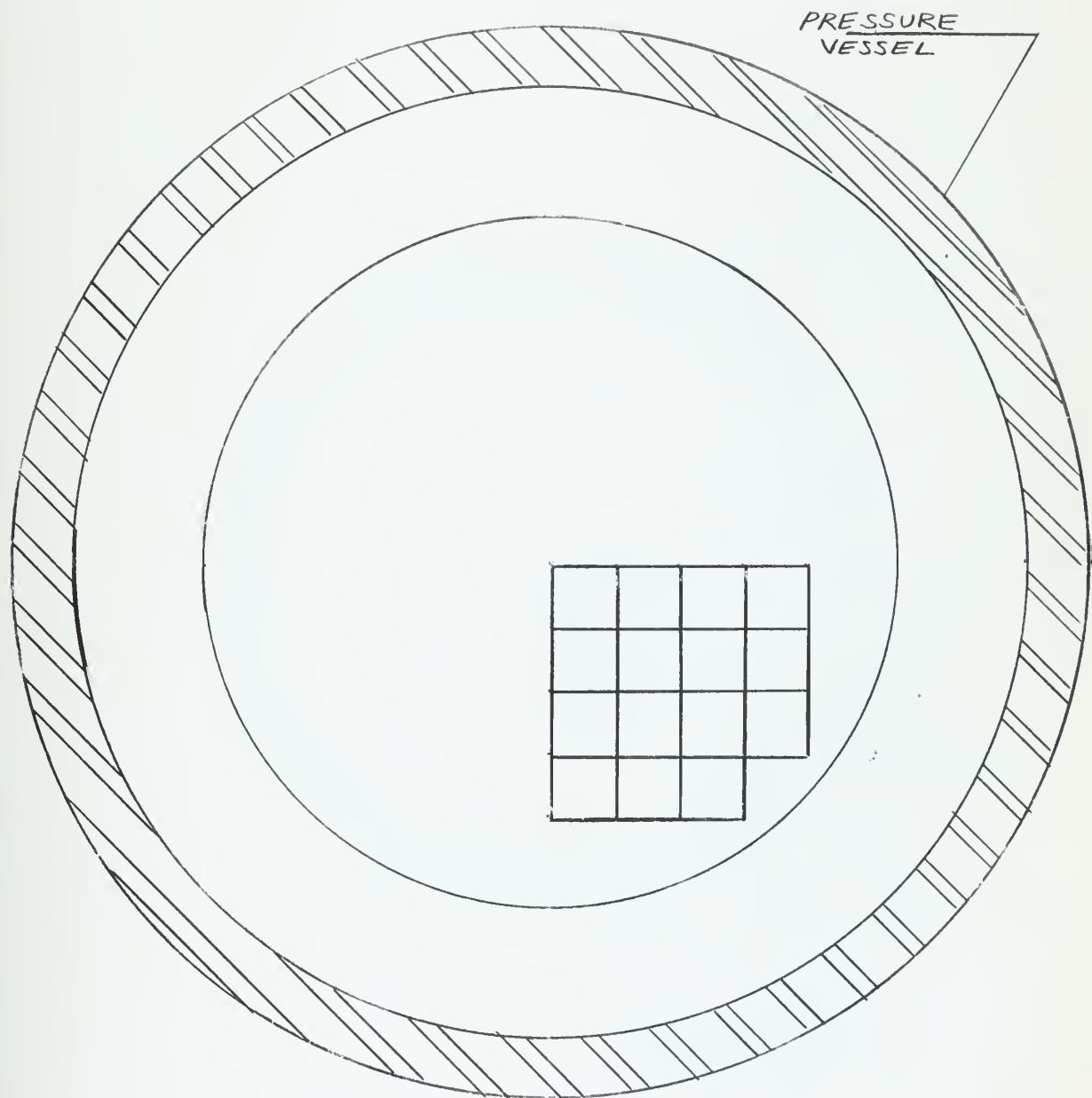
Pertinent Technical Data on Reactors

<u>Pressure Vessel</u>	PWR No. 1	PWR No. 2	PWR No. 2'	GCR
Op. pressure (psia)	2,000	2,000	2,000	1,150
I.D. (ft.)	11.83	6.83	5.75	11.0
Height (ft.)	30	22	19	26
Wall Thickness (in.)	9.48	5.46	4.6	7.5
<u>Core</u>				
Equiv. Dia. (ft.)	8.1	4.4	3.65	7.5
Height (ft.)	8.2	4.6	5.0	7.5
Fuel elements	164 rod rectangular	36 rod rectangular	81 rod rectangular	19 rod circular
No. elements	60	88	32	368
Fuel rod	0.50" SS clad	0.50" SS clad	0.50" SS clad	0.375" SS clad
No. rods	9,840	3,168	2,592	6,992
<u>Thermal</u>				
Thermal power, MW	102.1	102.1	93.2	78.6
Inlet pres. (psia)	2,050	2,070	2,075	1,135
Inlet temp. (°F)	506	544	546	745
Outlet pres. (psia)	2,000	2,000	2,000	1,120
Outlet temp. (°F)	536	584	586	1,300
Sat. temp. at P_2	636	636	636	--
Max. wall temp.	625	737	726	1,499
Max. coolant temp.	565	622	624	1,389
Max. heat flux (BTU/ ft^2 -hr)	106,500	588,000	600,000	--
B.O. heat flux	972,000	1,330,000	1,400,000	--
"S.F."	9.1	2.3	2.3	--

TABLE III-2 (continued)

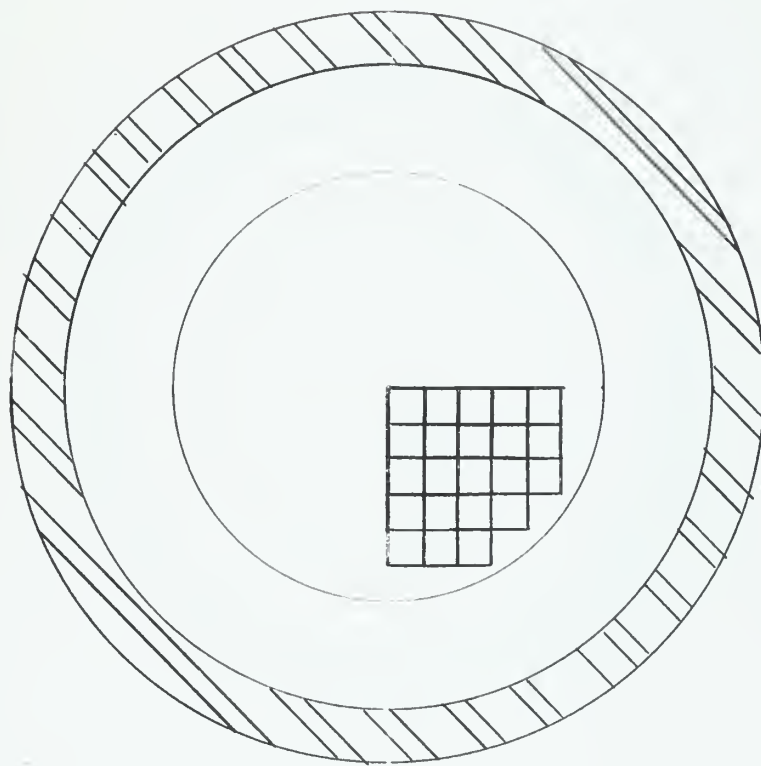
<u>HEAT EXCHANGERS</u>	PWR No. 1	PWR No. 2	PWR No. 2'	GCR
<u>Steam Gen.</u>				
<u>No.</u>	2	2	2	
Area/unit (ft ²)	1,900	1,625	2,100	
LMTD (°F)	122	168	101	
Q (BTU/HR)	174,000,000	174,000,000	159,000,000	
<u>Condenser</u>				
<u>No.</u>	4	4	4	
Area/Unit	1,070	1,070	1,000	
LMTD	44.7	44.7	44.7	
Q	479,000	479,000	419,000	
<u>Regenerator</u>				
<u>No.</u>				4
Area/Unit				4,290
LMTD				62
Q				46,000,000
<u>Intercooler</u>				
<u>No.</u>				4
Area/Unit				2,050
LMTD				80
Q				14,900,000
<u>Precooler</u>				
<u>No.</u>				4
Area/Unit				2,010
LMTD				110
Q				22,200,000

FIGURE III-12
CROSS SECTION OF PWR NO. 1 CORE
60 FUEL ELEMENTS
164 FUEL RODS PER ELEMENT
9840 FUEL RODS



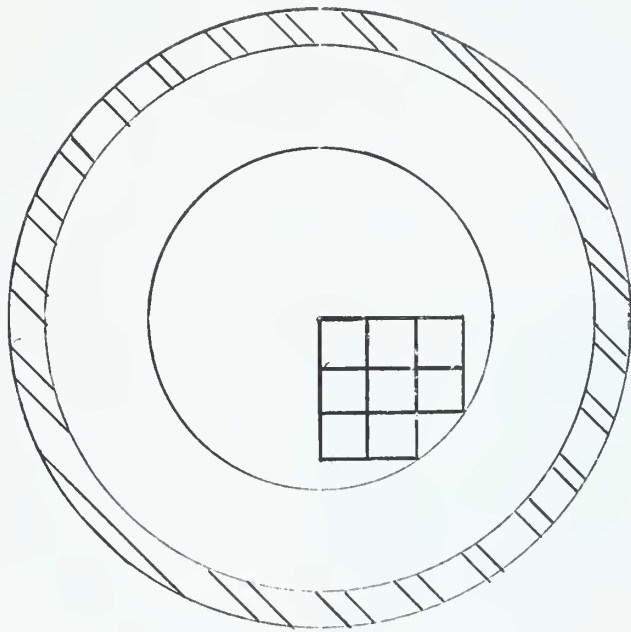
SCALE: $\frac{1}{2}'' = 1'$

FIGURE III-13
CROSS SECTION OF PWR NO. 2 CORE
88 FUEL ELEMENTS
36 FUEL RODS PER ELEMENT
3168 FUEL RODS



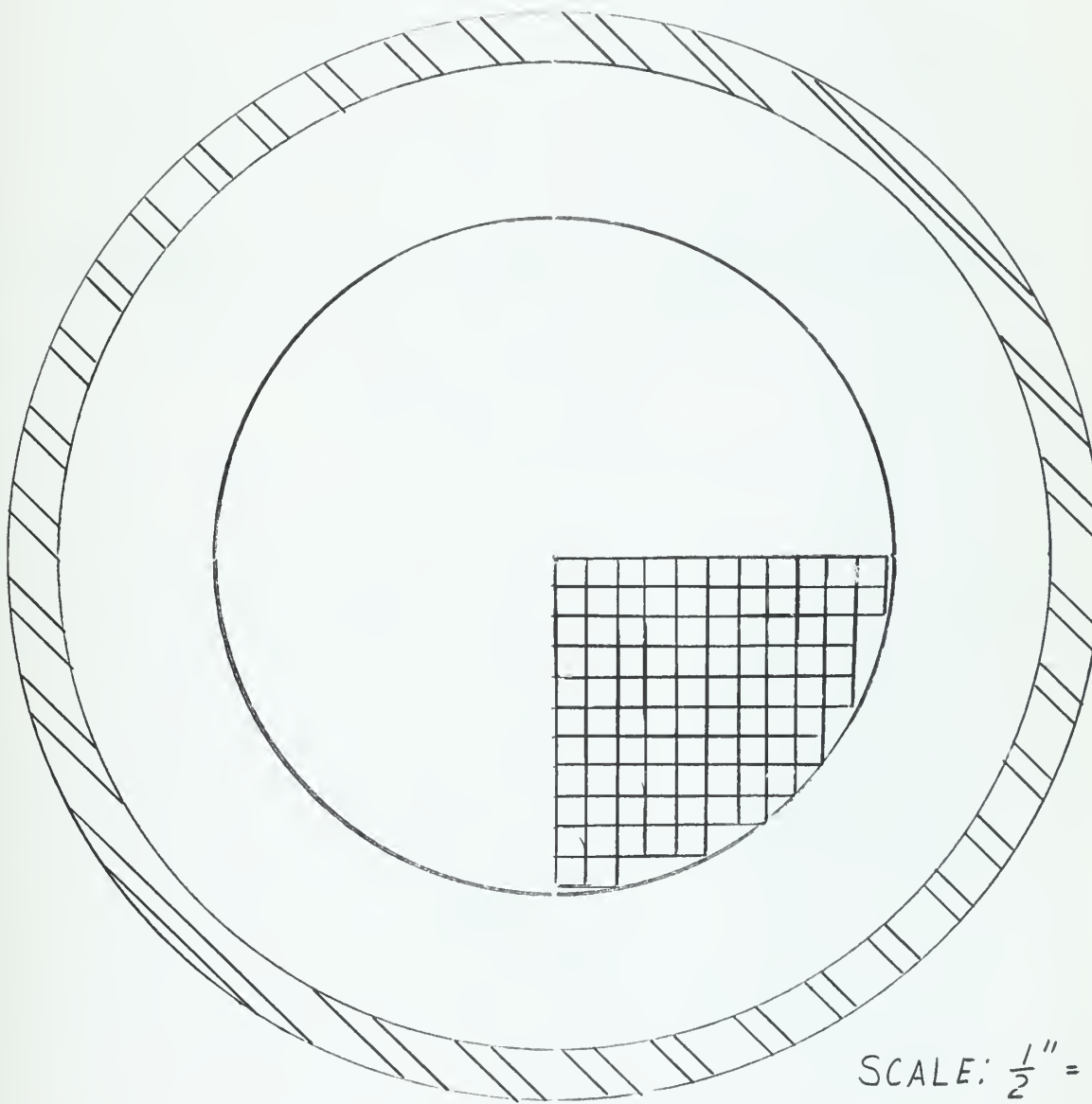
SCALE: $\frac{1}{2}'' = 1'$

FIGURE III-14
CROSS SECTION OF PWR NO. 2' CORE
32 FUEL ELEMENTS
81 FUEL RODS PER ELEMENT
2592 FUEL RODS



SCALE: $\frac{1}{2}'' = 1'$

FIGURE III-15
CROSS SECTION OF GCR CORE
368 FUEL ELEMENTS
19 FUEL RODS PER ELEMENT
6992 FUEL RODS



SCALE: $\frac{1}{2}'' = 1'$

FIGURE III-16
MAXIMUM WALL TEMPERATURE
VS
NUMBER OF FUEL ELEMENTS FOR GCR

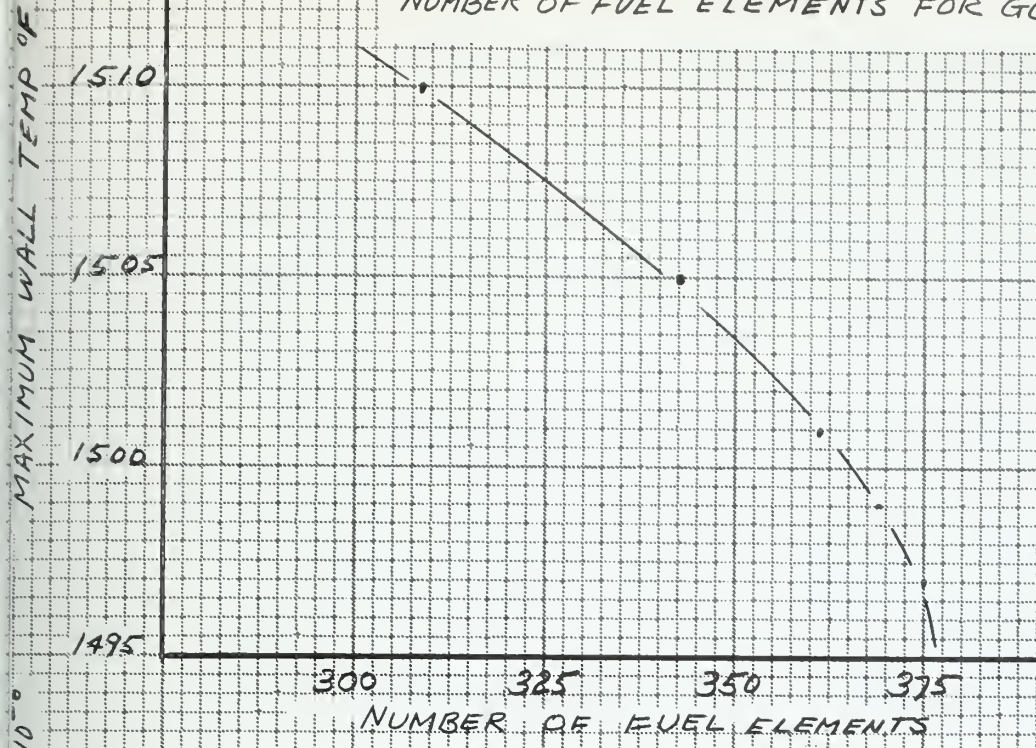
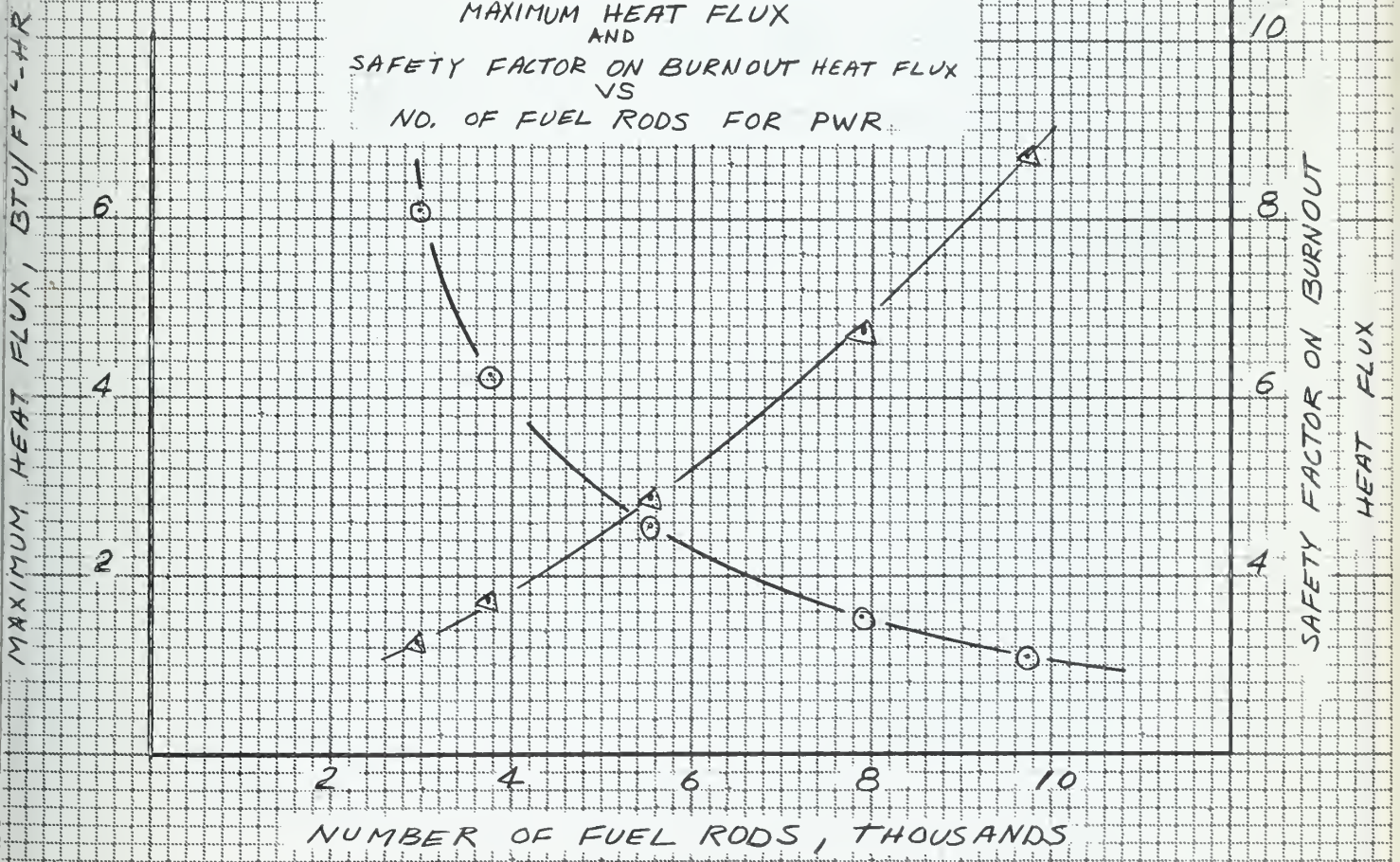


FIGURE III-17
MAXIMUM HEAT FLUX
AND
SAFETY FACTOR ON BURNOUT HEAT FLUX
VS
NO. OF FUEL RODS FOR PWR



III.3.2 Steam Plants, Results and Discussion

The steam plant proposed for these designs represents no radical departure from conventional systems. The deviations from what might be called ordinary designs are:

- (1) The degree to which the plant is broken into small units. This is done, not for reliability, but to limit the size of the D.C. generators required and to prevent the situation where a main propulsion motor is driven, through generators, by a single prime mover.

- (2) The use of saturated steam, which is becoming a more common practice as nuclear plants, with the attendant temperature limitations, are used more. However this is not conventional and requires special procedures in the turbine design.

For purposes of the heat balance calculations, fixed values were assigned to the miscellaneous steam demands. The electrical load was estimated from the loads on the U.S.S. GLACIER and principal pump requirements. Considerable excess capacity is provided to allow for the possible addition of a Tartar missile system and its attendant gear, as well as to allow for the characteristic growth in demand for power.

The selection of the pressure for cross-over between the high and low pressure turbines was based on a series of heat balances at different cross-over pressures. The results of these calculations are shown in Figures III-18 and III-19. The resulting heat balances in Figures III-20 and III-21 are self-explanatory.

III.3.3 Brayton Cycle, Results and Discussion

Since there are no large closed cycle gas turbine power plants, either mobile or fixed, in operation now, this whole concept is a departure from the conventional. Shaft-power-producing open cycle gas turbines of this capacity are reasonably commonplace. It can be expected therefore that the machinery can be developed without inordinate difficulty. The details of design may be different than practices used now, but the basic principles remain unchanged. Experimentation and construction of the actual hardware will be necessary to vindicate the various assumptions made. The pressure loss parameter assumed seems reasonable, but the plant performance is strongly dependent on this. Figure III-22 illustrates this dependence. Ducting and heat exchanger design will be

FIGURE III-18
 REACTOR THERMAL POWER
 VS
 TURBINE CROSSOVER PRESSURE
 PWR No 1 & PWR No. 2

THROTTLE COND:

$P = 546 \text{ PSIA}$

$T = 476^\circ\text{F}$

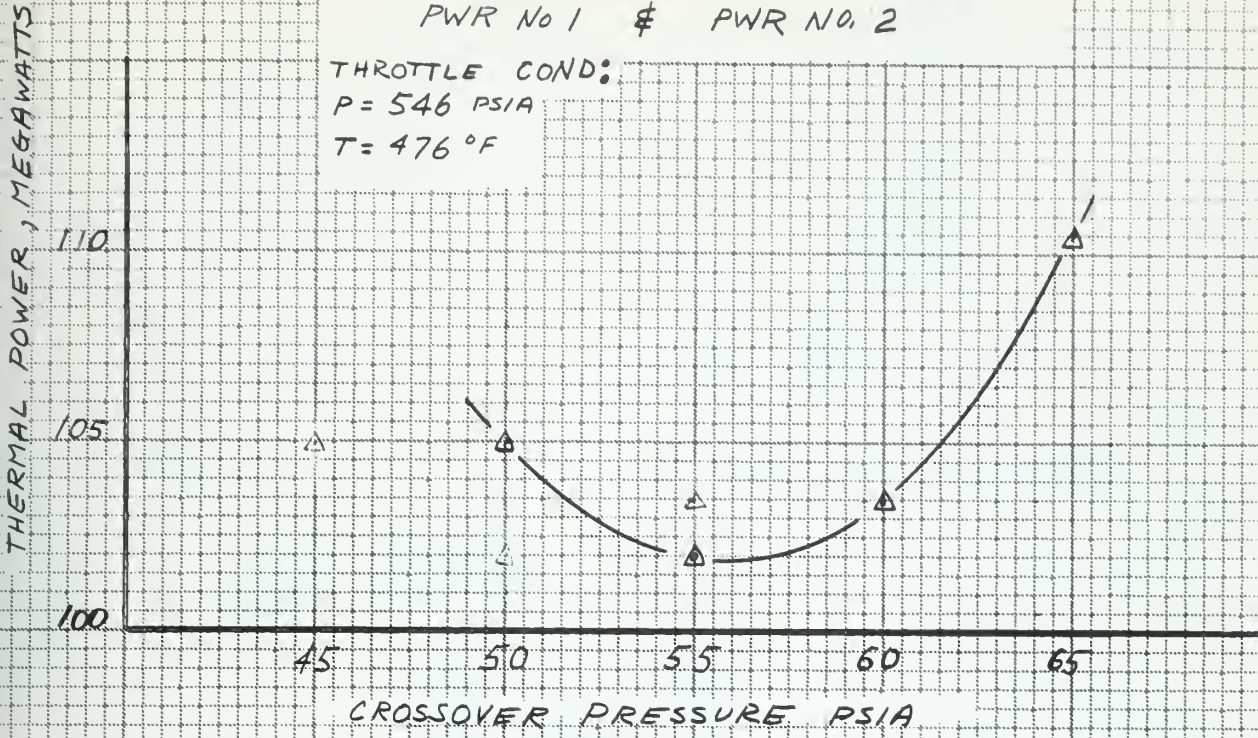


FIGURE III-19
 REACTOR THERMAL POWER
 VS
 TURBINE CROSSOVER PRESSURE
 PWR No. 2

THROTTLE
 COND:
 $P = 900 \text{ PSIA}$
 $T = 532^\circ\text{F}$

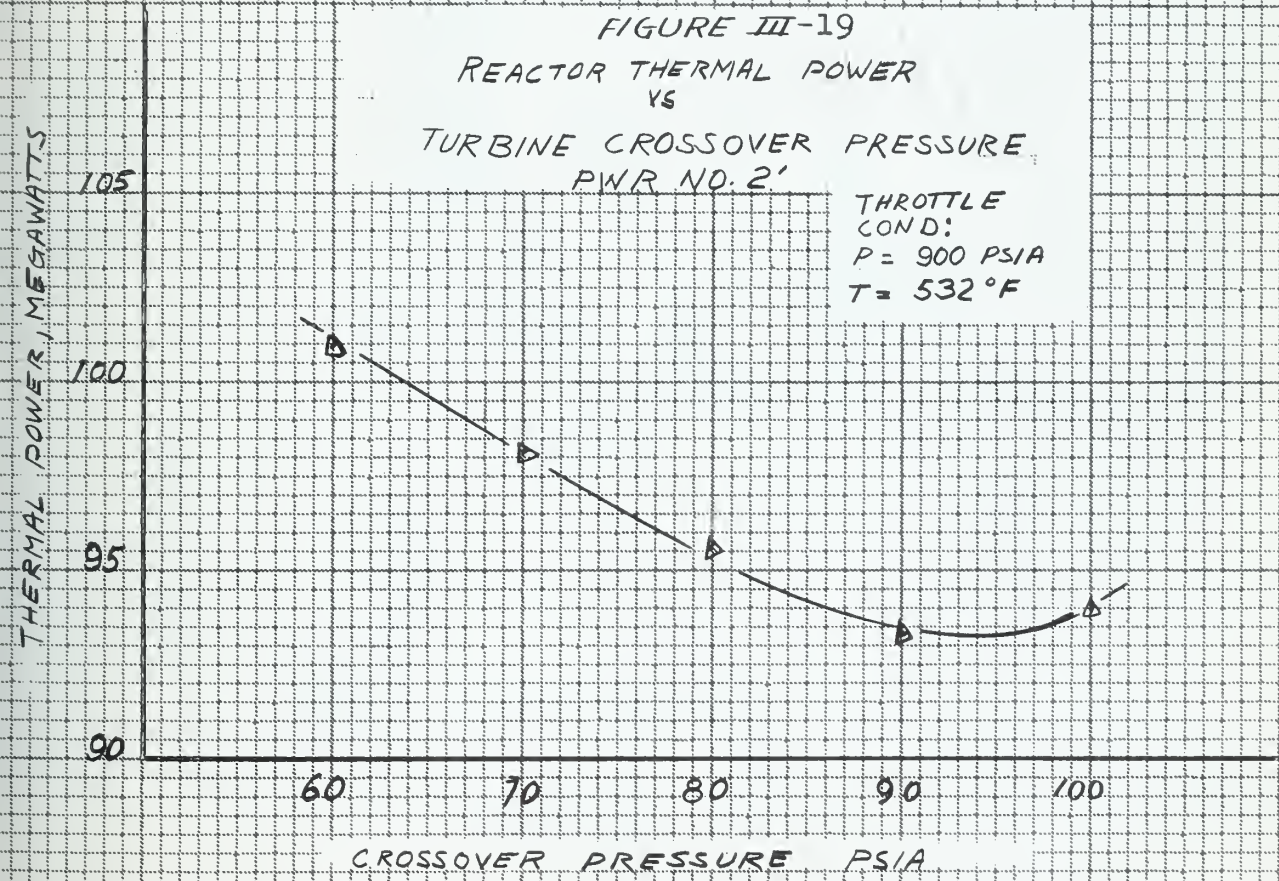


FIGURE III- 20

STEAM CYCLE HEAT BALANCE PWR NO. 1

25,500 SHP

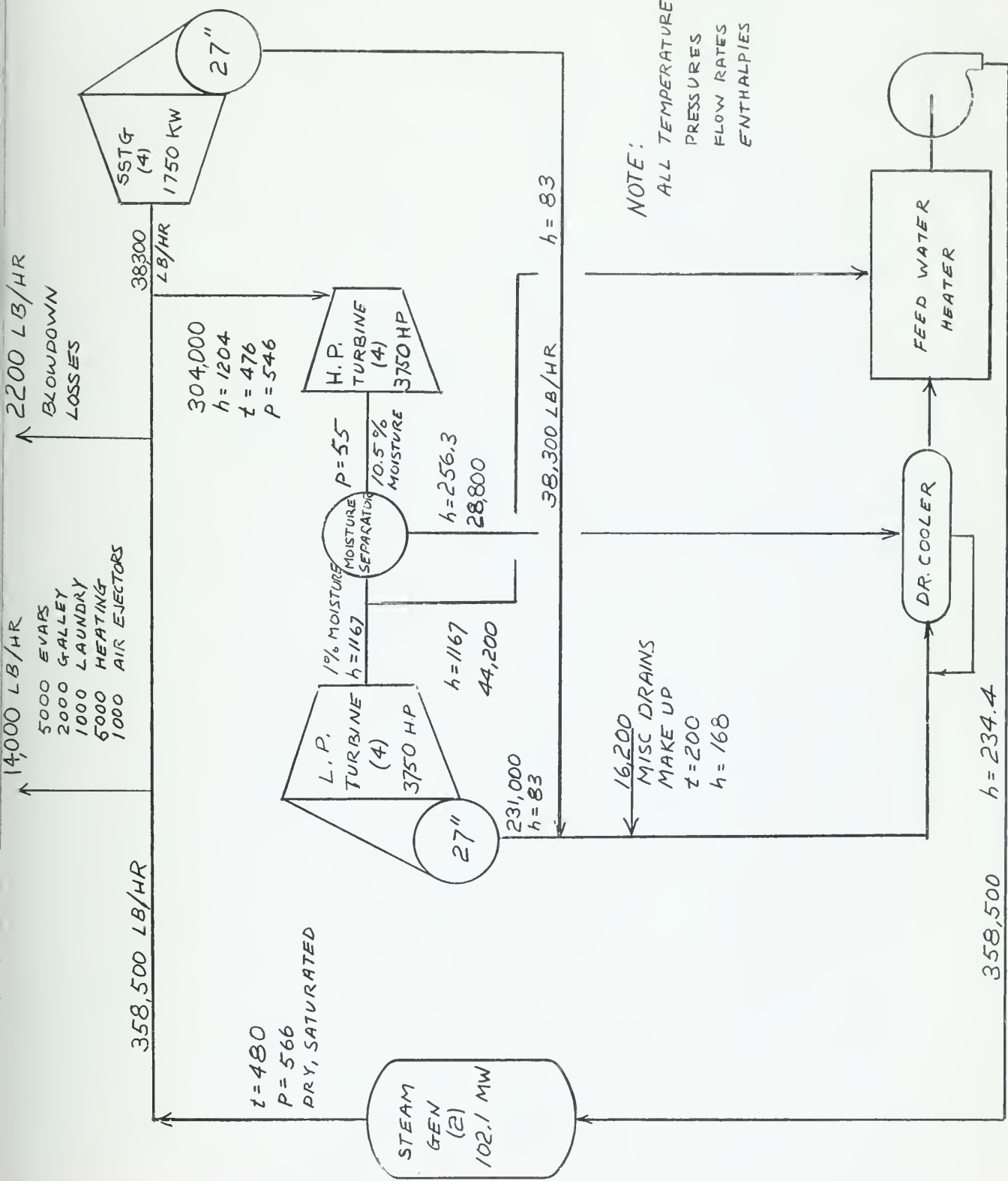
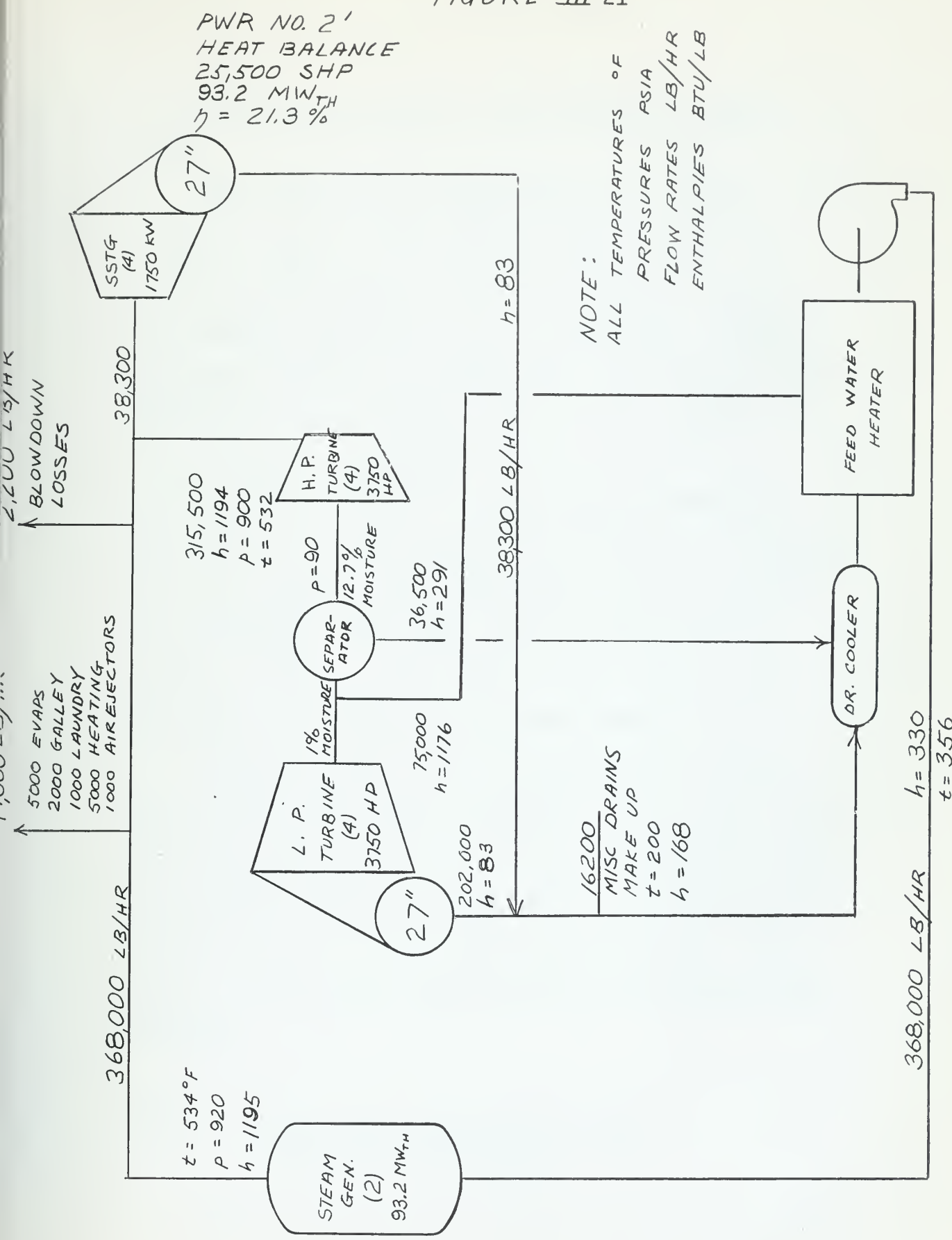
102.1 MW_{TH} $\eta = 19.4\%$ 

FIGURE III-21



influenced by an effort to keep pressure losses down.

For the slightly simplified case in which $\tau_{12} = \tau_{34} = \sqrt{\tau_{14}}$ Figure III-23 shows a result of calculations of cycle efficiency, η_{cycle} for various values of τ_{14} , the isentropic temperature ratio across the compressors. The rather broad maximum is in the region of $\tau_{14} = 1.49$. Since

$$\tau_{14} = \left(\frac{P_{04}}{P_{01}}\right)^{\frac{k-1}{k}}$$

, the resulting pressure ratio is 2.7. These values were used and the pressure level set more or less arbitrarily, based on that of the prototype. The final cycle is represented in Figure III-24. The effect of the SSTG sets was neglected in choosing the optimum pressure ratio.

The SSTG cycle itself is designed for maximum net work per unit mass of working fluid to keep its size down. Note that in lieu of a regenerative cycle, the turbine exhaust has been used to generate all the steam required for the ship's hotel services. Here again a large margin was allowed in power generating capacity.

III.3.4 Costs of Nuclear Power Plants, Results and Discussion

The costs of the major components of each of these

FIGURE III-22

GAS TURBINE CYCLE EFFICIENCY
VS.
PRESSURE LOSS PARAMETER

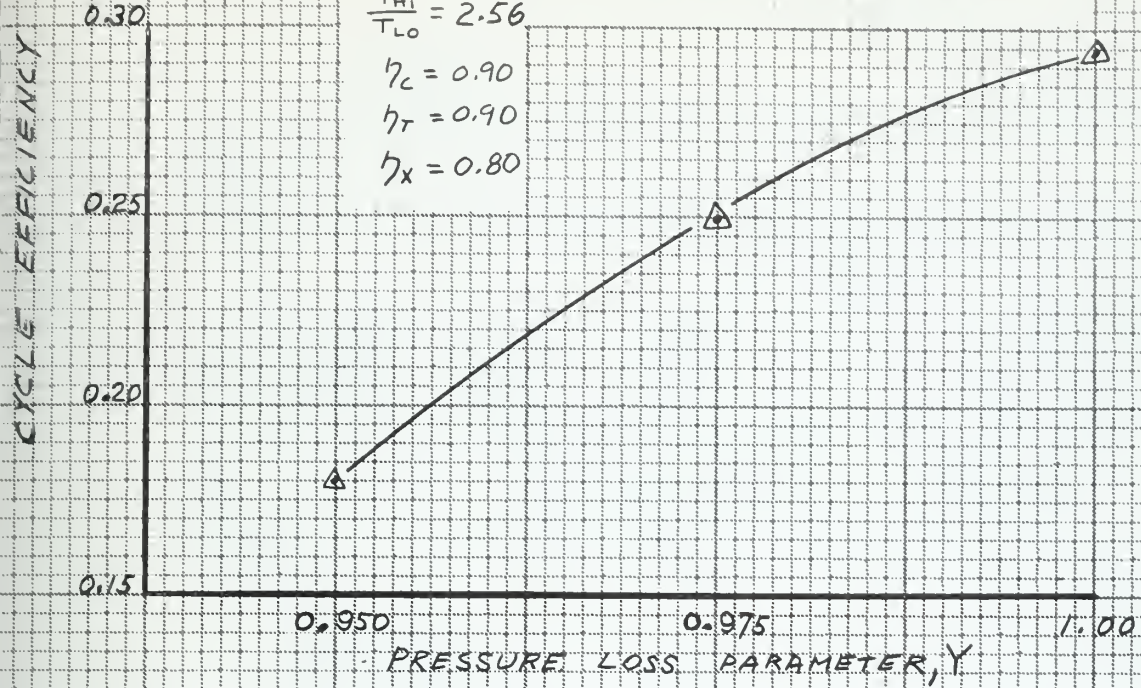


FIGURE III-
GAS TURBINE CYCLE EFFICIENCY
VS
COMPRESSOR ISENTROPIC TEMPERATURE
RATIO

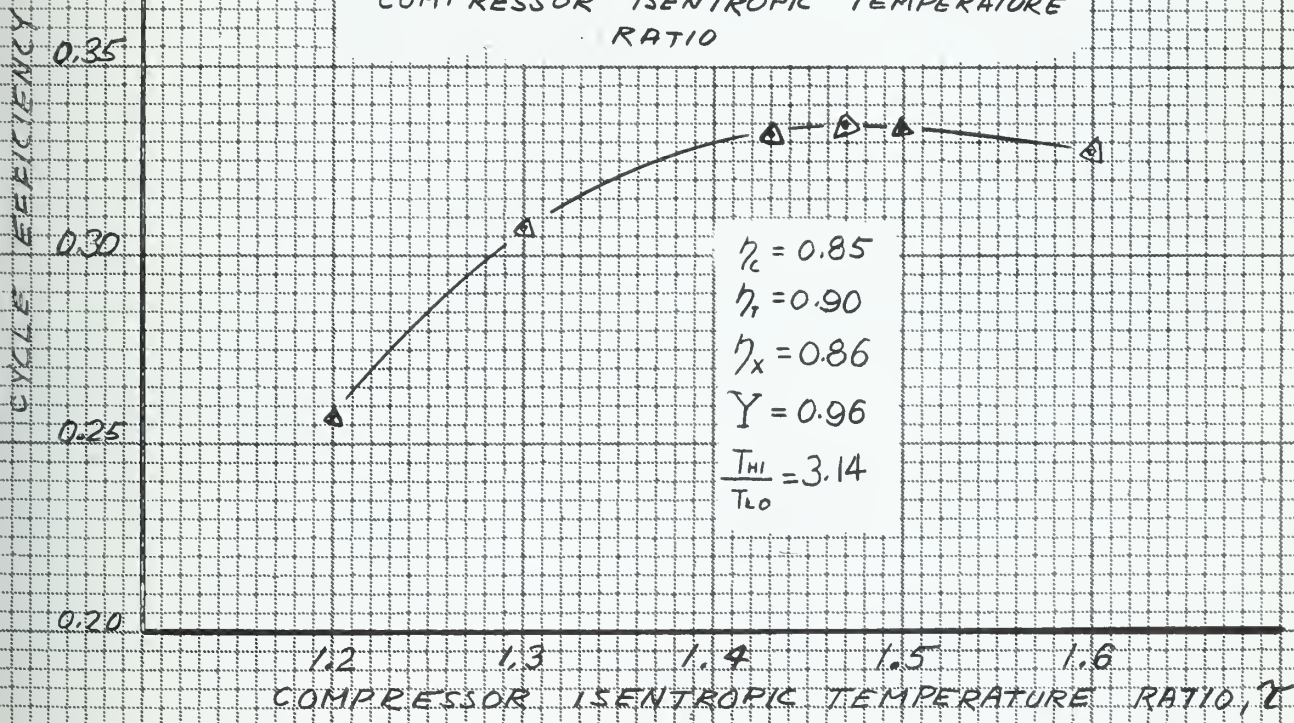


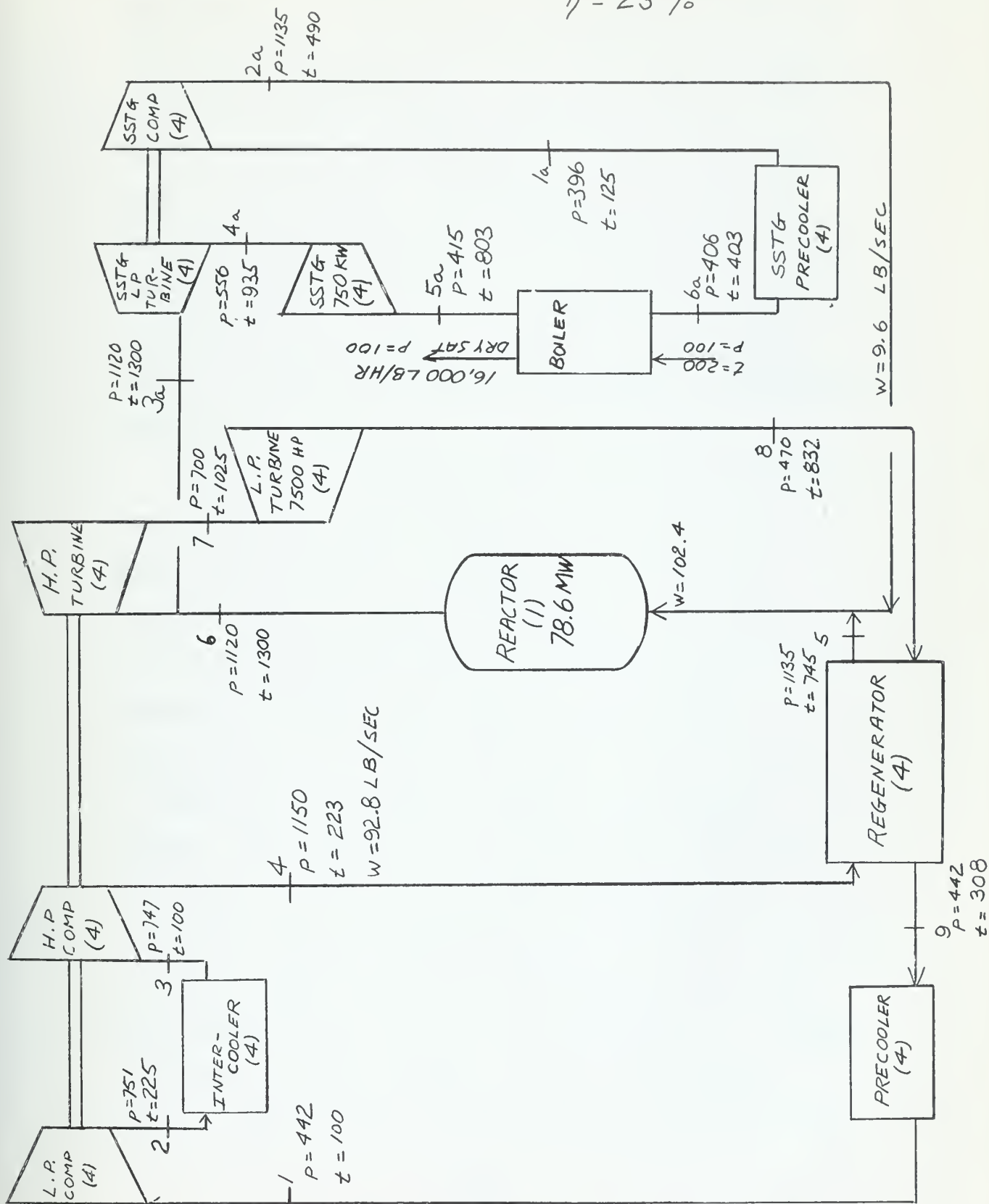
FIGURE III-24

GAS TURBINE CYCLE HEAT BALANCE

25,500 SHP

78.6 MW_{TH}

$$\eta = 23\%$$



four plants were estimated using the procedure of Appendix E. To reiterate a point made in Appendix E, these costs are, at best, only yardsticks to compare the four designs discussed. Wherever possible and where it seemed valid the same procedures were used for all four plants. The similarity of concept of the three PWR plants made it relatively easy to keep the cost estimates consistent among them. Certain deviations were necessary, however, in the case of the GCR. These deviations are mentioned in Appendix E and are there justified to the extent possible.

Table III-3 summarizes the cost data calculated and assumed for these designs. Those items with asterisks (*) are the components for which cost functions are developed in Appendix E. The items without asterisks are merely assumed to complete the comparison. It is hoped that errors in these assumptions do not cloud the results to the extent of making the comparison of total costs invalid. However, this possibility does exist and attention should be directed to the asterisked components.

Where research and development activity is necessary, the costs listed do not include developmental costs. Developmental costs will be slight for PWR No. 1 since its design is based closely on that of the NMSR. PWR No. 2 and PWR No. 2' will require considerable de-

velopment costs since research will be necessary to prove a design that will be stable with limited boiling and since specific boiling burnout data will be required. Even with these programs, reactors of this type could be produced in a relatively short time, say, two to four years.

The GCR design will undoubtedly require the greatest deal of development. The realization of this design is in the distant future of five to ten years. Study on the MGCR was begun in 1958 and has been pursued since by General Dynamics Corporation.

The costs of Table III-3 represent only the initial investment in the power plant. The cost of the first core has not been included in these costs since core costs are properly considered fuel costs and are included in annual operating expenses. A summary of the fuel costs as computed in Appendix E is given in Table III-4.

The fuel cycle costs of Table III-4 are based on assumed values of fuel enrichment. A more honest comparison could be made if each fuel cycle had been optimized for the best enrichment.

The burn-up used for PWR No. 1 is that used in calculations for the NMSR in the SAVANNAH. The other PWR burn-up figures reflect the univeral optimism in the performance of UO_2 fuel elements. Average burn-

ups of 10,000 - 15,000 MW-D/ton are frequently quoted as expected for this type of fuel rod (43). The fuel in the GCR is diluted in a ceramic mixture. This has been done in the prototype design to reduce the power density of the reactor to provide lower transient fuel element temperatures in the event the coolant is lost. The dilution in a ceramic mixture spreads out the bad effects of radiation damage and growth and thus, hypothetically, allows a greater exposure to irradiation before the elements become unserviceable.

The long life time calculated for these reactors is a direct result of the load factor chosen. The load factor for an average stationary power plant is around 87%, while for an ordinary warship may be less than 10%. The assumption made in choosing 30% for a load factor is that this ship will be operated more and at higher powers because it is nuclear powered.

Many references can be found commenting on the promise of gas-cooled reactors for reducing fuel costs (39,42). This hope is based upon the generally higher thermal efficiencies attainable with the proposed high temperatures, and the large burn-up hoped for in ceramic fuel elements. Both the high temperatures and the large burn-up depend upon a great deal of research and progress in the field of ceramic fuel elements.

The results listed in Table III-4 indicate that considerable improvement will be necessary to reduce annual fuel costs to that of PWR No. 2 or No. 2'. These costs also depend upon some progress, but it is felt that this development is in the nearer future than the developments required for the GCR.

TABLE III-3

NUCLEAR PROPULSION PLANT EQUIPMENT COSTS

<u>NUCLEAR PLANT</u>	PWR No. 1	PWR No. 2	PWR No. 2'	GCR
Reactor *	2,950,000	966,000	665,000	3,530,000
Heat Exchangers *	1,493,000	1,358,000	1,430,000	586,000
Waste disposal	65,000	65,000	65,000	Included below in turbine
Instrumentation and Controls	300,000	300,000	300,000	300,000
Containment and shielding	500,000	500,000	500,000	1,500,000
Spare parts	500,000	500,000	500,000	500,000
Installation and Indirect	3,000,000	3,000,000	3,000,000	3,000,000
Total Nuclear	8,808,000	6,689,000	6,470,000	9,416,000
<u>Propulsion Plant</u>				
Steam (gas) * turbine and auxiliaries	2,164,000	2,164,000	2,548,000	1,860,000
Reduction gears *	480,000	480,000	480,000	1,000,000
Main motors and generators	1,000,000	1,000,000	1,000,000	1,000,000
Shaft and propellers	600,000	600,000	600,000	600,000
Electrical system	400,000	400,000	400,000	200,000
Main propulsion control	50,000	50,000	50,000	50,000
Installation and Indirect	2,000,000	2,000,000	2,000,000	2,000,000
Total non-nuclear	6,694,000	6,694,000	7,078,000	6,710,000
TOTAL	15,502,000	13,500,000	13,548,000	15,126,000

TABLE III-4
FUEL CYCLE COST ESTIMATES

	PWR No. 1	PWR No. 2	PWR No. 2'	GCR
Thermal Power				
MW	102.1	102.1	93.2	78.6
Enrichment, %U ²³⁵	3%	3%	3%	20%
Burn-up, MWD/T	7,360	12,000	12,000	40,000
Inventory				
Kg U	19,700	3,730	3,310	1,820
Core Life at 30% L F. yrs	13	4	3.9	8.44
Initial cost, \$ U	7,390,000	1,400,000	1,200,000	5,870,000
Fuel use chg \$	3,840,000	224,000	187,000	1,980,000
Refund value \$	4,920,000	645,000	558,000	4,510,000
Net fuel burn-up charge \$	2,470,000	755,000	684,000	1,360,000
Fabrication \$	1,770,000	336,000	298,000	214,000
Reprocessing \$	425,000	180,000	170,000	152,000
Cooling \$				
Conversion to UF ₆	390,000	66,300	59,200	34,000
Pu credit \$ (est.)	-400,000	-100,000	-85,000	-160,000
Cost/cycle \$/cycle	8,495,000	1,461,000	1,313,000	3,580,000
Cost/year \$/year	652,000	365,250	336,700	424,000

III.4 Roll Stabilization, Results and Discussion

A stabilization system which uses anti-rolling tanks accomplishes its purpose by alternately filling and emptying tanks at the sides of the vessel with water or other liquid. If tanks on opposite sides of the vessel are connected at their lowest level by an athwartship duct the system is called a U-tube tank stabilizer.

If transfer of water is accomplished simply by the rolling of the ship, the system is said to be passive. In this case the period of oscillation of the water is adjusted until it is equal to the natural period of roll of the ship, and it then oscillates with the same period as the ship, but with a phase lag of a quarter period. The ship does not always roll with its natural period, and the effectiveness of the anti-rolling tanks diminishes as the rolling of the ship departs from its natural period.

An activated U-tube tank system of stabilization is one in which a pump is used to force the water to oscillate at any desired amplitude and frequency within the limits for which the system is designed.

The purpose of the study on the GLACIER was to determine the feasibility of installing an activated U-tube tank system on a ship of similar characteristics. An attempt was made to determine within reasonable accuracy the number and size of tanks, cross duct areas, and power re-

quirements. The installed heeling tanks were used wherever possible.

Table III-5 gives the particulars on the GLACIER used in the study. Figure III-25 shows the location of the heeling tanks within the ship. The heeling tanks are in pairs, port and starboard, six tanks in all. Figure III-26 gives the dimensions of one set of tanks.

The results of the study on the GLACIER are shown in Table III-6. Detailed calculations are given in Appendix F.

TABLE III-5
Particulars for USS GLACIER (AGB-4)

Displacement, full load, tons	8,640
Displaced volume, cu. ft.	302,000
LBP, ft.	290
Extreme breadth, ft.	74
Draft, full load, ft.	28.2
KM, ft.	35.9
KG, ft. (corrected for free surface)	24.4
GM, ft. (corrected for free surface)	11.5
KB, ft.	17 (estimated)
Period of roll, T_s , sec.	10 (estimated)

Figure III-25

Location of heeling tanks on the GLACIER

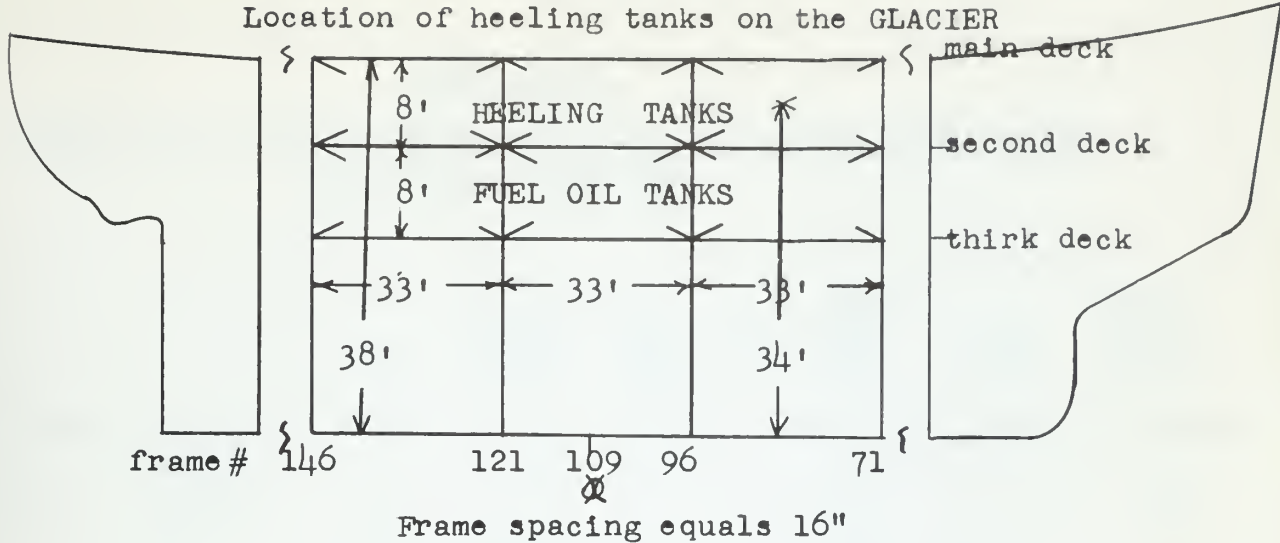


Figure III-26

Dimensions of one set of heeling tanks on the GLACIER
indicating possible location of cross duct
(Not to scale)

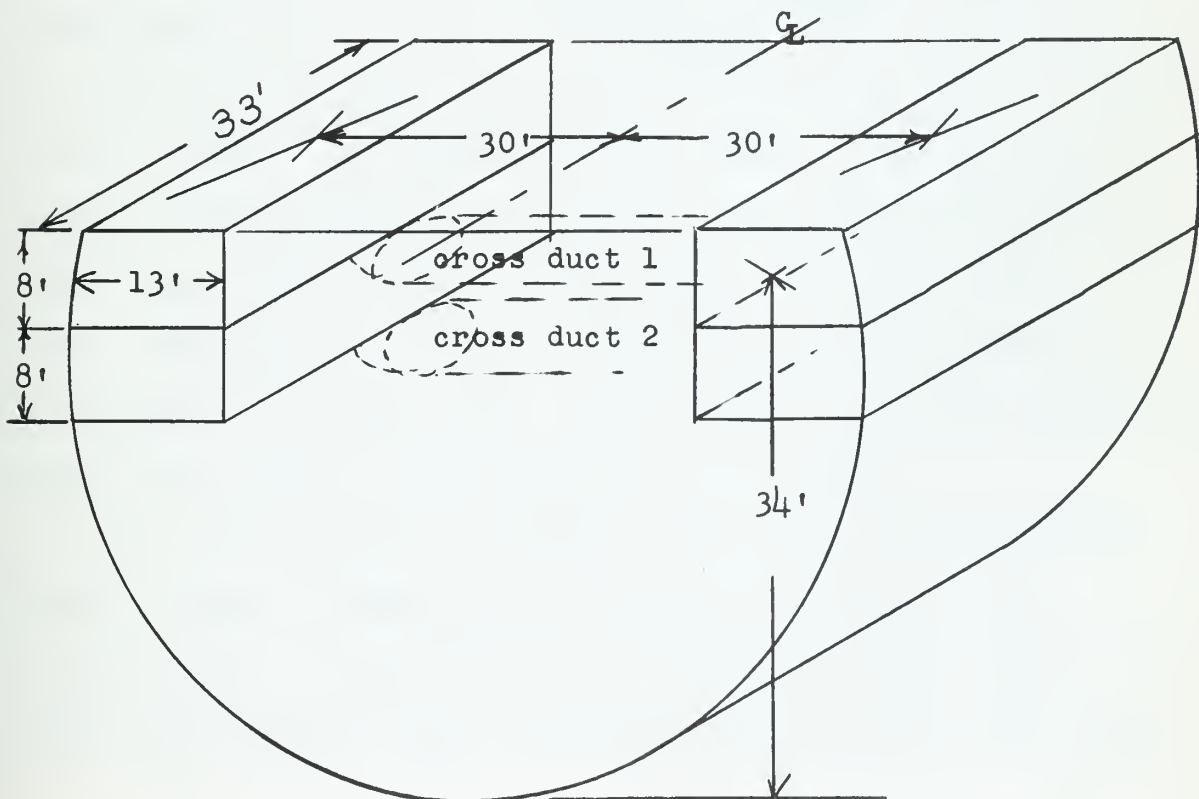


TABLE III-6

Results of Roll Stabilization Study on the GLACIER Using
Activated U-tube Tank

Trial Capacity		Max Head	Total Tank Area	No. of Sets of tanks	Cross Duct Area per set	Per-cent weight	Total Pump Output HP
No.	degrees	ft	ft ²		ft ²		
1	5.0	8.0	1,290	3	178		--
2	5.0	16.0	656	4	72	10.0	17,800
3	2.5	16.0	328	4	36	5.0	8,900

As shown three different conditions were looked into.

The capacity was based on a relationship given by Chadwick where desirable capacity = $\frac{(.36)(57.2)}{\log_{10} \Delta}$ degrees. The head is the maximum height differential between the fluid in each pair of tanks. An attempt was first made to use only the depth of the heeling tanks with the cross duct running beneath them. The maximum head for this system was eight feet. This turned out to be fruitless as the duct area required was 178 square feet, which is quite obviously impractical. This would require a duct diameter of 15 feet.

The next step was to increase the head to 16 feet which could be done by using the fuel tanks directly below the heeling tanks. These are shown in Figure III-25. This reduced the required cross duct area as well as the tank area.

To reduce the cross duct area even more four sets of tanks were used. A cross duct diameter of 9.5 feet was required. This is still a rather large pipe, however, the real stopper was the pump capacity required of 17,800 HP. The average power input to the fluid will be much less than the peak power, since the tanks are tuned for maximum passive effect. Nevertheless, the capacity of the pumps must be great enough to handle the maximum possible load demands within the design range.

Next the capacity of the system was cut in half which merely reduced the required area and pump HP by one half. It is readily apparent that even for a minimum capacity of 2.5° the required pump output rating prohibits the use of an activated tank system for the roll stabilization of icebreakers. Having concluded that an activated tank system is not even close to being practical, and ruling out the activated fin system for reasons already given in Chapter II, Section II.5, the only remaining possibility was a passive tank system. Since the activated system is tuned to get maximum passive effect, the procedure used in designing a passive system is the same as for an active system. The only difference is that no pumps are installed in the passive system.

The results of analog simulation of a passive tank system for a missile-range ship are given in DTMB Report

1322, May 1959 (58). These results were promising enough that a full scale evaluation was conducted aboard an AK-type ship in October, 1959. The results of the full scale evaluation are given in DTMB report 1414 (60). The data collected was limited, but the tanks reduced the roll by a factor of two under the sea conditions of the test.

Figure III-27 shows relatively what may be expected from a passive stabilizing system. This figure is based on the analog simulation of the missile range ship, taken from DTMB report 1322. The peak magnification of the unstabilized ship is not realistic, but the effect of the stabilizing system can be seen, including the effect of changing capacity ψ . It would appear that a design capacity ψ of 1° is as good as a design capacity of 3° . For this simulated test a capacity of 2° appears to be the optimum.

Contact was made with Mr. James Church, author of DTMB report 1322. It was hoped that an analog simulation using the parameters of the proposed design might be obtainable from the model basin. This hope was never realized. However, a study was made of the passive anti-roll tank stabilizing system installed on the ATKA.

Table III-7 gives the particulars for the ATKA. Figure III-28 gives the location of the heeling tanks on the ATKA, indicating the position of the newly installed anti-roll tanks. Figure III-29 gives the details of the anti-roll tanks.

Figure III-27

Magnification of Roll and Tank Water Angles
for a Stabilized Missile-Range Ship
(Analog Simulation)

ω = Apparent frequency of waves

ω_s = Natural frequency of ship in roll

Θ = Angle of roll of ship

Ψ = Effective instantaneous waveslope amplitude

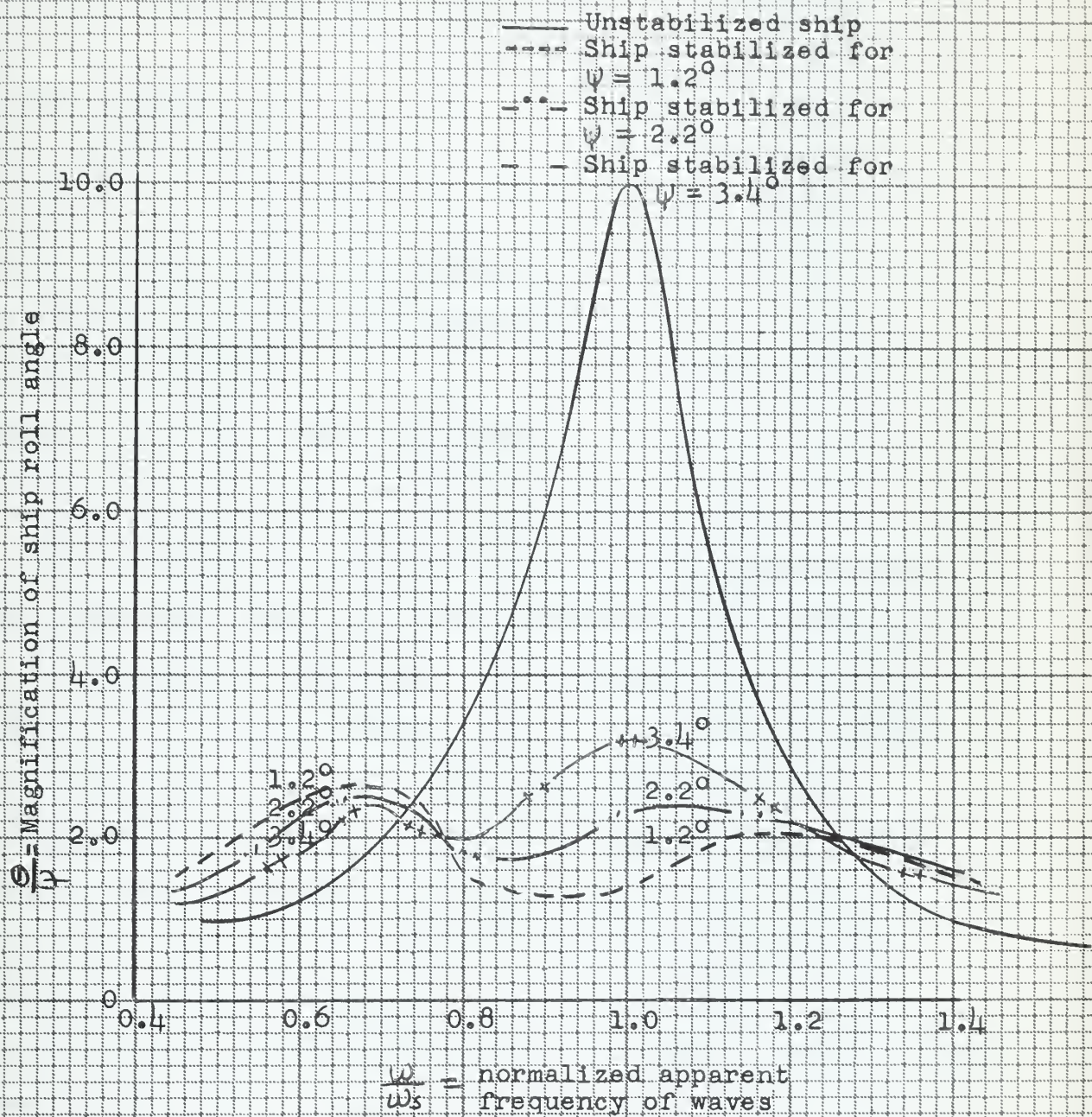


TABLE III-7
Particulars for the ATKA

Displacement, full load, tons	6,500
Displaced volume, cu. ft.	227,000
LBP, ft.	250
Extreme breadth, ft.	63.5
Draft, full load, ft.	29.1
KM, ft.	31.0
KG, ft. (corrected for free surface)	23.0
GM, ft. (corrected for free surface)	8.0
KB, ft. (estimated)	17.0
Period of roll, T_s , sec. (estimated)	10.0

The forward pair of heeling tanks were removed and anti-roll tanks were installed between frames 61 and 71 running the full breadth of the ship. The remaining space between frames 71 and 83 was converted into a living area to replace the living area lost to the anti-roll tanks cross duct. An athwartship bulkhead at frame 66 divides the tank volume into two separate tanks. For each tank the cross duct is part of the tank itself. The flow of water is controlled (tuned) by vertical standpipes with vertical fins attached to each pipe projecting athwartships, as shown in Figure III-29. These are installed at each end of the tanks fifteen feet inboard. The volume between the pipes is the cross duct.

Figure III-28
Location of heeling tanks on ATKA

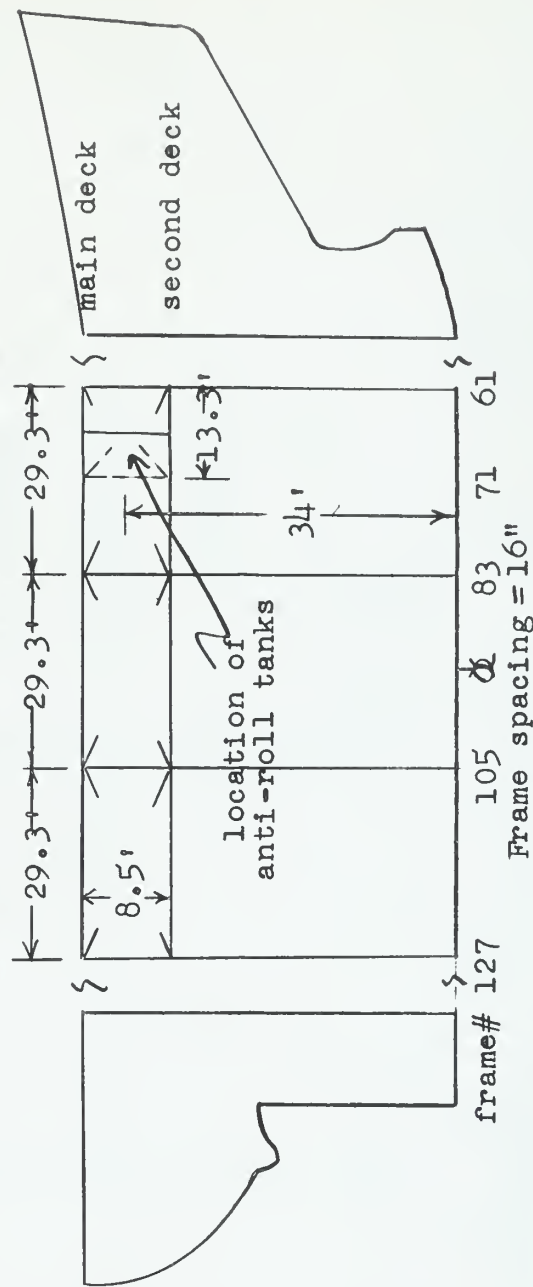
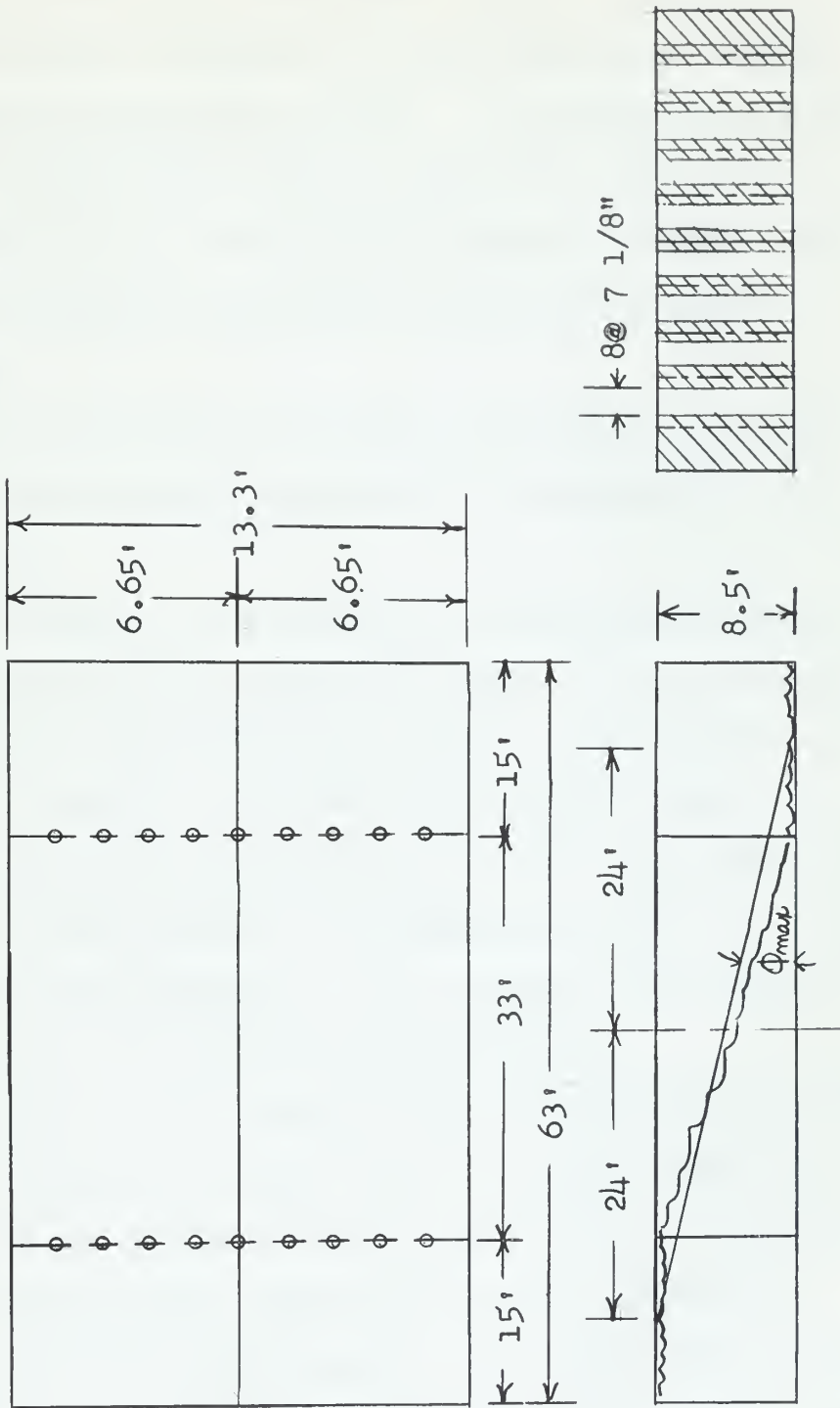


Figure III-29

Details of anti-roll tank installation on ATKA
(Not to scale)



In use the tanks are filled half full of liquid.

Figure III-30 shows a sequence of events which was used as an aid in understanding the system. It is noted that under the somewhat superficial, static, conditions shown, the amount of water in the "cross duct" remains constant. However, even in dynamic conditions this will be closely approximated.

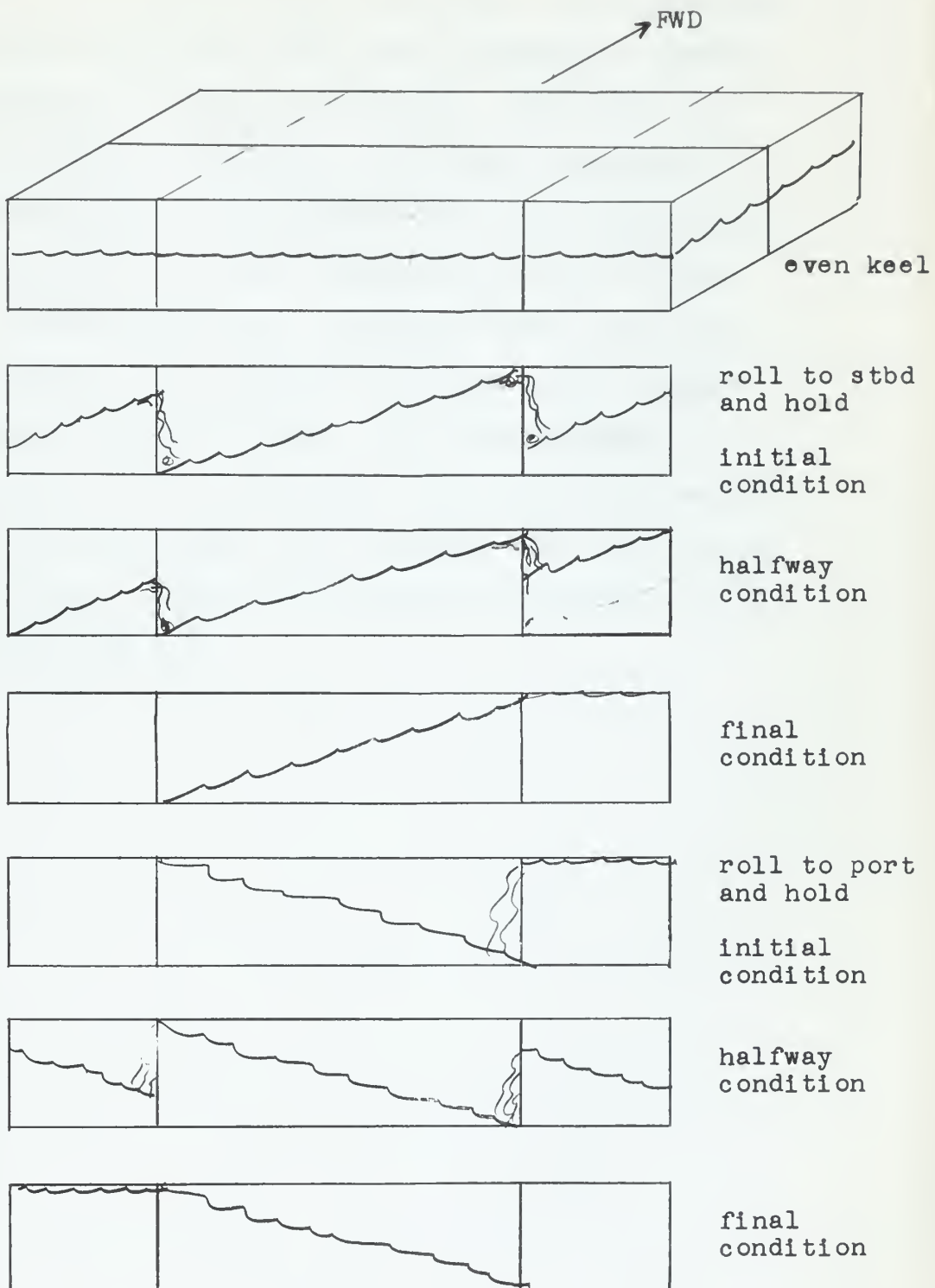
The fluid specified to be used in the tanks is diesel fuel oil as the system is connected to the ships fuel oil piping system.

The only result of the analysis of this system, which can be compared with the installed system is the open area between standpipe fins (cross duct area). Calculations given in Appendix F, Section F.2 showed the required area to be 42.7 ft^2 . The actual open area is 40.4 ft^2 . The slight difference may be attributable to the period of roll. For the analysis this was estimated at 10.0 seconds. The actual period of roll of the ATKA was not obtained.

The capacity of the system is 1.09° . Figure III-27 indicates that this may be enough to give adequate stabilization, although it is below Chadwick's minimum of 2.5° . The total stabilizing fluid weight using diesel oil is 83 tons or 1.28% of the full load displacement. The ATKA made a trial run from Boston to Norfolk, Virginia, arriving back in Boston on 28 April 1961. Data was taken during this voyage by the

Figure III-30

Sequence of Events



design branch of the Boston Naval Shipyard. The evaluation of this data was such that plans have been made to install a similar system on all Navy icebreakers. The results of the trial run were not available. Shipboard personnel in general expected more from the "anti-roll" tank installation. The comments of the few people contacted were not always favorable. The sea conditions during the trial run were quite mild, hence a full fledged evaluation under adverse sea conditions could not be made. The final success of the system will only be proven after much more sea experience under varied sea conditions, but a passive tank stabilizing system is certainly feasible and should be considered in all future icebreaker designs.

IV. CONCLUSIONS AND RECOMMENDATIONS

1. A more systematic recording of operational reports is required in order to properly evaluate the requirements of polar icebreakers.
2. A triple screw arrangement offers some distinct advantages over a twin screw arrangement if a broader, shallower stern is designed, and a large percentage of the power is applied on the centerline propeller.
3. While it is technically feasible to provide a large icebreaker with nuclear power, it is not economically feasible to do so. At this time the cost of such a ship is not justified by the advantages gained. This conclusion may be modified by either changes in the technical and economic fields of nuclear power or by changes in the operational requirements for United States' icebreakers.
4. Pressurized water reactor systems offer the most economical and technically feasible forms of nuclear propulsion. The degree of reliability shown in submarines and the operating and design experience with these systems dictate the use of a pressurized water reactor system in a nuclear powered icebreaker if built in the immediate future. Future developments and improvements in the design of

pressurized water reactors will help the pressurized water reactor system maintain its preeminence in the field of mobile nuclear power.

5. Activated tank stabilizing systems are not feasible for use on icebreakers.

6. Passive tank stabilizing systems offer adequate stabilization for icebreakers at a minimum cost. This type of stabilizing system should be considered for use on all future polar icebreaker designs.

7. The maximum beam is a more important characteristic than the length-beam ratio.

8. On the basis of Vinogradov's equations, there appears to be no particular optimum bow angles within the range of those angles found on past designs, i.e., 22° to 33° . Thus the bow angle must be determined from other, less tangible considerations.

9. The theoretical thickness of ice that an icebreaker can break is approximately proportional to the square root of the displacement if other parameters are held constant.

10. The theoretical thickness of ice that an icebreaker can break is approximately proportional to the square root of the thrust to displacement ratio. This indicates that it is desirable to provide an icebreaker with as much power

as is consistant with other requirements. However the power installed should be within the limitations of the propeller's ability to convert this power to thrust.

11. The condition of the ice is the most significant factor in determining a ship's ability to break ice. The effect of the coefficient of friction is partially illustrated in Figure III-1. The possibility of reducing this friction between the ship and the ice should be investigated.

12. An approach to analytically account for the effect of snow cover on icebreaking ability has been presented in Appendix C. It is recommended that this approach be used in an investigation into this effect.

13. At 100 percent slip a low pitch-diameter ratio and maximum propeller diameter give the highest thrust with the least cavitation.

ADDITIONAL RECOMMENDATIONS

1. Facilities should be provided by the United States government, most likely at the David Taylor Model Basin, for conducting model test on icebreakers under simulated ice conditions. The National Research Council in Ottawa, Canada, has provided facilities of this nature where active ice breaking tests can be carried out.

2. Reports from the David Taylor Model Basin indicate that all icebreaker model testing at the basin is being done with a WIND class hull. Variations are in the form of additions to this one hull design. The results of such tests are therefore of limited value. It is realized that building models is expensive, but at least one different type of basic hull configuration should be included in future tests.
3. On the return voyage from the ice, icebreaker operators should strive to reduce GM as much as possible. This in itself will make the ship ride more comfortably. It would also increase the beneficial effect of any type of stabilizing system. One practical method of doing this is by running with the double bottom tanks empty. On the WIND class this reduces GM by about 1.7 feet.

BIBLIOGRAPHY

GENERAL

1. Ferris, L.W., "The Proportions and Form of Ice-breakers", Society of Naval Architects and Marine Engineers Transactions, Vol. 67, 1959.
2. German, J. Gordon, "Design and Construction of Icebreakers", Society of Naval Architects and Marine Engineers Transactions, Vol. 67, 1959.
3. Matthews, F.W., Captain, RCN, "Stability and Control of HMCS LABRADOR", Society of Naval Architects and Marine Engineers Transactions, Vol. 67, 1959.
4. Lank, S.W. and Oakley, O.H., "Application of Nuclear Power to Icebreakers", Society of Naval Architects and Marine Engineers Transactions, Vol. 67, 1959.
5. Watson, A., "Operation of Department of Transport Icebreakers in Canada", Society of Naval Architects and Marine Engineers Transactions, Vol. 67, 1959.
6. Thiele, E.H., RADM, USCG, "Technical Aspects of Ice-breaker Operation", Society of Naval Architects and Marine Engineers Transactions, Vol. 67, 1959.
7. Rossell, H.E., and Chapman, L.B., Editors, Principles of Naval Architecture, Vol. II, Society of Naval Architects and Marine Engineers, 1939.
8. Saunders, H.E., Hydrodynamics in Ship Design, Vol. 2, Society of Naval Architects and Marine Engineers, 1957.
9. Johnson, Harvey F., RADM, USCG, "Development of Ice-breaking Vessels for the U.S. Coast Guard", Society of Naval Architects and Marine Engineers Transactions, Vol. 54, 1946.
10. Jansson, Jan-Erik, "Icebreakers and Their Design", Scandinavian Ship-Technical Conference in Oslo, October 12, 1956, European Shipbuilding, vol. 5, 1956.
11. Simonson, D.R., LT., USCG, "Bow Characteristics for Ice Breaking", American Society of Naval Engineers Journal, Vol. 48, 1936.

12. Nordstrom, H.F., Edstrank, H.E., and Lindgren, H., "Model Tests with Icebreakers", Swedish State Shipbuilding Experimental Establishment, 1952.
13. Milne, W.J., "Ice Breaking Vessels", Thesis, Department of Naval Architecture and Marine Engineering, Massachusetts Institute of Technology, 1951.
14. Hearings on the Committee on Interstate and Foreign Commerce, United States Senate, 85th Congress, on S. 3657. A bill "To Authorize the Construction of a Nuclear Powered Icebreaking Vessel for Operation by the United States Coast Guard, and for Other Purposes, May 28, June 17 and 20, 1958.
15. Kassell, B.M., "Russia's Ice Breakers", American Society of Naval Engineers Journal, Vol. 63, 1951.
16. Lank, R.B., "Influence of Arctic Operations on Future Ship Design", American Society of Naval Engineers Journal, Vol. 59, 1951.
17. van Manen, J.D., and Kamps, J., "The Effect of Shape of Afterbody on Propulsion", Society of Naval Architects and Marine Engineers Transactions, Vol. 67, 1959.
18. van Manen, J.D., "Open-Water Test Series with Propellers in Nozzles", International Shipbuilding Progress, No. 3, 1954.
19. van Manen, J.D., "Recent Research on Propellers in Nozzles", Journal of Ship Research, Vol. 1, Society of Naval Architects and Marine Engineers, July 1957.
20. Argyriadis, Doros A., "Modern Tug Design with Particular Emphasis on Propeller Design, Maneuverability, and Endurance", Society of Naval Architects and Marine Engineers Transactions, Vol. 65, 1957.
21. Fisher, R.E., "AGB 1 and 2, TMBModel 3705, Prediction of Performance with and without Ice Guards; Part 1 - Propulsion", David Taylor Model Basin Report 734, Sept. 1950.
- *22. Bradley, F.D., "Predictions of Performance with and without Ice Guards; Part 2 - Maneuvering", David Taylor Model Basin Report 745, Feb., 1951.

23. Gover, S.C., "Rolling Characteristics of Model 3705 Representing USS BURTON ISLAND (AG88)", David Taylor Model Basin Report 685, Feb., 1949.
- *24. Bradley, F.D., "Maneuvering Tests on Model 3705 Representing Twin Screw Ice Breakers (AGB1 and 2) with Inward Turning and Outward Turning Screws", David Taylor Model Basin Report 900, April, 1954.
- *25. Surber, W.G., Jr., "Maneuvering Tests of Model 3705-1 Representing the AGB-1 Class of Icebreakers with and without Kort Nozzles", David Taylor Model Basin Report 1181, Oct., 1957.
- *26. Hinterthan, W.B., and Heh, H.Y., "Prediction of Power Performances for AGB 1 Class Fitted with Kort Nozzles as Ice Guards from Tests with Model 3705-1", David Taylor Model Basin Report 1197, April, 1958.
27. Miscellaneous icebreaker design information, Naval Architecture files, Course XIII-A, Massachusetts Institute of Technology, Cambridge, Mass.
28. Troost, L., "Open Water Test Series with Modern Propeller Forms", North East Coast Institute of Engineers and Shipbuilders, Transactions, January, 1951.
29. Gertler, Morton, "A Reanalysis of the Original Test Data for the Taylor Standard Series", David Taylor Model Basin Report 806, March, 1954.

NUCLEAR POWER

30. Bonilla, C.F., editor, Nuclear Engineering, McGraw-Hill, New York, 1957.
31. Hogerton, J.F. and Grass, R.C., editors, Reactor Handbook, Vol. 2, Engineering, AECD-3646, Technical Information Service, U.S. Atomic Energy Commission, 1955.
32. Etherington, H., editor, Nuclear Engineering Handbook, McGraw-Hill, New York, 1958.
33. Glasstone, S. and Edlund, M.C., The Elements of Nuclear Reactor Theory, D. Van Nostrand, Princeton, N.J., 1952.
34. Kramer, A.W., Boiling Water Reactors, Addison-Wesley, Reading, Mass., 1958.

35. Benedict, Pigford and Mason, Nuclear Chemical Engineering, Ch. 3, "Fuel Cycles in Thermal Nuclear Reactors", McGraw-Hill, New York, 1960.
36. Keenan, J., Thermodynamics, Wiley, New York, 1941.
37. U.S. Atomic Energy Commission, Naval Reactors Branch, The Shippingport Pressurized Water Reactor, Addison-Wesley, Reading, Mass., 1958.
38. Sorenson, H.A., Gas Turbines, Ronald Press, New York, 1951.
39. Sargent and Lundy, "Power Cost Normalization Studies, Civilian Power Reactor Program-1959", U.S. Atomic Energy Commission, 1959.
40. Powell, S.C., "Estimation of Machinery Weights", New England Section, Society of Naval Architects and Marine Engineers, 1958.
41. Alexandrov, A.P., et al, "The Atomic Icebreaker Lenin", United Nations Second International Conference on the Peaceful Use of Atomic Energy, Proceedings, P/2140 USSR, 1958.
42. U.S. Atomic Energy Commission, Proceedings of the 1958 Nuclear Merchant Ship Symposium, TID-7563, 1959.
43. U.S. Atomic Energy Commission and U.S. Maritime Administration, "Three Design Studies for Selecting a Prototype Reactor for a Nuclear Tanker", TID-8528, 1960.
44. Smith, W.R. and Turner, M.A., Babcock and Wilcox Co., "Nuclear Merchant Ship Reactor; Design of NMSR Primary Shield", BAW 1101, 1958.
45. Babcock and Wilcox Co., "Nuclear Merchant Ship Reactor Project Quarterly Technical Reports", BAW-1102, BAW-1124, BAW-1138, 1958.
46. Landis, J.W., "The Power Plant for the First Nuclear Merchant Ship (N. S. SAVANAH)", Proceedings of the 1958 Nuclear Merchant Ship Symposium, U. S. Atomic Energy Commission, TID-7563, 1959.
47. General Dynamics Corporation, "Evaluation of Coolants and Moderators for the Maritime Gas-Cooled Reactor", GA 570, Dec. 10, 1958.

48. General Dynamics Corporation, "Maritime Gas Cooled Reactor Program, Quarterly Progress Reports", Periods ending 30 Sept. 1959; 31 Dec. 1959; and 31 March 1960, GA 1183, GA 1195, GA 1259.
49. Rohsenow, W.M., Lewins, J. and Barger, J.P., "Steady State Temperature Distribution in a Nuclear Reactor with End- and Center-Fed Coolant", Unpublished Notes, NT-269, Nuclear Engineering Department, M.I.T., 1957.
50. Fenech, Henri, Unpublished Notes and Problems on Gas Cooled Reactors for Course 22.23, M.I.T., Cambridge, Mass., 1960.
51. Wadleigh, K R., Unpublished lectures on gas turbine theory, Course 2.412, Massachusetts Institute of Technology, 1960.

ROLL STABILIZATION

52. Chadwick, J.H., Jr., "Ship Stabilization in the Large. A General Analysis of Ship Stabilization Systems", Final Report, Contract N6-ONR-25129 Department of Electrical Engineering, Stanford University, February 27, 1953.
53. Chadwick, J.H., Jr., and Morris, A.J., "Ship Stabilizer Cost in Weight, Space, and Power as a Function of System Parameters", Technical Report No. 3, Contract N6-ONR-25129 Department of Electrical Engineering, Stanford University, February 20, 1953.
54. Chadwick, J.H., Jr., "The Anti-Roll Stabilization of Ships by Means of Activated Tanks", Part D, Technical Report No. 15, Contract N6-ONR-251, Division of Engineering Mechanics, Stanford University, July, 1955.
55. Chadwick, J.H., Jr., "On the Stabilization of Roll", Society of Naval Architects and Marine Engineers Transactions, 1955.
56. Vane, Francis F., "Activated Antirolling Tanks Tested on the USS PEREGRINE (E-AM373)", David Taylor Model Basin Report C-356, June 1951.

57. Thews, J.G. and Landweber, L., "The Power Cost of Roll Stabilization on the Conte Di Savoia", David Taylor Model Basin Report 430, January 1947.
58. Church, J.W., "Analog Simulation of a Passive Anti-Rolling Tank System for a Missile-Range Ship", David Taylor Model Basin Report 1322, May 1959.
59. Hagen, Grant R., "Feasibility Studies of the Roll Stabilization of the USS BOSTON (GAC-1)", David Taylor Model Basin Report 950, September 1955.
60. Golovato, Paul, "A Full-Scale Evaluation of Passive Antiroll Tanks Aboard an AK-Type Ship", David Taylor Model Basin Report 1414, April 1960.

* Included to make the bibliography as complete as possible, but not available to the authors.

A P P E N D I C E S

APPENDIX A

BRAYTON CYCLE ANALYSIS

APPENDIX A. BRAYTON CYCLE ANALYSIS

Figure A-1 is the classical representation on temperature-entropy coordinates of the CICBTX cycle to be used. The nomenclature used is fairly standard in the field. The subscript "o" denotes stagnation states. In the following analysis, this subscript will be dropped for convenience, but all temperatures and pressures refer to stagnation states. The following definitions are necessary:

$$\eta_T = \frac{(h_{in} - h_{out})_{actual}}{(h_{in} - h_{out})_{isentropic}} = \text{turbine efficiency} \quad (1)$$

$$\eta_C = \frac{(h_{out} - h_{in})_{isentropic}}{(h_{out} - h_{in})_{actual}} = \text{compressor efficiency} \quad (2)$$

$$\eta_{cycle} = \frac{W_{net}}{Q_{in}} = \text{cycle efficiency} \quad (3)$$

$$\eta_x = \frac{T_5 - T_4}{T_8 - T_4} = \text{regenerator "effectiveness"} \quad (4)$$

$$\tau_{12} = \left(\frac{P_1}{P_2}\right)^{\frac{k-1}{k}} = \frac{T_1}{T_{2s}} \quad (5)$$

$$\gamma = \frac{\tau_{68}}{\tau_{14}} = \text{pressure loss parameter} \quad (6)$$

The total work done by the compressor,

$$W_c = (h_4 - h_3) + (h_2 - h_1).$$

To simplify the analysis, specify that $T_3 = T_1$ and that $\gamma_{12} = \gamma_{34}$. Then

$$W_c = \frac{c_p}{\gamma_c} (T_{2s} - T_1) + \frac{c_p}{\gamma_c} (T_{4s} - T_1).$$

In nondimensional form,

$$\frac{W_c}{c_p T_1} = \frac{2}{\gamma_c} (\sqrt{\gamma_{14}} - 1). \quad (7)$$

Similary the total turbine work,

$$\frac{W_T}{c_p T_1} = \gamma_T \frac{T_6}{T_1} \left(1 - \frac{1}{\gamma_{68}}\right).$$

which is

$$\frac{W_T}{c_p T_1} = \gamma_T \frac{T_6}{T_1} \left(1 - \frac{1}{\gamma_{14}}\right). \quad (8)$$

The net work performed by the cycle,

$$\frac{W_{net}}{c_p T_1} = \frac{W_T}{c_p T_1} - \frac{W_c}{c_p T_1}, \quad (9)$$

which is

$$\frac{W_{net}}{c_p T_1} = \gamma_T \frac{T_6}{T_1} \left(1 - \frac{1}{\gamma_{14}}\right) - \frac{2}{\gamma_c} \left(\sqrt{\gamma_{14}} - 1\right). \quad (10)$$

The heat added to the system is the enthalpy increase from the state leaving the regenerator, 5, to the state entering the turbine, 6.

$$Q_{in} = c_p (T_6 - T_5) = c_p (T_6 - T_4) - c_p (T_5 - T_4) \quad (11)$$

Normalizing and using the definition of equation (4);

$$\frac{Q_{in}}{c_p T_1} = \frac{T_6}{T_1} - \frac{T_4}{T_1} - \gamma_x \frac{T_8}{T_1} + \gamma_x \frac{T_4}{T_1} \quad (12)$$

From equations (1), (2), (5) and (6)

$$1 - \frac{T_8}{T_6} = \gamma_T (1 - \frac{1}{\sqrt{\gamma_{14}}}) \quad (13)$$

and

$$\frac{T_4}{T_1} - 1 = \frac{1}{\gamma_c} (\sqrt{\gamma_{14}} - 1). \quad (14)$$

Using equations (13) and (14) in (12);

$$\begin{aligned} \frac{Q_{in}}{c_p T_1} &= \left(\frac{T_6}{T_1} - 1 \right) - \frac{1}{\gamma_c} (\sqrt{\gamma_{14}} - 1) \\ &\quad - \gamma_x \frac{T_6}{T_1} \left\{ 1 - \gamma_T (1 - \frac{1}{\sqrt{\gamma_{14}}}) - \frac{T_1}{T_6} \left[1 + \frac{1}{\gamma_c} (\sqrt{\gamma_{14}} - 1) \right] \right\} \end{aligned} \quad (15)$$

The cycle efficiency as defined in equation (3) becomes, if $\gamma = \gamma_{14}$,

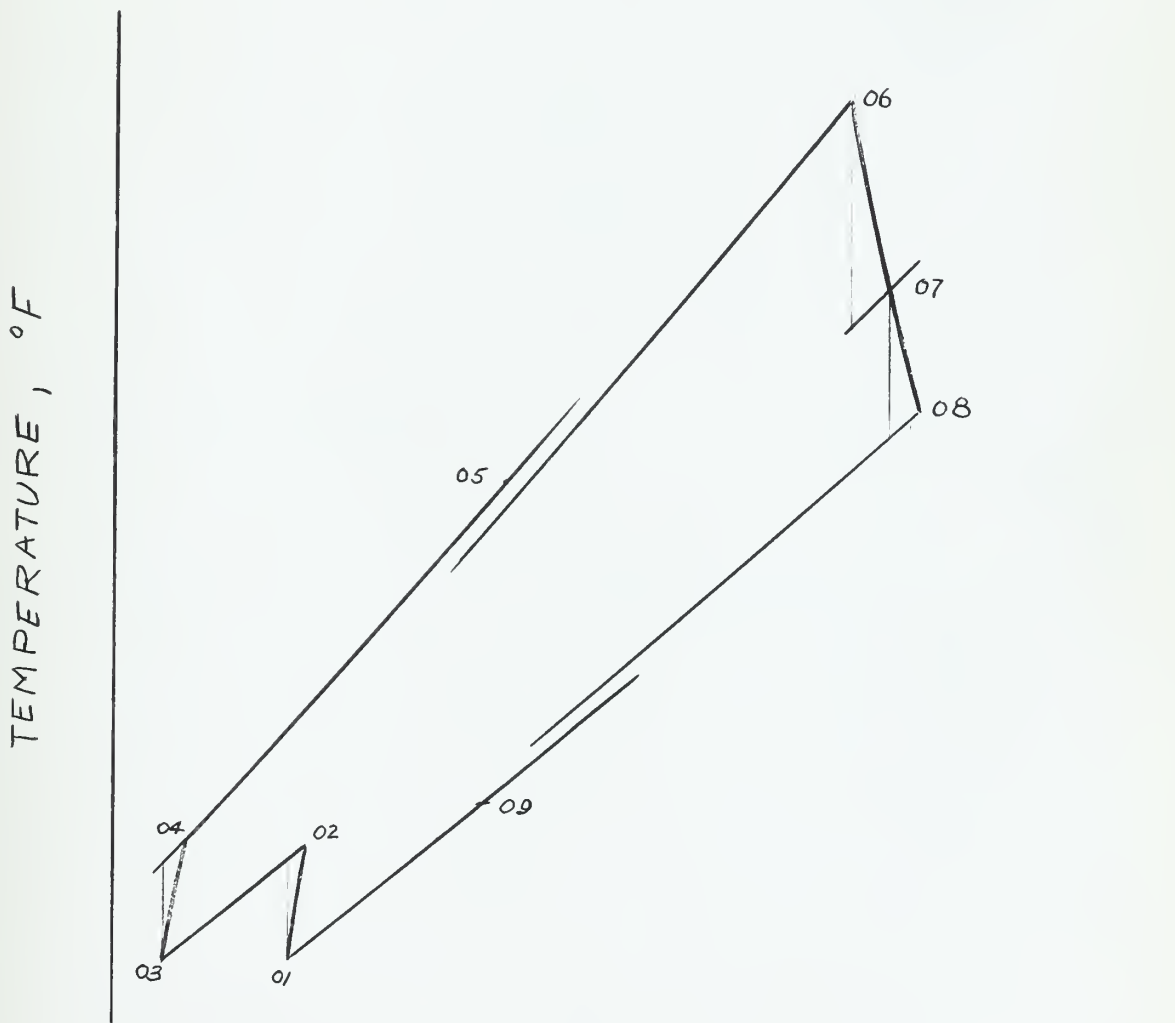
$$\eta_{\text{cycle}} = \frac{\frac{T_6}{T_1} \left(1 - \frac{1}{Y\gamma}\right) - \frac{2}{\eta_c} (\sqrt{\gamma} - 1)}{\frac{T_6}{T_1} - 1 - \frac{1}{\eta_c} (\sqrt{\gamma} - 1) - \eta_x \frac{T_6}{T_1} \left\{ 1 - \eta_T \left(1 - \frac{1}{Y\gamma}\right) - \frac{T_1}{T_6} \left[1 + \frac{1}{\eta_c} (\sqrt{\gamma} - 1) \right] \right\}}$$

(16)

In general, a maximum cycle efficiency exists for some value of γ . Equation (16) is so complex, that an analytic approach to find the optimum value of γ gets bogged down in the algebra. It is easier to plot several points and get a curve of cycle efficiency as a function of the isentropic pressure ratio across the compressor.

FIGURE A-1
TEMPERATURE - ENTROPY DIAGRAM
FOR CICBTX BRAYTON CYCLE

01-02	1 ST STAGE OF COMPRESSOR
02-03	INTERCOOLER
03-04	2 ND STAGE OF COMPRESSOR
04-05	REGENERATOR, COLD SIDE
05-06	REACTOR
06-07	1 ST STAGE OF TURBINE
07-08	2 ND STAGE OF TURBINE
08-09	REGENERATOR, HOT SIDE
09-01	PRECOOLER



APPENDIX B

DETAILS OF EHP CALCULATION

APPENDIX B. DETAILS OF EHP CALCULATION

$$EHP = \frac{R_t V}{550} \quad (1)$$

where

R_t = total resistance in pounds

V = ship speed in fps

$$R_t = C_t \frac{1}{2} \rho V^2 S \quad (2)$$

where

S = wetted surface area in ft^2

ρ = mass density $\frac{lbs \ sec^2}{ft^4}$

$$C_t = \text{total resistance coefficient} \quad (3)$$

$$= C_r + (C_f + \Delta C_f)$$

where

$$C_r = \frac{(Rr/\Delta)\Delta}{\rho/2SV^2}$$

Δ = displacement in lbs.

Rr/Δ = dimensionless residual resistance

C_f = frictional resistance coefficient

ΔC_f = roughness allowance

The values used were

$$LWL = 310'$$

$$\Delta = 9000 \text{ tons}$$

$$\rho = 1.995 \frac{\text{lbs sec}^2}{\text{ft}^4} \text{ for salt water at } 42^\circ\text{F.}$$

$$S = 24,700 \text{ ft}^2 \text{ from Gertler (29)}$$

Rr/Δ = values were taken from model test data presented by Dr. Jansson (10). He gives curves of Rr/Δ versus Froude number F where

$$F = \frac{V}{\sqrt{gLWL}}$$

Table B.1 gives the values taken from Dr. Jansson's work and also gives the resulting EHP at different ship speeds.

TABLE B.1

Residual Resistance Rr/Δ from Reference (10)
and EHP versus Ship Speed

V knots	F	Rr/Δ	EHP
14.0	.237	1.25	2080
16.0	.270	2.20	4000
18.0	.304	4.20	7250
20.0	.338	6.60	11640

APPENDIX C

Ice Breaking Analysis

APPENDIX C. ICEBREAKING ANALYSIS

C.1. Vinogradov's Analysis

A summary of Vinogradov's derivation is included in reference (1) and will not be repeated here. However, the final form of the equation given for the icebreaking force does contain an error. Using the same notation, equation 19 on page 12 of reference (1) should read:

$$p_1 = XT \pm \left\{ X^2 T^2 + \frac{Y}{A} W^2 \left[\frac{v_o^2}{g D} \frac{1 - (1-e^2) \sin^2}{-v_1^2} \right] \right\}^{\frac{1}{2}}$$

The error resulted from having the heavy square brackets misplaced.

The principle of conservation of energy is applied in the derivation. The energies accounted for are (1):

E_0 = kinetic energy of ship when the ice is first touched.

E_1 = kinetic energy of ship when ice collapses or at instant when the force is desired.

E_2 = energy derived from propeller thrust.

E_3 = energy dissipated by impact in non elastic collisions.

E_4 = potential energy of attitude and position acquired by ship.

E_5 = energy lost by friction.

The statement of conservation of energy with these terms becomes:

$$E_0 + E_2 = E_1 + E_3 + E_4 + E_5$$

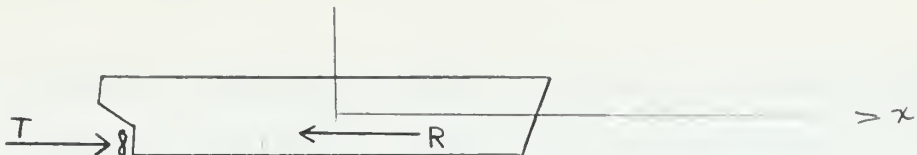
The energies are evaluated by various means and the resulting equation expresses the icebreaking force as a function of the displacement, thrust, and some physical parameters of the ship and some of the properties of the ice. The ice breaking force so derived is a static vertical force. This force, which is related to the potential energy of attitude and position of the ship, E_4 , is that force which would be required to change the draft and trim of the ship to the values of draft and trim at the time of interest. The force is usually, but not necessarily always, evaluated at that instant when the ship has lost all forward velocity, i.e., $E_1 = 0$, since by this analysis, this is the instant of maximum ice breaking force. No truly dynamic effects are accounted for in this analysis.

A preliminary analysis showed that the dynamic force would be greatest at, and immediately after, the instant of contact when the accelerations of the ship are maximum. At this instant the static force is zero, and by the time

the static force has built up to an appreciable fraction of its maximum value, the dynamic force has diminished to almost zero. Thus the neglect of dynamic forces is not an unreasonable approximation.

The velocity of the ship as it strikes the ice, v_o , is a significant parameter. Other treatments (1,4) assume a value for this speed, and when comparing the expected ice-breaking performance of different ships hold v_o constant. Since the calculated forces resulting from Vinogradov's equation are valid only for comparison, every effort must be made to keep the proper variables constant. It is argued that the distance available to accelerate, not the velocity achieved, is the true variable to keep constant when comparing different ships. In this way the power to displacement ratio is reflected in the kinetic energy of the initial contact as well as the thrust available to force the ship up on the ice.

In order to calculate the velocity a ship will attain after a charge of a given distance, the equations of motion must be solved. With the ship as a free body the following equation results:



T - thrust of propeller

R - resistance of ship

M - mass of ship

$$T - R = M \frac{d^2 x}{dt^2}$$

or

$$T - R = M \frac{dv}{dt} \quad (1)$$

Both the thrust and the resistance are functions of the ship's speed. These functions are fairly complicated, but they may be approximated by the following linearizations:

$$T(v) = T_0 + C_T \cdot v \quad (2)$$

$$R(v) = C_R \cdot v \quad (3)$$

In (2) T_0 is the maximum thrust at zero speed or the "bollard pull". C_T may be evaluated from a knowledge of the ship's propeller characteristic. In this case C_T has been evaluated for a propeller with somewhat the same characteristics as those of the USS GLACIER. Using the propeller charts of Professor Troost (28), a plot of thrust can be made against ship's speed. The slope of this curve

in the region of interest, near $v = 0$ is the coefficient C_T . As seen in Figure C-1, the curve is essentially linear in this region.

From the calculations and from Figure C-1,

$$T = 2 \left[1.86 \times 10^5 - 720 \cdot v \right]$$

where

$$T_0 = 3.72 \times 10^5 \text{ ft. lbs.}$$

and

$$C_T = -1440 \frac{\text{lbs.}}{(\text{ft/sec})}.$$

The coefficient, C_R , in equation (3) was evaluated by a similar process, using a derived curve of resistance as a function of ship speed. Note again in Figure C-2 that the linear approximation is good in the region of interest. From this curve, $C_R = 1650 \frac{\text{lbs.}}{(\text{ft/sec})}$. With the thrust and resistance in the form of equations (2) and (3), equation (1) becomes

$$M \frac{dv}{dt} + (C_R - C_T)v - T_0 = 0. \quad (4)$$

The solution of this for $v = 0$ at time $t = 0$ is

$$v = \frac{T_0}{(C_R - C_T)} \left[1 - e^{-\frac{(C_R - C_T)t}{M}} \right]. \quad (5)$$

For simplification let $C = C_R - C_T$

then

$$v = \frac{T_o}{C} \left(1 - e^{-\frac{C/Mt}{C}} \right) \quad (6)$$

and

$$x = \frac{M T_o}{C^2} \left(e^{-\frac{Ct}{M}} - 1 \right) + \frac{T_o}{C} t \quad (7)$$

The procedure followed was to select an arbitrary charge distance, $X_o = 100$ feet, and to solve equation (7) by trial and error to find the time to go this distance. This time was then used in equation (6) to find the velocity, V_o , attained after a full power charge of X_o feet from a complete stop. This velocity was then used in Vinogradov's equation.

The important ship and ice parameters in Vinogradov's equation are listed below with explanations as required. The symbols are those used in the IBM 709 Fortran program which was used to investigate the effects of varying some of these parameters.

DISP	Displacement of ship in tons.
THRSTO	Thrust at zero speed.
C	Resistance coefficient, $(C_R - C_T)$, as determined above.
PHI D	Angle of bow with horizontal in degrees.
XO	Distance of charge to ice in feet.
CB	Block coefficient.

CWP	Waterplane coefficient.
Q	Position of LCB from forward perpendicular.
GML	Longitudinal metacentric radius.
D	Draft
BETAD	A measure of the angle of flare at the bow. β is the angle between a normal to the bow plating and the ϕ plane measured in a plane perpendicular to the stem.
	$\tan \frac{\alpha}{2} = \sin \phi \cos \beta$
	$\alpha/2$ is one-half the angle of entrance
CR	A function of the coefficient of restitution of the ice, $CR = (1-e^2)$. This represents the fraction of kinetic energy of the ship dissipated in the collision with the ice.
F	The coefficient of friction for the sliding motion between the ice breaker's bow and the ice.

The program was set up to systematically vary DISP and PHID with other values changing in correct proportions to DISP. A series of data decks was used to investigate the effects of varying THRSTO, CWP and Q at various values of DISP and PHID.

Although not necessary for the general use of the program, certain assumptions were made to simplify the process of systematically varying the displacement and other parameters. It was assumed that the ratios Q/GML and Q/D would be constant for similar ships of different displacements. Unless data is specifically introduced to the contrary, the program will

keep the ratio THRSTO/DISP constant as DISP is varied by the program.

The two ice parameters, CR and F merit further discussion. For all calculations performed, e was taken as 0.95 (1) which means that $(1 - e^2)$ or 9.75% of the initial kinetic energy is completely lost at impact. Calculations were made with $F = 0.20$ (1,10) and (inadvertently) with $F = 0.0$. Any value chosen for these factors may be nearly right at one time and grossly in error another time due to different ice conditions. An approximate method to account for the effect of snow cover on an icebreaker's performance is seen in the values chosen for CR and F. A heavy snow cover will adsorb the impact of the icebreaker without transmitting the impact of the ice. Hence a simulation of snow cover would be to reduce e towards zero at which value all of the kinetic energy of the ship is dissipated inelastically. Snow, clinging to the sides of the ship tends to drag or slow the ship, and actually an increased value of F is present.

APPENDIX D

Reactor Thermal Design Techniques Used

APPENDIX D. NOMENCLATURE

A_{ht} = heat transfer area of a fuel element or channel, ft^2

A_f = flow area of a fuel element or channel, ft.^2

C_p = specific heat at constant pressure. $\text{BTU/lb.} - ^\circ\text{F.}$

D = diameter, ft.

D_e = equivalent diameter ft. $D_e = \frac{4 \text{ area}}{\text{wetted perimeter}}$

F_c hot channel factor for coolant bulk temperature rise.

F_e = hot channel factor for film temperature rise.

F_f = hot channel factor for fuel temperature rise.

h = surface film coefficient of heat transfer $\text{BTU}/\text{ft}^2 \cdot \text{hr.}^\circ\text{F.}$

J_0 = zeroth order bessel function of the first kind.

J_1 first order bessel function of first kind.

k = thermal conductivity $\text{BTU}/\text{ft} \cdot \text{hr.}^\circ\text{F.}$

L/D = length to diameter ratio.

N = number of fuel elements in reactor.

n = number of fuel rods in element.

Nu = Nusselt number $Nu = \frac{hk}{D}$

P = thermal power of reactor M watts or $\text{BTU}/\text{hr.}$

Pr = Prandtl number $Pr = \frac{C_p \mu}{K}$

(\bar{q}/A) = average heat flux $\text{BTU}/\text{ft}^2 \cdot \text{hr.}$

$(q/A)_{\max}$ = maximum heat flux $\text{BTU}/\text{ft}^2 \cdot \text{hr.}$

r = radius. ft.

R_o = physical radius of reactor core.

R' = extrapolated radius of reactor core. $R'_o = R_o +$ reflector savings.

Re = Reynolds number $Re = \frac{\rho V D}{\mu}$

t = temperature °F.

t_c = bulk coolant temperature, °F.

t_{c1} = bulk coolant temperature at reactor outlet, °F.

t_f = fuel temperature, °F.

t_w = wall or cladding temperature at surface, °F.

t_{w_o} = maximum t_w , °F.

V = velocity, ft/sec.

w = mass rate of flow per fuel element or channel, lbs/hr. This must be consistent with A_f and A_{ht} .

w_T = total mass rate of flow through reactor, lbs./hr.

z = axial direction from mid-plane of core, ft.

z_o = axial distance from mid-plane to physical end of core, $z_o = 1/2$ core height.

z' = $z' = z_o +$ reflector savings.

Δt_c = bulk temperature rise in coolant. May apply to a particular element or whole reactor, °F.

Δt_e = temperature rise across surface film, $\Delta t_e = (t_w - t_c)$, °F.

Δt_f = temperature rise to center of fuel, °F.

γ_T = turbine thermodynamic efficiency, $T = \frac{h_1 - h_2}{h_1 - h_{2s}}$

γ_{T-G} = mechanical and electrical efficiencies of main propulsion generator units.

γ_M = mechanical and electrical efficiencies of main propulsion motors.

μ = viscosity, ft.lbm/hr.ft.

ρ = density, lbm/ft²

ϕ = neutron flux. neutrons/cm²-sec.

$\bar{\phi}$ = **average** neutron flux.

ϕ_o = maximum neutron flux.

D.1. Temperature Distribution

The rate of heat generation within a reactor at a point is proportional to the rate of nuclear fissions at that point. This is expressed

$$P = \text{constants } \phi \sum_f \delta \text{ Vol.}$$

For reactors which have a "single region" or are "uniformly loaded" the fission cross-section, \sum_f , is independent of gross position within the reactor. The ideal distribution of flux within such a reactor is the "chopped cosine distribution".* Thus the ideal power distribution may be expressed analytically and integrated averages obtained. However, the presence of adsorbers in the reactor core such as control rods cause radical departures of the flux from the ideal distribution. This treatment will consider an average fuel element. The average defined by the total power of the reactor and its volume. This average fuel element will, however, be endowed with the chopped cosine flux distribution in the axial direction. The results of calculations, i.e., coolant or wall temperature, based on these average fuel elements will be corrected for the radial flux distribution and other unknowns by the application of "hot channel factors".

* Actually the distribution is chopped cosine in a rectangular reactor or in the axial direction of cylindrical reactors. The radial distribution in a cylindrical reactor is "chopped J_0 Bessel function."

Following the development of Rohsenow, et al (49), the temperature rise in the coolant at any point, z , along the channel is

$$t_c - t_{c1} = \frac{\Delta t_c}{2} \left[\frac{\sin \frac{\pi}{2} \frac{z}{z'}}{\frac{z}{z'}} + 1 \right] \quad (1)$$

and the film temperature rise is

$$t_w - t_c = \frac{\Delta t_c}{2} \pi \frac{z_o}{z'} \frac{wC_p}{A_{ht}h} \left[\frac{\cos \frac{\pi}{2} \frac{z}{z'}}{\frac{z}{z'}} \right] \quad (2)$$

The sum of these two temperature rises is $(t_w - t_{c1})$, which will allow the calculation of the maximum wall temperature, t_{w_o} .

$$t_w - t_{c1} = \frac{\Delta t_c}{2} \left[\frac{\sin \frac{\pi}{2} \frac{z}{z'}}{\frac{z}{z'}} + 1 + \pi \frac{z_o}{z'} \frac{wC_p}{A_{ht}h} \frac{\cos \frac{\pi}{2} \frac{z}{z'}}{\sin \frac{\pi}{2} \frac{z}{z'}} \right]. \quad (3)$$

Still following Rohsenow, these expressions may be put in the form

$$P = \sin \frac{\pi}{2} \frac{z}{z'} + Q \cos \frac{\pi}{2} \frac{z}{z'}. \quad (4)$$

For equation (3)

$$P = \left[\frac{(t_w - t_{c1})}{\Delta t_c} - 1 \right] \sin \frac{\pi}{2} \frac{z_o}{z'}. \quad (5)$$

and

$$Q = \pi \frac{z_o}{z'} \frac{w C_p}{A_{ht} h}.$$

Differentiation and manipulation of equation (4) will lead to the result

$$P_{max}^2 = 1 + Q^2. \quad (6)$$

Using (6) with values of P and Q from (5) and using the definition of tw_o

$$(tw_o - tc_1) = \frac{\Delta tc}{2 \sin \frac{\pi}{2} \frac{z_o}{z'}} \left\{ \left[\left(\frac{\pi w C_p}{A_{ht} h} \cdot \frac{z_o}{z'} \right)^2 + 1 \right]^{\frac{1}{2}} + \sin \frac{\pi}{2} \frac{z_o}{z'} \right\} \quad (7)$$

In the designs to be investigated here, the average Δtc has been specified. The other variables, z_o , z' , w , A_{ht} and h are directly or indirectly functions of the size of reactor chosen.

The surface film coefficient of heat transfer, h , may be calculated by one of several correlations (30,31,32). The Colburn analogy will be used here. This is

$$Nu = 0.023 R_e^{0.8} P_r^{1/3}.$$

This correlation is based on empirical data for turbulent flow heating inside a pipe, with $Re > 10^4$ and

$0.7 < Pr < 120$. There will be some unknown error introduced by using this correlation for flow outside of the fuel rods, but the use of an equivalent diameter is reasonably justified and an accepted practice. Actual experimental data, for the geometry to be used, would be necessary to determine a more accurate correlation. In dimensional form the Colburn analogy becomes:

$$h = 0.023 \frac{k}{D_e} \left(\frac{w D_e}{A_f \mu} \right)^{0.8} P_r^{1/3} \quad (8)$$

Using equation (8) in (7) a working equation evolves:

$$t_{wo} - t_{cl} = \frac{\Delta tc}{2 \sin \frac{\pi}{2} \frac{z_o}{z'}} \left\{ \left[\frac{\pi C_p}{A_{ht}} \frac{z_o}{z'} \frac{D_e}{K} \frac{P_r^{-1/3}}{0.023} \left(\frac{A_f \mu}{D_e} \right)^{0.8} w^{0.2} \right]^2 + 1 \right\}^{\frac{1}{2}} + \frac{\Delta tc}{2 \sin \frac{\pi}{2} \frac{z_o}{z'}} \quad (9)$$

For a given configuration, only z_o , z' and w depend upon the size of the reactor. w is determined by the relationship:

$$w = \frac{w_T}{N} . \quad (10)$$

w_T is calculated from the total power of the reactor by

$$P = w_T C_p \Delta tc. \quad (11)$$

D.2. Hot Channel Factors

Hot channel factors for the PWR designs have been taken from Bonilla (30) and are considered conservative. The hot channel factors are divided into three categories. First, those that derive from uncertainties in the coolant bulk temperature rise in a channel, F_c . Second, those that reflect uncertainties in the temperature rise across the film of coolant at the wall, F_f . Third, those that take into account uncertainties in the temperature rise to the center of the fuel, F_e .

F_c takes into account known and unknown flux deviations and physical eccentricities in dimension and fuel concentration. F_f attempts to correct for the same factors as F_c in addition to the uncertainty of prediction of h . F_e corrects for the same factors as F_c in addition to uncertainties in the physical properties of the fuel and its dimensions. From Bonilla (29), page 443:

$$F_c = 1.95$$

$$F_f = 2.28$$

$$F_e = 1.76$$

These factors are applied to the nominal value of the appropriate temperature rise at the location of the "hot spot" being investigated.

The axial location of the maximum wall temperature, from Rohsenow et al (43) is:

$$z_{H.S.} = z' \frac{2}{\pi} \tan^{-1} \frac{1}{Q} = \frac{z' 2}{\pi} \tan^{-1} \left(\frac{A_{ht} h |z'|}{w C_p z_o} \right). \quad (12)$$

Δt_c at this point can be calculated from equation (1) and

$$\Delta t_f = (t_{wo} - t_{cl}) - \Delta t_c = t_{wo} - t_c. \quad (13)$$

Finally,

$$t_{wo} = 1.95 (\Delta t_c) + 2.28 (\Delta t_f) + t_{c_1}. \quad (14)$$

Hot
Spot

The hot channel factors used for the GCR are those used in the prototype calculations and are much less conservative (47). There is some controversy over the method of determining and applying hot channel factors. The current trend is toward a rational reduction of these through the application of statistical techniques (30).

From reference (47):

$$F_c = 1.15$$

$$F_f = 1.63$$

D.3. Heat Flux

The average heat flux, (\bar{q}/A) is related to the size, power and geometry of the reactor.

$$(\bar{q}/A) = \frac{P}{N A_{ht}} \quad (15)$$

For the uniformly loaded reactors being considered,

$$(q/A)_{max} = \frac{\phi_o}{\phi} (\bar{q}/A) \quad (16)$$

If the flux distribution is known, $\frac{\phi_o}{\phi}$ may be calculated. For any distribution other than a simple chopped cosine or Bessel function, the integrations must be made by a computer. Most flux distortions tend to depress the flux, and control rods are usually centrally located where the flux is the highest. Therefore the analytic expression for ϕ_o/ϕ will be larger than the actual ratio. That is, the actual flux will probably be less peaked in the center of the reactor, and the $(q/A)_{max}$ calculated using the analytical value of $\frac{\phi_o}{\phi}$ will be higher than the actual maximum heat flux.

For a right circular cylindrical reactor, reflected on both ends and sides, the ideal flux distribution is:

$$\phi = \phi_o \cos \left(\frac{\pi}{2} \frac{z}{z'} \right) J_o \left(\frac{2.405 r}{R'} \right). \quad (17)$$

The volume weighted average flux is:

$$\bar{\frac{\phi}{\phi_o}} = \frac{\int_0^{R_o} \int_{-z_o}^{+z_o} \cos\left(\frac{\pi}{2} \frac{z}{z'}\right) J_o\left(\frac{2.405}{R'} r\right) 2\pi r dr dz}{\int_0^{R_o} \int_{-z_o}^{+z_o} 2\pi r dr dz} \quad (18)$$

This integrates to:

$$\bar{\frac{\phi}{\phi_o}} = \frac{R' z' 4}{R_o z_o \pi (2.405)} \sin\left(\frac{\pi}{2} \frac{z_o}{z'}\right) J_1\left(\frac{2.405 R_o}{R'}\right) \quad (19)$$

The Jens-Lottes correlation is used to establish the burnout heat flux (30). The correlation is:

$$(q/A)_{bo} = 10^6 a_3 \left(\frac{\rho V}{10^6}\right)^m (\Delta t_{sub})^{0.22} \quad (20)$$

a_3 and m are determined by the pressure as follows:

p	a_3	m
500	0.817	0.16
1000	0.626	0.28
2000	0.445	0.50
3000	0.250	0.73

This equation is based on experiments with the variables limited as follows:

- (a) water in 0.226" I.D. tubes.
- (b) flow at 5 to 30 fps.
- (c) $L/D = 110$.
- (d) $p = 250$ to 3000 psia.
- (e) $\Delta t_{sub} = 3$ to 160°F .

This correlation is easy to use and accounts for some of the most important variables of the burnout phenomenon. However, there are other variables, particularly the texture of the heating surface and the flow geometry, that are not accounted for in equation (20). The use of this correlation for materials and shapes other than those actually used in the experiments must be done with the realization that errors of unknown magnitude may enter the results.

APPENDIX E

COST ESTIMATING PROCEDURE

APPENDIX E. COST ESTIMATING PROCEDURE

E.1 General

Engineering cost estimating falls into either of two categories. The first is the group of estimates based on an almost firm and detailed design. These estimates are usually accurate within plus or minus ten percent limits. The second category of estimating is the class of estimates based on a very rough design embodying the major concepts only. These estimates can only reasonably be made by "old pros", that is, engineers with a large backlog of experience in the particular field of interest. These estimates may be in error by as much as a factor of two or five or more. However, if the knowledge of the estimator is considerable and specific, and the original concepts are not changed in the realization of the design, the plus or minus ten percent confidence limits may well apply in this case.

Unfortunately, this report embodies neither the complete detailed design of the first case mentioned above, nor is there available a great backlog of experience and information to be drawn upon. The estimates developed in this appendix are not offered to represent the actual cost of the equipment to any particular accuracy. The

estimates are offered as a means of comparing the costs of components and the whole concept.

E.2 Reactor Costs

These three reactors have one major component in common. This is the pressure vessel, which in all three cases is large, must withstand a large pressure and is exposed to intense radiation and thermal stresses. This pressure vessel is an expensive item and it is argued that its cost is proportional to the total reactor cost excluding the fuel elements. All the reactor internal construction and the expensive control rod mechanisms and drives are lumped into a single reactor cost, C_R .

The cost function can be assumed to be functions of many different variables. However the number of variables chosen must be limited so the problem can be solved with data available. In this case the pertinent variables were chosen to be the size or volume enclosed by the pressure vessel and the pressure it must withstand. By limiting the variables to these two, three tacit assumptions are made:

- 1) Similarity exists in the control systems.

- 2) Similarity exists in the construction of reactor internals.
- 3) Similarity exists in the method and degree of support of the pressure vessel.

These are not unreasonable restrictions to place upon the designs, but they must be borne in mind.

The reactor cost function was assumed to be of the form:

$$C_R = K_R \left(\frac{P+100}{1000} \right)^n \left(\frac{Vol}{1000} \right)^m$$

C_R = cost of reactor in dollars

K_R ; m ; n = constants to be evaluated

P = operating pressure of reactor in psia

Vol = enclosed volume of pressure vessel in ft^2

Data from reference (37), TID-8528 were used to evaluate the constants K_R , m and n . The data of TID-8528 are only estimates, but it is felt that these estimates are more nearly in the first category of estimates discussed in Section E.1. The influence of company partisanship has been reduced in TID-8528 by the refereeing of the U.S. Atomic Energy Commission and the U.S. Maritime Administration.

The values of K_R , m and n used came from the solution of three simultaneous equations. Using the data from TID-8528:

$$K_R = 586,000$$

$$m = 0.765$$

$$n = 0.898$$

and

$$C_R = 586,000 \left(\frac{Vol}{1000} \right)^{0.765} \left(\frac{p+100}{1000} \right)^{0.898}$$

The construction of the GCR reactor core is definitely not similar to that of the PWR. There is no justification to use the cost function just derived for estimating GCR costs. The approach taken was to re-evaluate the constant K_R with the estimates of reference (47). Enough data to reevaluate the exponents m and n were not available and it was reasoned that these might not be too different for the two different reactor concepts. The final cost function as used for the GCR is:

$$C_R = 1,450,000 \left(\frac{Vol}{1000} \right)^{0.765} \left(\frac{p+100}{1000} \right)^{0.898}$$

E.3 Heat Exchanger Costs

The main parameter reflecting heat exchanger costs is, of course, the heat transfer area. Another parameter which influences the cost is the pressure difference between the tubes and shell of the heat exchangers. The cost function was assumed to be of the form:

$$C_x = K_x (A_x +) \Delta P + 10 \right)^n$$

C_x = heat exchanger cost in dollars.

K_x ; m ; n = constants to be evaluated.

A_x = heat transfer area in ft^2 .

ΔP = pressure difference between two sides of heat exchangers.

Data from reference (39), SL-1674, were used to evaluate K_x , m , and n . These are based upon steam generator costs for four-loop stationary power plants. The evaluation of the constants resulted in:

$$C_x = 113 (A_x)^{0.684} (\Delta P + 10)^{0.50}$$

In this form, A_x is the area per loop and the resulting cost is cost per loop.

The reference heat exchanger is a steam generator, with the complexities of risers, downcomers, and provisions for separating the moisture. The regenerator, precooler, and intercooler of the GCR are simple shell and tube type heat exchangers, and are much less expensive. The constant, K_x , was reevaluated from MGCR data (47) and the resulting cost function is:

$$C_x = 8.93 (A_x)^{0.684} (\Delta P + 10)^{0.50}$$

Again the heat transfer area and costs are per loop.

E.4 Main Propulsion Equipment Costs

An attempt was made to follow the same procedure used above to establish a cost function for the steam power plant. The important parameter in this case was assumed to be the exhaust annulus area of the low pressure turbine. This approach was pursued and several forms of cost functions resulted for trial and rejection.

This approach might be reasonably valid for turbines made by the same manufacturer and for similar service. However, the exhaust annulus areas were not given in any of the cost data references, and assumptions of the steam leaving losses were necessary to calculate the areas. The pyramiding assumptions led to a situation where almost any desired cost for a given steam plant could be calculated.

The situation was resolved by a conference with personnel of General Electric's Medium Steam Turbine, Generator and Gear Department in Lynn, Massachusetts. The estimates from this source are in Table E-1, and are probably within fifteen percent of actual current costs.

The GCR propulsion equipment costs were estimated based on the estimates of reference (47). The major change from the conditions of the MGCR of reference (47) is not power capacity, but the complexity of four

complete units instead of one large one. Table E-2 lists the cost estimates of the prototype and the estimates used in this paper.

TABLE E-1

Cost Estimates for 7500 H.P. Cross-Compounded Steam Turbine and Auxiliary Equipment

Steam Conditions	546 psia 476°F	900 psia 532°F
Basic Turbine Cost	364,000	392,000
Two Single Reduction Gears	120,000	120,000
Condenser and Air Ejector	110,000	110,000
Lube Oil System	11,000	11,000
Main Feed Pump with Motor and Control	18,000	22,000
Piping, Valves, etc.	60,000	70,000
De-aerating Feed Heater	32,000	32,000

TABLE E-2

Cost Estimates for Gas Turbine Cycle Power Producing Equipment

System	Single, 20,000 HP Unit (47)	4 - 7500 HP Units
Turbo Compressors	644,000	1,200,000
Valves and piping	102,000	200,000
Insulation	33,000	60,000
Coolant Storage System	116,000	150,000
Lube Oil System	125,000	250,000
Reduction Gear	810,000	1,000,000

E.5 Fuel Cycle Costs

The fuel cycle costs are directly related, through reactor physics, to the nuclear properties of materials in the reactor, their concentration in the reactor and to the spacing of fuel elements, or the lattice parameters, of the reactor. In this treatment, this dependence has been avoided by relying on the results worked out for the prototypes. Thus, with the assumed enrichment of fuel, a given reactor may not have a long enough lifetime to provide the fuel burn-up assumed. On the other hand, the reactor may reach the allowable burn-up with excess U-235 left over. It is felt, however, that within the range of the extrapolations, these errors will be no greater than others introduced elsewhere.

The initial inventory of fuel in the PWR reactors was calculated by simply figuring how much UO_2 would be required to fill the fuel rods. A density of 10.4 grams/cm³ was used for the UO_2 . The GCR fuel is a mixture of UO_2 and Al_2O_3 and the inventory was based on an assumed volume concentration of 20% UO_2 .

The initial value of the fuel was based on the current AEC prices for enriched UF_6 , as reported in reference (35). This UF_6 must then be converted to UO_2 and fabricated into pellets of the desired size. A cost of \$90/Kg U, including conversion to UO_2 , was chosen from data in reference (35).

Enriched Uranium is not sold by the AEC but leased at 4% per year on the initial value of the Uranium. The time the charge is based on is the total time from the time the user gets UF_6 until UF_6 is returned for credit. This time therefore includes all fabrication and processing times as well as the "cooling off" time the highly radioactive fuel elements must undergo before they can be handled. For these calculations, it was assumed that Government agencies would be required to pay the fuel use charge, just as civilian companies must.

A charge for the actual amount of Uranium burned is levied by the AEC in addition to the fuel use charge of 4%. This burn-up charge is the difference in value between the returned UF_6 and the UF_6 originally procured from the AEC. The final value is determined from the same tables that determined the initial value. An extract of these tables is given in Table E-3.

TABLE E-3 (condensed from ref. 35)

Base Charge for Uranium Established by U.S.A.E.C.

In form of UF_6 , FOB, Oak Ridge, Tennessee

Weight Fraction U-235	\$/K gm Uranium	\$/gm U-235
0.00715 (natural U)	39.25	5.52
0.01	75.75	7.58
0.03	375.50	12.52
0.10	1529.00	15.29
0.95	16258.00	17.11

Note that the cost of Uranium increases sharply with enrichment.

The spent fuel rods must be stored safely somewhere while the shorter lined and more intense radioactivity dies out. A charge of \$12.45/K gm of fuel is quoted for this storage including shipping to the reprocessing plant.

To date no commercial attempts have been made to reprocess fuel elements to recover the Uranium. The A.E.C. does this with charges based on a hypothetical plant with a capacity of 1000 Kg of Uranium per day. The charge is \$15,200/day with eight days added to the processing time for decontamination. The result of this process is $\text{UO}_2(\text{NO}_3)_2$ which must be converted to UF_6 before the cycle has been completed and it is accepted by the A.E.C. The cost of this conversion, again accomplished by the A.E.C., is \$5.60 per Kg of Uranium.

The production of Plutonium in a reactor has several effects. The process begins as a neutron is adsorbed by a U-238 nucleus. This has a deleterious effect on the neutron economy. However one of the eventual products of this reaction is Pu-239 which is a fissile material itself. The presence of Pu-239 adds some lifetime to the core due to fissions of Pu-239 in place of U-235 and the presence of Pu-239 adds value to the spent fuel elements. The current price guaranteed by the A.E.C. until 1963 is \$30 per gram Pu. After that time, it is expected that the

price will be about \$12 per gram (35). The latter price has been used in this report.

A knowledge of the energy released in a fission enables the conversion of burn-up in units of MW-Days/Ton, E, to burn-up measured as a fraction of Uranium fissioned, β . Using A as the atomic weight of the fuel, usually about 238,

$$192 \frac{\text{Mev}}{\text{fission}} \times \frac{6.023 \times 10^{23} \text{ fissions}}{\text{g. atom fissioned}} \times \frac{1.854 \text{ Mev}}{\text{MW - Day}}$$

$$= 214.5 \frac{\text{MW - Days}}{\text{g. atom fissioned}}.$$

Therefore,

$$E \left(\frac{\text{MW-Days}}{\text{TON}} \right) = \frac{214.5 \text{ MW-Days}}{\text{g. atom fissioned}} \times \frac{1}{A \text{ g}} \times \frac{10^6 \text{ g}}{\text{TON}} \times \beta \frac{\text{g. fissioned}}{\text{g}}$$

$$= \frac{2.145 \times 10^8}{A} \beta.$$

For $A \approx 238$

$$E = 9.0 \times 10^5 \beta.$$

The amount of fuel remaining, R, after a burn-up of β is approximately

$$R = (1 - \beta)I.$$

where I is the initial inventory of fuel.

The final enrichment after burn-up β is approximately

$$x_f = \frac{x_i - \beta}{1 - \beta}.$$

Where X_f is the final enrichment and X_i is the initial enrichment. These approximations neglect the effect of Pu^{239} fissions. In certain reactors this effect is significant, but in the kinds of reactors considered, this effect is small.

These relations enable calculation of the amount and enrichment of the remaining fuel and therefore the burn-up charge.

APPENDIX F

Details of Roll Stabilization Calculations

APPENDIX F. DETAILS OF ROLL STABILIZATION CALCULATIONS

NOTATION

This notation is in agreement with the notation of reference (59) Hagen,

<u>Symbol</u>	<u>Description</u>
ψ	Effective instantaneous waveslop amplitude, in radians
ψ_{\max}	Actual capacity of stabilizer
ψ_{static}	Maximum (static) capacity of tank stabilizer
ψ_0	Required peak capacity of tank stabilizer at any time
ω	Apparent frequency of waves
ω_s	Natural frequency of ship in roll
ω_t	Natural frequency of tanks
ω_{st}	"Decoupling" frequency
Ω	Normalized apparent frequency of waves = ω/ω_s
Ω_t	Normalized frequency of tank fluid = ω_t/ω_s
Ω_{st}	Normalized "decoupling frequency" = $\omega_{\text{st}}/\omega_s$
Δ	Displacement of ship in long tons
VOL	Volume displacement of ship
B	Maximum beam of ship at load waterline
\overline{GM}	Transverse metacentric height
T_s	Natural roll period of ship
b	Normalized beam of ship = $B/(\text{VOL})^{1/3}$
R	Radius of roll = $(T_s/2\pi)^2 g$

P_o	"Standard Horsepower" = $\Delta(VOL)^{1/6} (g)^{1/2} 2240/550$
θ	Angle of roll of ship
α	Angle of tank-water level with respect to ship
K_{ss}	Ship-sea coefficient. Torque of waves = $K_{ss} \psi$
K_s	Static righting coefficient of ship. Righting moment = $K_s \theta$
K_t	Static righting coefficient of tank water. Torque = $K_t \theta$
A_o	Average cross-sectional area of side tank
A_s	Area of U-tube at any point
A_d	Cross-sectional area of cross duct
D_s	Perpendicular distance from center of rotation to any tank-water element
y_o	Average athwartships dimension of side tank
L	Tank lever arm
H	Maximum change of water level in side tanks
$S' & S''$	"Weighted" lengths of U-tube
n	Number of sets of U-tubes
K_p	Power coefficient
Q'_t	Magnification ratio of tanks (without pump)
ρ_{fl}	Density of stabilizing fluid
ρ_{sw}	Density of salt water

Figure F-1

Cross-Section of Ship and Tanks, Showing Nomenclature

θ = angle of roll of the ship

ϕ = angle of water surface against deck

L =lever arm of tank

D_s =perpendicular distance from "virtual" center of rotation to tangent at any point on trajectory

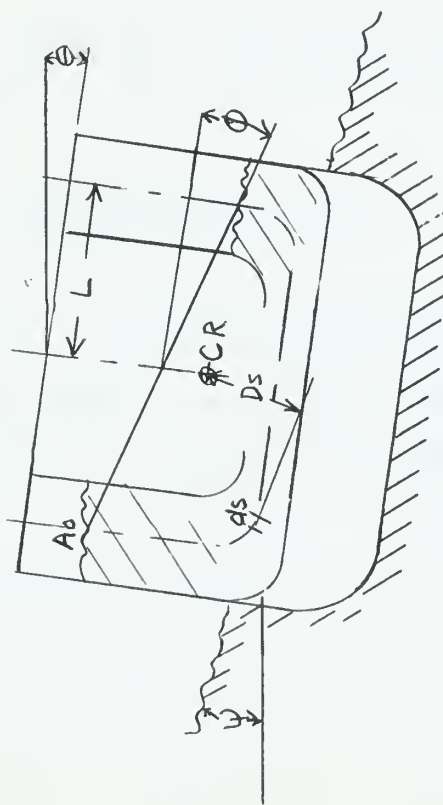
ψ = effective waveslope

A_o =tank cross-section

A_s =tank cross-section at any point s

A_D =duct cross-section

f_{fl} = density of stabilizing fluid



F.1 Activated Tank System Based on the Characteristics of the USS GLACIER (AGB-4)

Table III-5 gives the particulars for the GLACIER. Figure III-25 shows the general location of the heeling tanks and Figure III-26 gives the dimensions of one set of tanks. These are presented near the beginning of Section III.4. Figure F-1 shows a general cross-section of a ship and tanks, showing the nomenclature used in the calculations.

Capacity

Chadwick (53) offers the following empirical formula as a guide in selecting a desirable system capacity:

$$\text{Desirable capacity} = .36 / \log_{10} \Delta \text{ radians} \quad (1)$$

For the GLACIER

$$\text{Capacity} = \frac{(.36 \times 57.3)}{\log_{10} 8640} = 5.2^\circ$$

Since almost the sole purpose of stabilizing an icebreaker is for personnel comfort, it is felt that this is an upper limit on the capacity required. For initial calculations a

$$\text{Capacity} = 5.0^\circ = \psi_{\text{max}}$$

will be used.

Geometry

Table F-1 compares the critical ship parameters of the GLACIER to the average characteristics of a wide group of naval vessels given by Chadwick (53). Refer to the notation list for the definition of terms.

TABLE F-1
Comparison of Critical Ship Parameters

	GM/B	b	r	B/R	$\frac{GM}{B \log_{10} \Delta}$
Average	.0729	.087	2.1	0.44	.0176
GLACIER	.1555	1.102	1.215	.907	.0394

Calculations for the parameters of the GLACIER are as follows:

$$b = \frac{B}{\sqrt[3]{VOL}} = \frac{74}{\sqrt[3]{302 \times 10^3}} = 1.102$$

$$R = (T_s/2\pi)^2 g = \left(\frac{10}{6.28}\right)^2 32.2 = 81.6$$

$$r = \frac{R}{\sqrt[3]{VOL}} = \frac{81.6}{67.1} = 1.215$$

$$B/R = \frac{74}{81.6} = .907$$

$$\frac{GM}{B \log_{10} \Delta} = \frac{11.5}{(74)(3.94)} = .0394 \quad (2)$$

It is readily apparent that an icebreaker is far from being an average naval vessel. In particular the large GM makes it a hard ship to stabilize. Using pertinent quantities,

the frequency of roll is

$$\omega_s' * = \frac{2\pi}{T_s} = \frac{2\pi}{10} = .628 \text{ radians/sec}$$

the roll-righting coefficient is

$$K_s' = \Delta GM = (8640)(11.5) = 99,400 \text{ ft-tons/radian} \quad (3)$$

and the roll-inertia coefficient is

$$J_s' = \frac{K_s'}{(\omega_s')^2} = \frac{99,400}{(.628)^2} = 252,000 \text{ ft-tons/radian} \quad (4)$$

It will be assumed that the tank system can be designed on a static basis, so that

$$K_t \times \phi_{\max} = K_{ss} \psi \text{ static} \quad (5)$$

K_t is the static moment in roll produced by the tank water per unit of ϕ ,

K_{ss} is the static moment in roll produced by the sea per unit of ψ ,

ϕ_{\max} is the maximum angle of tank water level with respect to the ship, and

ψ static is the maximum effective waveslope (capacity).

* Primes refer to ship unmodified by tanks.

Because the problem is one of dynamics rather than statics, the above assumption is permissible only if

$$\omega_{st} > 2.5 \omega_s \text{ (from reference 54)}$$

ω_s is the resonant frequency of the ship system, and ω_{st} is the "decoupling" frequency; when the tank water oscillates sinusoidally at this frequency, the torque due to static head is exactly neutralized by the torque due to the acceleration forces acting on the water.

Whether the required condition is satisfied will appear later.

System Parameters

Stabilizer weight and space costs will depend primarily on the following parameters:

$$\frac{B}{L} = \frac{\text{beam}}{\text{tank lever arm}}$$

$$\frac{H}{L} = \frac{\text{maximum possible change in tank water level}}{\text{tank lever arm}}$$

$$\Omega_t = \frac{\omega_t}{\omega_s} \frac{\text{natural frequency of tanks}}{\text{natural frequency of ship}}$$

$$\Omega_{st} = \frac{\omega_{st}}{\omega_s} \text{ normalized decoupling frequency}$$

$$Q_t' = \text{magnification ratio of tanks (without pump)}$$

It is shown in (53) that the total fluid weight is a strong function of L/H . For minimum weight L/H should be made small. However, as will be seen later, power goes up with decreasing L/H . In the present study for icebreakers weight and space are available at relatively low cost, therefore low power requirements will govern the design. As a first try the heeling tanks as presently installed, shown in Figures III-25 and III-26, will be used. Using nomenclature shown in Figure F-1

$$H = 6 \text{ feet}; \quad L = 30 \text{ feet}; \quad B = 74 \text{ feet}$$

Calculations for duct size

$$\phi_{\max} = \tan^{-1} \frac{H}{B-13} = \tan^{-1} \frac{6}{61} = 5.65^\circ$$

It is assumed (see reference 54) that

$$K_{ss} = K_s = K'_s = 99,400 \text{ ft-tons/radian}$$

Then

$$K_t = K_{ss} \times \frac{\phi_{\max}}{\phi_{\max}} = (99,400) \left(\frac{5}{5.65} \right) = 88,000 \text{ ft-tons/radian}$$

But also

$$K_t \phi = \frac{(\rho_f \ell g) L h A_o}{2240}$$

where

$$\phi = \frac{h}{2L}$$

and

h = head at any time

therefore

$$K_t = \frac{2 \rho_{s.w.} g L^2 A_o}{2240} \text{ using salt water} \quad (6)$$

and

$$A_{o\text{total}} = \frac{K_t}{2 \rho_{s.w.} g L^2} = \frac{(88,000)(2240)}{(2 \times 64)(30)^2} = 1710 \text{ ft}^2$$

A_o for the tanks installed = $(13)(33) = 430 \text{ ft}^2$ per tank,
which means four sets of tanks would be needed. By using
part of the fuel oil tanks directly below the heeling
tanks, shown in Figure III-25, H can be increased.

Let

$$A_{o\text{total}} = 3 \times 430 = 1290 \text{ ft}^2$$

then

$$K_t = \frac{A_o^2 \rho_{s.w.} g L^2}{2240} = \frac{(1290)(128)(900)}{(2240)} = 66,300 \text{ ft-ton/radian}$$

$$\phi_{\max} = \frac{(99,400)(5)}{66,300} = 7.49^\circ$$

$$H = (B-13) \tan 7.49^\circ = (.61 \times 1312) = 8.0'$$

Thus the tanks can be used as they are with the cross duct running from the fuel tanks. Further calculations will be based on the above numbers which utilize 3 sets of tanks.

To prevent yawing moment on the ship due to acceleration of water, the tanks should be equidistant fore and aft from the longitudinal center of gravity LCG of the ship. This is the case for the heeling tanks as installed as can be seen from Figure III-25.

The behaviour of a set of tanks depends upon the frequency to which they are tuned. After the tanks themselves are fixed, this depends on the length and cross-sectional area of the cross-connecting duct. The most reasonable value for the natural frequency of the tank ω_t is a value equal to the ship frequency as this satisfies the criterion for optimum passive damping.

Therefore

$$\omega_t = \omega_s = 0.628 \text{ radians/sec}$$

Following the procedure used by Hagen (59), the resonant frequency of the tank system can be determined from the following formula:

$$t = \sqrt{\frac{2g}{S'}} \quad (7)$$

where S' is the "weighted" length of the U-tube formed by a set of tanks and the connecting duct and is defined as

$$S' = \int_0^S \frac{A_o}{A_s} ds \quad (8)$$

From equation (7)

$$S' = \frac{2g}{(\omega_t)^2} = \frac{64.4}{(.628)^2} = 163 \text{ ft}$$

The total length of water in each tank pair is 8.0'. There must be a transition section connecting the tank to the duct which will be taken to be essentially vertical and 4 feet on each side. The weighted length of the duct alone

$$S_D' = 163 - 8.0 - 2(4) = 147 \text{ ft.}$$

The actual length of the cross duct

$$L_D = \text{is approximately } 74-13 = 61 \text{ ft.}$$

Using equation (8)

$$A_D = \frac{A_o L_D}{S_D} = \frac{(430)(61)}{147} = 178 \text{ ft}^2$$

This is quite obviously not a practical size for the duct, therefore some adjustments are necessary at this point. If the full depth of the fuel tanks below the heeling tanks is used with the cross duct below the fuel tanks

$$H = 16 \text{ ft}$$

$$\phi_{\max} = \tan^{-1} \frac{16}{61} = 14.7^\circ$$

$$K_t = 33,800 \text{ ft-tons/radian}$$

$$A_o \text{ total} = 656 \text{ ft}^2$$

Using 4 sets of tanks, rather than three, to bring A_o down to a size which will make A_D reasonable

$$A_o = \frac{656}{4} = 164 \text{ ft}^2$$

$$S'_D = 163 - 16 - 8 = 139 \text{ ft}$$

$$A_D = \frac{(164 \times 61)}{139} = 72 \text{ ft}^2$$

Using eight sets of tanks

$$A_o = 82 \text{ ft}^2$$

$$A_D = 36 \text{ ft}^2$$

Now a check can be made on validity of assumption made earlier that

$$\frac{\omega_{st}}{\omega_s} > 2.5$$

Taking

$$_{st} = \sqrt{2g/S''} \quad (9)$$

where

$$S'' = \int_0^S \frac{D_s}{L} d s \quad (10)$$

S'' equals the weighted length of the fluid trajectory.

Hagen arrives at equation (10) with the following argument. "The ship-tank system is one having two degrees of freedom, and it is characterized by three natural

frequencies: ω_s , ω_t and ω_{st} , each of which can be written in terms of a moment coefficient K and an inertia coefficient J . For example, $\omega_{st} = \sqrt{K_t/J_{st}}$, where J_{st} is a "mutual" inertia coefficient. The derivation of the equations of motion shows that J_{st} is dependent on a "weighted" length of the fluid trajectory; that is, upon $S'' = \int_{S_s}^S \left(\frac{D_s}{L}\right) ds$. Referring to Figure F-1, D_s is the perpendicular distance from the center of rotation to the velocity vector of the tank-water element under consideration. The center of rotation of the fluid element is assumed to be midway between the center of buoyancy and the center of gravity (54). KG equals 24.4 feet. KB is estimated at 17 feet. Therefore the center of rotation is 20.7 feet above the base line. For $H = 16$ feet the centerline of the cross ducts is approximately 20 feet above the base line and for the cross duct

$$D_s = 20.7 - 20 = 0.7 \text{ ft.}$$

For the side tanks the total length of water in each pair is $16 + 8 = 24$ feet
and

$$D_s = 30 \text{ feet}$$

Therefore

$$S'' = \int_0^{24} \frac{30}{30} ds + \int_0^{60} \frac{.7}{30} ds = 24 + 1.4$$

$$S'' = 25.4 \text{ feet}$$

and

$$\omega_{st} = \sqrt{\frac{2g}{S''}} = \sqrt{\frac{64.4}{25.4}} = 1.59$$

$$\frac{\omega_{st}}{\omega_s} = \frac{1.59}{.628} = 2.54$$

It was only necessary that $\omega_{st} > 2.5 \omega_s$, therefore the condition is satisfied. The addition of the tanks does change the ship parameters slightly, however calculations made in reference 54 indicate that such changes would be very small. All that would be required to account for this is a change in the cross-sectional area of the cross duct.

If CR is lower than estimated, S'' will decrease and ω_{st} will increase. This is favorable. However, if CR is higher than estimated, S'' will increase and ω_{st} will decrease. A large error in the latter case would drop ω_{st}/ω_s below the 2.5 limit.

Weight of the System

Weight of stabilizing water per set of four tanks is

$$64 (164 \times 20) + (60.0 \times 72) 1220 =$$

$$\frac{64}{2240} (3280 + 4320) = \frac{(64)(7600)}{2240} = 217 \text{ tons per set}$$

Therefore total weight = $(4)(217) = 868 \text{ tons}$

Percent stabilizing weight = $868/8640 = 10.0\%$

of which 5.68% is in the ducts.

Required Power

From Chadwick (53)

$$\text{Peak real power} = K_p P_o \frac{\underline{\Omega}}{Q_t} \frac{\underline{\Omega}}{\underline{\Omega}_t}$$

$$\text{Peak reactive power} = K_p P_o \underline{\Omega} \left[1 - \left(\frac{\underline{\Omega}}{\underline{\Omega}_t} \right)^2 \right]$$

where

$$K_p = \frac{1}{2} \left(\frac{H}{L} \right) \left(\frac{GM}{B} \right) \left(\frac{B}{R} \right)^{\frac{1}{2}} \left(\frac{\Psi_o}{\Psi_{\text{static}}} \right)^2 \left(\Psi_{\text{static}} \right)^{\frac{1}{2}} b^{\frac{1}{2}}$$

and

$$\frac{1}{Q_t} = 3.0 \times 10^{-2} \left[b^{3/2} \left(\frac{H}{B} \right)^2 \left(\frac{L}{H} \right)^{\frac{1}{2}} \left(\frac{R}{B} \right)^2 \left(\Psi_{\text{static}} \right)^{\frac{1}{2}} \frac{\sqrt{n}}{\underline{\Omega}_t^3} \right]$$

$$\left[\left(\frac{P_{f1}}{P_{ssw}} \right)^{\frac{1}{2}} \left(\frac{\Psi_o}{\Psi_{\text{static}}} \right) \left(\frac{\underline{\Omega}}{\underline{\Omega}_t} \right) \right]$$

$$\begin{aligned}
\Delta &= 8,640 \\
H &= 16 & \frac{H}{L} &= .533 & \frac{H}{B} &= .216 \\
L &= 30.0 \\
CM &= 11.5 & \frac{CM}{B} &= .1555 \\
B &= 74 \\
R &= 81.6 & \frac{B}{R} &= .907 \\
b &= 1.102 \\
\Psi_{\text{static}} &= 5^\circ = .0873 \text{ radians} \\
n &= 4 = \text{number of ducts} \\
\text{Therefore,} \\
K_p &= \frac{1}{2} (.533) (.1555) (.907)^{\frac{1}{2}} \left(\frac{\Psi_o}{\Psi_{\text{static}}} \right)^2 (.0873 \times 1.102)^{\frac{1}{2}} \\
K_p &= 3.64 \times 10^{-3} \left(\frac{\Psi_o}{\Psi_{\text{static}}} \right)^2 \\
\Psi_o &= \frac{(\Delta)(VOL)^{1/6}}{550} (g)^{\frac{1}{2}} (2240) = \frac{(8640)(8.19)(5.67)(2240)}{550} \\
\Psi_o &= 1.63 \times 10^6
\end{aligned}$$

$$\text{If } \omega_t = \omega_s, \text{ then } \omega_t = \omega_t / \omega_s = 1.0$$

$$\text{Maximum power is required when } \Psi_o / \Psi_{\text{static}} = 1$$

$$\text{Power requirements are based on } \omega / \omega_s = \omega = 2.0$$

which is the worst condition.

Therefore

$$\frac{1}{Q_t'} = 3.0 \times 10^{-2} \quad (1.102)^{3/2} \quad (.216)^2 \quad (1.865)^{\frac{1}{2}} \quad \times \\ \frac{1}{(.907)^2} \quad \frac{1}{(.0873)^{\frac{1}{2}}} \quad \frac{\sqrt{4}}{(1)^3} \quad [2]$$

$$\frac{1}{Q_t'} = 3.0 \times 10^{-2} \quad \frac{(1.157)(.0467)(1.365)}{(.822)(.296)} \quad (2)(2) = .0361$$

$$Q_t' = 27.7$$

$$\text{Peak real power} = K_p P_o \frac{\omega^2}{Q_t' \omega_t} = \frac{(3.64 \times 10^{-3})(1.63 \times 10^6)(4)}{27.7}$$

$$\text{Peak real power} = .8560 \times 10^3 = 856 \text{ HP}$$

$$\text{Peak reactive power} = K_p P_o \omega \left[1 - \left(\frac{\omega}{\omega_t} \right)^2 \right] = (3.64 \times 10^{-3})(1.63 \times 10^6) \\ (2)(-3)$$

$$\text{Peak reactive power} = -35.6 \times 10^3 = 35,600 \text{ HP}$$

$$\text{Pump output rating} = \frac{1}{2} \sqrt{(\text{peak real power})^2 + (\text{peak reactive power})^2}$$

$$\text{Pump output rating} = \frac{1}{2} \sqrt{(856)^2 + (35,600)^2} = \frac{1}{2} (35,600)^2$$

$$\text{Pump output rating} = 17,800 \text{ HP}$$

The average power of the pump will be considerably less than the rated output but will still be quite large.

Summary

$$\psi_{\text{static}} = \text{capacity} = 5^\circ$$

Cross sectional area of each duct using 4 sets of tanks = 72 ft²

Percent weight = 10.2%

Pump output rating = 17,800 HP

These figures make this system clearly prohibitive. However, they are based on an effective waveslope ψ of 5° which gives a large degree of stabilization. Therefore the next step is to look into the requirements of a system with a smaller capacity.

Calculations for a Reduced Capacity System

Another method of reducing the cost of the system is to reduce GM.

Therefore, before starting calculations for a lower capacity system, it will be of interest to see how much the GM is reduced by the free surface in the four sets of tanks used in the previous calculations.

$$CG_v = \frac{i}{V} \text{ for one tank, where } i = \frac{bh^3}{12}$$

$$i = \frac{(32.5)(11)^3}{12} = 3.6 \times 10^3$$

$$V = 3.02 \times 10^5 \text{ ft}^3$$

$$CG_v = \frac{3.6 \times 10^3}{3.02 \times 10^5} \times 8 = .0954 \text{ ft.}$$

which is negligible.

Chadwick is of the opinion that a capacity below 2.5° will not be effective, therefore 2.5° will be used for the reduced capacity calculations.

Therefore,

$$K_t = 16,900 \text{ ft-tons/rad.}$$

$$A_o = 328 \text{ ft}^2 \text{ total}$$

Again using four sets of tanks

$$A_o \text{ per tank} = 328/4 = 80.2 \text{ ft}^2$$

$$A_D = 36 \text{ ft}^2$$

$$\text{Total weight} = \frac{1}{2}(868) = 434 \text{ tons}$$

$$\text{Percent stabilizing weight} = 5.0\%$$

$$\text{static} = \text{capacity} = 2.5^\circ$$

$$K_p \sim \psi_{\text{static}}, \text{ therefore, } K_p = \frac{3.64 \times 10^{-3}}{2} = 1.82 \times 10^{-3}$$

$$Q_t' \sim \frac{1}{(\psi_{\text{static}})^{\frac{1}{2}}} \text{ therefore, } Q_t' = 27.7 (\sqrt{2}) = 39.3$$

$$\text{Peak reactive power} = 17,800$$

$$\text{Pump output rating} = 8,900 \text{ HP}$$

Thus, even at a minimum capacity, the cost in power is clearly prohibitive, and an activated tank system cannot be used on a ship with a GM as large as that of an icebreaker.

F.2 Analysis of Passive Anti-Roll Tanks Installed On the USS ATKA

Figure III-28 gives the general location of the heel-ing tanks indicating the location of the anti-roll tank. Figure III-29 gives details of the anti-roll tank installation. Table III-7 gives the particulars for the ATKA. These are presented in Section III.4. The analysis of this system follows the same procedure as used in Section F.1 on the GLACIER and hence is briefer.

Calculations

$$\text{Desirable capacity} = \frac{.36}{\log_{10} \Delta} = \frac{.36}{\log_{10} 6500} = \frac{.36}{3.81} = 5.4^\circ$$

The frequency roll is

$$\omega_s' = \frac{2\pi}{T_s} = \frac{2\pi}{10.0} = .628 \text{ radians/sec}$$

the roll-righting arm coefficient is

$$K_s' = \Delta GM = (6500)(8.0) = 52,000 \text{ ft-tons/radian}$$

From Figure III-29,

$$H = 8.5' \quad L = 24.0$$

Therefore,

$$\phi_{\max} = \tan^{-1} \frac{H}{2L} = \tan^{-1} \frac{8.5}{48} = 10.0^\circ$$

$$K_{ss} = K_s' = 52,000 \text{ ft-tons/radian}$$

$$K_t = K_{ss} \frac{\phi_{\max}}{\psi_{\max}} = \frac{52,000}{10.0} \quad \psi_{\max} = 5,200 \quad \psi_{\max}$$

But also

$$K_t = \frac{2 \rho_{fp} g L^2 A_o}{2240} \text{ ft-tons/radian}$$

where

$$\rho_{fp} g = 55 \text{ lbs/cu.ft for diesel oil}$$

$$A_o = (15)(13.3) = 200 \text{ ft}^2$$

Therefore

$$K_t = \frac{(2)(55)(24.0)^2(200)}{2240} = 5660 \text{ ft-tons/radian}$$

and

$$\psi_{max} = \frac{5660}{5220} = 1.09^\circ = \text{system capacity}$$

The open area between standpipe fins can be determined as follows:

$$\omega_t = \omega_s = .628 \text{ radians/sec}$$

$$\omega_t = \sqrt{\frac{2g}{S'}}$$

Therefore, $S' = \frac{2g}{(\omega_t)^2} = \frac{64.4}{(.628)^2} = 163 \text{ ft}$

Also $S' = \int_0^S \frac{A_o}{A_s} ds$

The total length of water in each tank, where the tanks are designated as the volume outboard of the standpipe and fins, is 8.5 feet.

The weighted length of the duct alone

$$S'_D = 163 - 8.5 = 154.5 \text{ ft.}$$

The actual length of the cross duct

$$L_D \text{ is } 33 \text{ feet}$$

and

$$A_{D_{\text{total}}} = \frac{A_o L_D}{S'_D} = \frac{(200)(33.0)}{154.4} = 42.7 \text{ ft}^2$$

which is the total area of the cross duct open in both tanks.

The height of the opening under condition of maximum head is the full height of the tank, therefore the total open distance athwartships is

$$42.7/8.5 = 5.02 \text{ feet}$$

This compares favorably with the actual total open distances between standpipe fins as installed of $\frac{(8)(7-1/8)}{12} = 4.75 \text{ feet.}$

A check on the validity of assumption that

$$\frac{\omega_{st}}{\omega_s} > 2.5$$

revealed that this ratio equals 2.86. Therefore assumption was valid.

The weight of the fluid in the system using diesel oil at 55 lbs per cubic foot is 41.5 tons per tank. This is 12,600 gallons. Therefore the total weight of the fluid is 83 tons or 1.28 percent of the full load displacement.

thesH533
A design study for a polar icebreaker /



3 2768 002 06048 5
DUDLEY KNOX LIBRARY